Department of Chemistry
Faculty of Science
University of Helsinki
Finland

Development of Materials and Methodologies for Microextraction Techniques

Hangzhen Lan

DOCTORAL DISSERTATION

To be presented, for public examination with the permission of the Faculty of Science of the University of Helsinki, in Chemicum Auditorium A129, A. I. Virtasen Aukio 1, on the 23rd of August 2019 at 12 o'clock.

Helsinki 2019

Supervisor: Professor Marja-Liisa Riekkola
Department of Chemistry
University of Helsinki
Finland

Co-supervisor: Docent Kari Hartonen
Department of Chemistry
University of Helsinki
Finland

Reviewers: Professor Rosa Maria Marcé
Department of Analytical Chemistry and Organic Chemistry
Universitat Rovira i Virgili
Spain

Professor Torsten C. Schmidt
Instrumental Analytical Chemistry
University of Duisburg-Essen
Germany

Opponent: Professor Antonio Canals Hernandez
Departamento de Química Analítica, Nutrición y Bromatología
Universidad de Alicante
Spain

ISBN 978-951-51-5310-4 (Paperback)
ISBN 978-951-51-5311-1 (PDF)
http://ethesis.helsinki.fi/

https://unigrafia.fi/
Helsinki 2019

Abstract

Traditionally, sampling and sample preparation can occupy up to 70-80% of total analysis time in an analytical process that calls for state of the art technologies to reduce the time and the labor needed. In addition, authorities and researchers increasingly demand more sensitive and reliable analytical methods. Solid phase microextraction (SPME) Arrow and in-tube extraction (ITEX) techniques meet these requirements by combining sampling and sample preparation procedures into one, resulting in decreased total analysis time and improved accuracy without any need for organic solvent. The type and amount of sorbent phase, which is immobilized on/in SPME Arrow and ITEX devices, volume of the system and affinity towards targeted analytes are the four main parameters that affect the sensitivity and capability of an analytical method.

The main goals of this thesis were to develop new materials, useful as the extraction sorbent in SPME Arrow and ITEX devices, and to clarify their applicability for semi-automated and automated sampling and/or extraction systems for the analysis of volatile organic compounds (VOCs) in environmental, food and biogenic samples.

Atomic layer deposition and molecular deposition-conversion methods were employed to fabricate directly iron, aluminum, and zirconium-based metal organic frameworks (MOFs) SPME Arrow coatings. The efficiency of these hydrophobic MOF coatings to isolate hazardous organic compounds from wastewater was evaluated. SPME Arrows were coated also with acidified zeolitic imidazolate framework-8 (A-ZIF-8), ordered mesoporous silicas (OMSs) and functionalized OMSs with different mesopore sizes and multidimensional pore-channel structures by dipping method. Extraction selectivities of these materials were systematically studied. The dipped coatings were reproducible and reusable. The applicability of electrospun and electroblown nanofibers as the packing materials of ITEX was also evaluated. Polyacrylonitrile (PAN) nanofibers with good gas permeability, thermal stability, and excellent affinity to VOCs made them a good alternative of commercial adsorbents for ITEX packing materials.

Fully automated dynamic PAN-ITEX system on-line coupled to gas chromatography-mass spectrometry (GC-MS) for continuous analysis of VOCs in air was developed for long-term campaigns. The applicability of aerial drone as the carrier for SPME Arrow and ITEX devices was tested as well for passive and active air sampling in the field. The effects of accessories used in the sampling device, drone flight displacement and sampling location on the sampling results were evaluated.

The results demonstrated the great potential of new materials as the extraction sorbents for SPME Arrow and ITEX. They provided better or similar performance in terms of extraction capacity, extraction selectivity and extraction kinetics when compared to commercial materials for enrichment and isolation of analytes from various sample matrices. Further, the developed SPME Arrow and on-line dynamic ITEX methods offered flexibility and versatility for analysis of VOCs. The drone was an ideal platform for miniaturized passive and active air sampling in remote and difficult access regions.

Preface

This thesis is based on research carried out at the Department of Chemistry, University of Helsinki, during the years 2015-2019. China Scholarship Council (grant no. 201508330310), the Finnish Centre of Excellence in Atmospheric Science-From Molecular and Biological Processes to the Global Climate (grant no. 307331), and the Doctoral Programme in Materials Research and Nanosciences of the Doctoral School in Natural Sciences financially supported the research.

First, I want to express my sincere gratitude to my supervisor, Professor Marja-Liisa Riekkola, for providing me the opportunity to carry out my doctoral studies under her supervision. I am especially grateful for all the guidance, valuable comments, encouragement, and support for my life, study, and research during these years.

I also want to thank Dr. Kari Hartonen for the thorough discussion about the research when I was completely confused and the help to improve my writing language in my publications and dissertation time-to-time.

Many thanks to Dr. Jevgeni Parshintsev for giving your hand and encouragement for my study and research. Tuukka Rönkkö is especially acknowledged for your help about living in Finland and your demonstration and discussion.

Special thanks to laboratory engineer Matti Jussila and laboratory technician Karina Moslova, I cannot finish my researches on time without your kind of friendly and patient persons. Matti Jussila helped to construct so many different devices, thermal desorption unit, liquid nitrogen cryotrap, electronic controller, air-sampling tubes, which all were so important during my study. Karina Moslova, such an energetic human being helped me to look for the right chemicals or consumables from every corner in Chemicum.

I would like to express my gratitude to all the co-authors who contributed to my work. Leo Salmi, Jani Holopainen, and Wenzhong Zhang are thanked for their help in material synthesis. Mikko Ritala is thanked for the collaboration for the development of new materials. Ning Gan is thanked for stimulating discussions related to material application. Marianna Kemell is thanked for SEM measurements. Jan-Henrik Smått, Motolani Sakeye, and Jawad Sarfraz are thanked for the BET measurement. Timo Hatanpää for TGA measurements. Nicola Zanca and Jose Ruiz-Jimenez are thanked for the great teamwork in air sampling at Hyytiälä with our lovely 'EUNICE' drone.

The present and former laboratory staff members: Norbert Maier, Heli Sirén, Evegen Multia, Thanaporn Liangsupree, Luís Barreira, Aku Helin, Crystal Tear, Magdalena Okuljar, Henri Avela, Xinpei Li, ChenYeh Tsai, Yu Tat Tse, Geoffroy Duporté and Xinghua Wang are acknowledged for creating an enjoyable and stimulating working atmosphere.

I would like to thank my Chinese friends, Chao Zhang, Zheng Yang, Zhongmei Han, Junhua Xu, Xiaodong Li, Ming Guo, for the entertainments and other activities.

Finally, I would like to thank my parents for their continuous support and encouragement.

Helsinki, February 2019
Hangzhen Lan

Table of contents

Abstract ... 3
Preface ... 4
List of original publications ... 7
Abbreviations ... 8
List of symbols ... 10
1 Introduction ... 11
2 Background to the work ... 13
2.1. Sampling ... 13
2.1.1. Passive sampling ... 13
2.1.2. Active sampling ... 15
2.2. Sample preparation ... 16
2.2.1. Non-exhaustive microextraction techniques ... 16
2.2.2. Exhaustive microextraction techniques ... 20
2.3. Trends in the development of analytical process ... 23
2.3.1. New materials ... 23
2.3.2. Automation ... 26
2.3.3. New platform ... 26
2.3.4. Applications ... 27
3 Experimental ... 28
3.1. Materials synthesis and fabrication for microextraction devices ... 32
3.1.1. Metal organic frameworks for solid phase microextraction Arrows ... 32
3.1.2. Ordered mesoporous silicas for solid phase microextraction Arrows ... 32
3.1.3. Nanofibers packed in-tube extraction ... 33
3.2. Material characterization ... 34
3.3. Construction of the permeation systems ... 34
3.3.1. Permeation system for standard volatile organic compounds ... 34
3.3.2. Permeation system for internal standard ... 35
3.4. Construction of the air sampling unit for the drone ... 35
3.5. Thermal desorption units ... 36
3.5.1. Thermal desorption unit for blade solid phase microextraction ... 36
3.5.2. Thermal desorption unit for in-tube extraction ... 36
3.6. Gas chromatography-mass spectrometry conditions ... 38

3.7. Solid phase microextraction and in-tube extraction procedures 38
3.7.1. Static solid phase microextraction procedures 38
3.7.2. Dynamic solid phase microextraction Arrow procedures 38
3.7.3. Headspace dynamic in-tube extraction 39
3.7.4. Online dynamic in-tube extraction 39
3.7.5. Aerial drone as the platform of microextraction sampling systems 40
3.8. Sampling and sample pretreatment 40
3.8.1. Air samples 40
3.8.2. Liquid samples 40
3.8.3. Solid samples 41
3.9. Software 41
4 Results and discussion 42
4.1. Development of new materials for microextraction techniques 42
4.1.1. Solid phase microextraction Arrow coatings 42
4.1.2. In-tube extraction packing material 44
4.2. Comparison of laboratory-made and commercial solid phase microextraction devices 45
4.3. Comparison of laboratory-made and commercial in-tube extraction 51
4.4. Reusability and reproducibility of laboratory-made microextraction devices 52
4.5. Performance of laboratory-constructed permeation systems 53
4.6. Optimization of solid phase microextraction Arrow conditions 54
4.7. Optimization of in-tube extraction conditions 56
4.7.1. Online dynamic in-tube extraction 56
4.7.2. In-tube extraction sampling accessories 57
4.8. Performance of the developed solid phase microextraction and in-tube extraction methods 57
4.9. Developed solid phase microextraction Arrow and in-tube extraction methods for natural sample analysis 58
4.10. Drone as the platform for the microextraction devices in air sampling 59
5. Conclusions 61
References 63

List of original publications

This dissertation is based on the following publications:

I. **H. Lan**, L.D. Salmi, T. Rönkkö, J. Parshintsev, M. Jussila, K. Hartonen, M. Kemell, M.-L. Riekkola, Integrated atomic layer deposition and chemical vapor reaction for the preparation of metal organic framework coatings for solid-phase microextraction Arrow, ***Analytica Chimica Acta***, 2018, 1024: 93-100. DOI: 10.1016/j.aca.2018.04.033

II. **H. Lan**, T. Rönkkö, J. Parshintsev, K. Hartonen, N. Gan, M. Sakeye, J. Sarfraz, M.-L. Riekkola, Modified zeolitic imidazolate framework-8 as solid-phase microextraction Arrow coating for sampling of amines in wastewater and food samples followed by gas chromatography-mass spectrometry, ***Journal of Chromatography A***, 2017, 1486: 76-85. DOI: 10.1016/j.chroma.2016.10.081

III. **H. Lan**, W. Zhang, J.H. Smått, R. Koivula, K. Hartonen, M.-L. Riekkola, Selective extraction of aliphatic amines by functionalized mesoporous silica coated solid phase microextraction Arrow, ***Microchimica Acta***, 2019, 186 (7): 412. DOI: 10.1007/s00604-019-3523-5

IV. **H. Lan**, J. Holopainen, K. Hartonen, M. Jussila, M. Ritala, M.-L. Riekkola, Fully automated online dynamic in-tube extraction for continuous sampling of volatile organic compounds in air, ***Analytical Chemistry***, 2019, 91 (13): 8507-8515. DOI: 10.1021/acs.analchem.9b01668

V. J. Ruiz-Jimenez, N. Zanca, **H. Lan**, M. Jussila, K. Hartonen, M.-L. Riekkola, Aerial drone as a carrier for new miniaturized air sampling systems, ***Journal of Chromatography A,*** 2019, 1597:202-208. DOI: 10.1016/j.chroma.2019.04.009

Contribution of the author:

Hangzhen Lan carried out the research and all the experiments related to modification and conversion of materials, coatings, packings and testing of microextraction devices, sample preparation, chromatography, mass spectrometry and data analysis (Papers I-IV). He also prepared the coatings for SPME Arrow and the packing materials for ITEX devices for air sampling (Paper V). He had the main responsibility for writing the manuscripts (Papers I-IV).

Abbreviations

ADAP	Automated Data Analysis Pipeline
ALD	Atomic layer deposition
AS	Active sampling
CA	Cluster analysis
DEA	Diethylamine
DI	Direct immersion
DMA	Dimethylamine
DVB	Divinylbenzene
EA	Ethylamine
EI	Electron ionization
GC	Gas chromatography
HmIM	2-Methylimidazole
HS	Headspace
ISTD	Internal standard
ITEX	In-tube extraction
LC	Liquid chromatography
LLE	Liquid-liquid extraction
LMWAA	Low-molecular-weight aliphatic amine
LOD	Limit of detection
LOQ	Limit of quantitation
m/z	Mass-to-charge ratio
MA	Methylamine
MLD	Molecular layer deposition
MOF	Metal organic framework
MS	Mass spectrometry
NT	Needle trap
NTME	Needle trap microextraction
OMS	Ordered mesoporous silica
PA	Polyacrylate
PAN	Polyacrylonitrile
PCA	Principal component analysis
PDMS	Poly(dimethylsiloxane)
PS	Passive sampling
PVC	Poly(vinyl) chloride
SBSE	Stir bar sorptive extraction
SEM	Scanning electron microscopy
SMEAR II station	Station for Measuring Ecosystem-Atmosphere Relations II
SPE	Solid phase extraction
SPME	Solid phase microextraction
T.P.	Temperature program
TD	Thermal desorption
TDU	Thermal desorption unit

TEA	Triethylamine
TGA	Thermogravimetric analysis
THF	Tetrahydrofuran
TMA	Trimethylamine
TWA	Time-weighted average
VOCs	Volatile organic compounds
XPS	X-ray photoelectron spectroscopy
XRD	X-ray diffraction

List of symbols

C_0	Original concentration of analytes in the sample (M)
C_h^∞	Equilibrium concentration of analytes in the headspace (M)
C_S^∞	Equilibrium concentration of analyte in the sample (M)
$C_{f\ max}$	Maximum concentration of active sites on the coating (M)
C_f^∞	Equilibrium concentration of analyte in SPME coating (M)
C_{fA}^∞	Equilibrium concentration of analyte A (M)
C_{fB}^∞	Equilibrium concentration of competing compound B (M)
K_{hs}	Distribution constant of analytes between the sample matrix and sample headspace
K_A	Adsorption equilibrium constant for analyte A
K_B	Adsorption equilibrium constant for competing compound B
K_{es}	Distribution constant of analytes between the sorbent phase and the sample matrix
K_{fh}	Distribution constant of analytes between the SPME coating and the sample headspace
K_{fs}	Distribution constant of analytes between the SPME coating and the sample matrix
L_d	Diffusive path length of the passive sampler (cm)
L_p	Membrane thickness of a permeation passive sampler (μm)
V_h	Sample headspace volume (mL)
V_S	Sorbent phase volume (μL)
V_b	Breakthrough volume (mL)
V_f	SPME coating volume (μL)
V_s	Sample volume (mL)
V_v	Void volume of the sorbent bed (μL)
k_p	Permeability of the sorbent bed in the needle trap device
t_b	Breakthrough time (min)
$\emptyset$	Porosity of the sorbent bed
Δp	Pressure drop of the sample through the needle
μ	Sample viscosity
A	Cross-sectional area of the diffusion path in the passive sampler (cm^2)
A	Cross sectional area of the needle (cm^2)
C	Analyte concentration in the sampled medium ($ng\ mL^{-3}$)
D	Diffusion coefficient of the analyte in the passive sampler ($cm^2\ min^{-1}$)
K	Adsorption affinity constant of the analyte
L	Length of the packed sorbent bed (cm)
N	Theoretical plate number of the sorbent bed
P	Partial pressure of the analyte close to the membrane surface of a permeation passive sampler
Q	Flow rate of the sample in the needle trap device ($mL\ min^{-1}$)
Q'	Collected mass amount of the analyte in the passive sampler (ng)
S	Permeability coefficient of a certain analyte ($cm^2\ min^{-1}$)
T	Passive sampling time (min)
k	Retention factor
n	Mass amount of analytes that extracted by the SPME coating at equilibrium (ng)
v	Linear flow rate of the gas sample through the sorbent bed ($mL\ min^{-1}$)

1 Introduction

Employment of new sorbent materials to improve and immobilize miniaturized sampling and sample preparation devices, and to widely utilize these devices and extend their applicability have become a trend in analytical chemistry. For example, nanomaterials with porous structures, diverse surface chemistries, and specific physical and chemical properties allow them to capture a certain compound or a group of compounds based on size exclusion and chemical selectivity. Miniaturized devices, that enable studies with minimized operation steps and analytical errors, have been widely used. Furthermore, small devices are particularly suitable for automation. New approaches, combining selective materials, microextraction devices, advanced controlling systems, and platforms, have the potential to provide comprehensive and time-dependent information of analytes of interests and contribute to understand the fundamental mechanism of environmental pollution, biogenic activity, food spoilage, and physiological processes. This work was focused on the development and application of selective materials as coating and/or packing materials in the miniaturized devices that can be exploited for quantitative analysis of volatile organic compounds (VOCs) in environmental, food and biogenic samples.

The solid phase microextraction (SPME) Arrow and in-tube extraction (ITEX) were selected as miniaturized sampling and sample preparation devices for further development. Atomic layer deposition (ALD)- and molecular layer deposition (MLD)-converted metal organic frameworks (MOFs) films were coated on SPME Arrows and applied to environmental studies. Acidified zeolitic imidazolate framework-8 (ZIF-8), ordered mesoporous silicas (OMSs) and functionalized OMSs with diverse pore size distribution and surface functional groups proved to be appropriate for the harvesting of chemical compounds selectively and they were exploited as new SPME Arrow coatings in multiple analytical applications. Electrospun and electroblown nanofibers were also utilized as the packing sorbent for ITEX system. A specific objective was to compare the new materials with commercial materials in terms of extraction affinity, extraction selectivity and extraction kinetics for the selected analytes in various sample matrices. A fully automated online dynamic ITEX system was developed for continuous monitoring of VOCs in atmospheric air in urban areas. The system allows studying the fundamental mechanism of aerosol formation and furthering their effect on Earth's climate. The potential of an aerial drone as the platform for passive and active sampling systems, SPME Arrow and ITEX, was demonstrated.

Aims of the study

The main aim was to develop different materials, study their applicability as sorbents for miniaturized sampling, and sample preparation techniques.

The more specific aims of the study were:

1. To evaluate the applicability of ALD- and MLD-conversion methods for coating of SPME Arrow. (***Paper I***).
2. To develop new SPME Arrow coating materials for selective extraction of VOCs and organic pollutants from wastewater, atmospheric air, mushroom, and salmon samples (***Papers I-III***).
3. To develop new packing materials for ITEX trap (***Paper IV***).
4. To develop a fully automated online dynamic ITEX system for continuous sampling of VOCs in atmospheric, exhaled and indoor air samples (***Paper IV***).
5. To evaluate the applicability of aerial drone as the carrier for SPME Arrow and ITEX sampling of atmospheric VOCs at remote regions (***Paper V***).
6. Comparison of tailor-made and commercial materials (***Papers I-V***).

2 Background to the work

An analytical process is useful for qualitative and/or quantitative analysis of chemical substances in a sample of matter [1]. Sampling, sample preparation, analysis, and data processing are four essential and inter-related steps needed for the results.

The initial sampling procedure requires a proper plan to collect a representative sample whose properties and composition correspond to that of the whole materials [2]. Sample size, sampling location, sampling methods, packing, transportation, and preservation are the key aspects that need to be taken into consideration before sampling [3]. After the sampling, sample preparation converts the complex sample into an instrument-compatible medium (gas, liquid or solid) for the subsequent instrumental analysis. The main task is to homogenize the sample, reduce the sample size, remove unnecessary matrix components, isolate, and concentrate the analytes of interest so that the sample can be directly introduced into the analytical instruments [4-6]. In the past three decades, analytical chemists have taken extensive efforts to 1) simplify operation steps, 2) miniaturize sample preparation devices, 3) reduce sample and/or organic solvent consumption and 4) automate the system to achieve more efficient and environmentally friendly sample preparation without sacrificing the reliability of the analysis [7-11]. The techniques that merge the sampling and sample preparation procedures into one-step were emphasized in this thesis targeting at shortened total analysis time and decreased total analytical errors. After the sample preparation, the sample is generally introduced into an analytical instrument, e.g. chromatograph, spectrometer, for separation and/or detection. These sophisticated instruments provide nowadays sensitive, selective, fast, automated, and multi-targeted detection of analytes [1]. In particular, chromatography coupled with mass spectrometry is the most powerful system to the analysis of complicated samples. Data processing is then used for data assessment, identification, and quantification purposes.

2.1. Sampling

2.1.1. Passive sampling

Passive sampling (PS) technique was invented in 1927 [12] for semi-quantitative analysis of CO and later quantitative analysis was done in 1973 [13, 14]. In the PS process, a passive sampler collects analytes by the driving force of different chemical potentials of the analytes in the sampler and the sample medium. The analytes move by either diffusion or permeation from the higher concentration area in the sample medium to the sampler, where concentrations of the analytes are lower until the equilibrium is reached between these two mediums [15, 16]. Therefore, the most general classification of PS mode includes two categories, diffusion, and permeation (Figure 1).

Fick's First Law of Diffusion (equation (1)) interpreted the diffusional mass transfer of analytes [15, 17, 18]:

$$Q' = D(\frac{A}{L_d})CT \quad (1)$$

where: Q' is the collected mass amount of the analytes (ng), D is the diffusion coefficient of the analyte ($cm^2\ min^{-1}$), A is the cross-sectional area of the diffusion path (cm^2), L_d is the diffusive path length (cm), C is the analyte concentration in the sampled medium ($ng\ mL^{-3}$) and T is the sampling time (min). D is specific to the analyte, which is varied by chemical and physical properties. The term of DA/L is considered as the sampling rate of the passive sampler for a certain analyte.

The Fick's First Law of Diffusion in equation (2) can also describe the permeative mass transfer of analytes through a membrane [15, 17, 18]:

$$Q' = S(\frac{A}{L_p})PT \quad (2)$$

where S is the permeability coefficient of a certain analyte ($cm^2\ min^{-1}$), L_p is the membrane thickness and P is the partial pressure of the analyte close to the membrane surface. In this case, at a constant temperature, S and P are constant, thereby the concentration of the analytes can be determined easily once Q' and T are known.

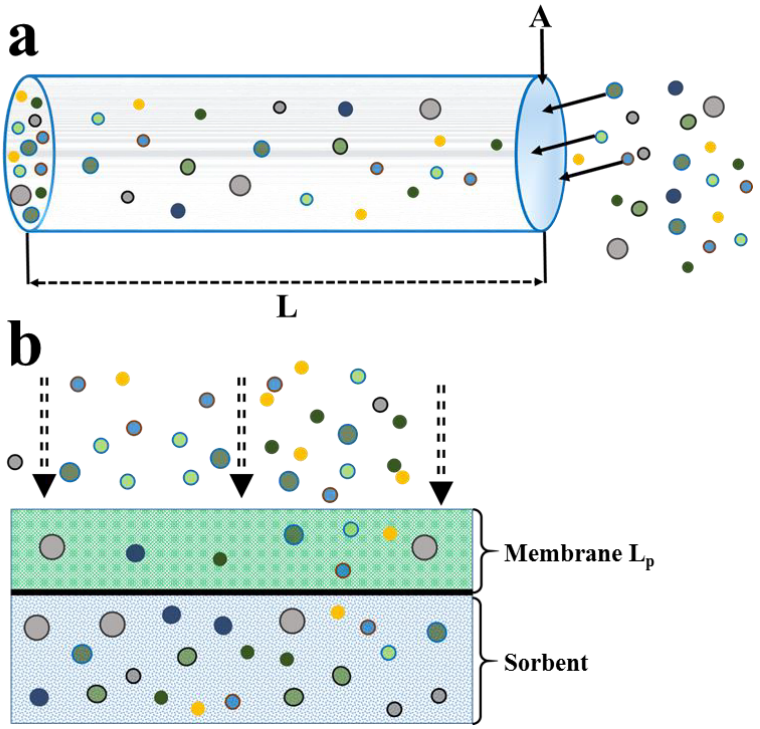

Figure 1. (a) Tube-type diffusion and (b) badge-type permeation passive samplers. Reproduced with modification from Elsevier [15]. A, L and L_p are the cross-sectional area of the diffusion path, the diffusive path length, and membrane thickness, respectively.

These theories have then been derived and applied for equilibrium-based microextraction techniques to interpret their extraction mechanism and corresponding method development. For example, solid phase microextraction (SPME) technique (detailed description is in **section 2.2.1**).

The biggest advantage of passive samplers is their possible operation without electricity in a fixed location for a long period of time [15]. Therefore, they are particularly suitable for long-term exposure sampling in the remote region and for the determination of time-weighted average (TWA) concentration of analytes [19-21]. In addition, simplified and miniaturized sampler allows personal sampling at home, school, or hospital without professional training.
PS techniques are also compatible with gaseous, liquid, and solid samples due to the diverse sampler systems and implementation instructions [16, 19, 20]. The various sampler geometries, e.g. sorbent

coated silicon or metal fiber, metal bar (Arrow), tube, and thin film, were developed to meet the diverse requirements in various applications [19, 22]. Among them, fiber formatted SPME is the most successful product in the commercial market. Recently, the coupling of SPME techniques with portable analytical instruments, for example, portable gas chromatography (GC) and/or mass spectrometry (MS), for on-site analysis are becoming popular [23-29]. SPME Arrow and thin film SPME have been coupled with portable GC-MS for analyzing of volatile organic compounds (VOCs) in boreal forest and detection of persistent organic contaminants in the water sources, etc. [23, 24, 26, 27, 29].

The first and most relevant limitation of PS techniques is the difficulty in quantitation due to their temperature and/or analyte concentration dependent nature. The environmental conditions, not only temperature but also pressure, humidity, and concentration of analytes, are varying all the time. Alternatives to diffusive passive samplers, e.g. fiber-retracted SPME device, were developed to decrease their dependence on above-mentioned conditions but they are still negligible [21]. Competitive sorption between different chemical substances in passive samplers can also cause questionable quantitative results [16]. Low time-resolution and as a consequent provides impractical results for the researchers who need more data points in a period for real-time monitoring of the variation of a certain chemical compound. Terminating the sampling before equilibrium, improve the sorbent volume and collection performance are solutions to address these challenges [15].

2.1.2. Active sampling

Active sampling (AS) uses an extra pressure or vacuum as the driving force to actively push or pull samples through a collection device which can be a filter or an adsorbent/absorbent packed tube, etc. (Figure 2) [9, 16, 30-34]. It is an exhaustive technique and concentrations of the analytes can be calculated easily and straightforwardly by dividing the quantified masses of the analytes by the total sample volume/mass. Nowadays, most of the active samplers are utilized for air sampling due to the simple matrix, low viscosity, and easy to achieve a high flow rate of air compared to that achieved with liquid or solid samples. For air sampling, up to 13000-m^3 air can be collected in a few days [33]. AS [30, 34] is also available for water but still not as common as for air and it is challenging for solid sampling because of the inhomogeneous distribution of the analytes in the solid samples.

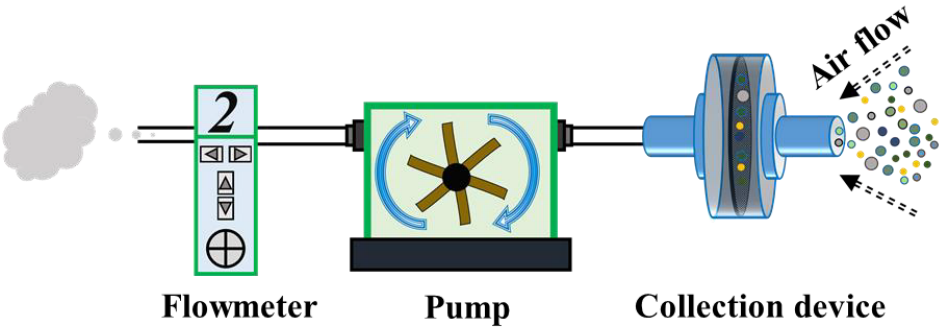

Figure 2. Scheme of active air sampling.

AS enables accurate and reliable quantitation, which is more independent of the environmental conditions such as wind speed, temperature, and pressure. AS is relatively costlier compared to PS, but it offers shorter sampling time, higher sampling efficiency, and lower detection limit. In practical, the artifact of the collection device and sorbent, the type of sampling device and sorbent, the

degradation of analytes and sorbent, and breakthrough all influence the sampling efficiency and consequent quantitation [16]. Therefore, a specialized sampling configuration should be used for a certain application. To avoid the loss of the analytes (breakthrough), the type or geometry of the sampling device, sampling flow rate and time should be evaluated before starting the sampling.

2.2. Sample preparation

Solvent-based liquid-liquid extraction (LLE) (since ca. 1870) and sorbent-based SPE (first cartridges at 1978) are two types of well-known and commonly accepted sample preparation techniques [35, 36]. LLE isolates the analytes from the sample matrix by one-step equilibrium based on the distribution constant (K_{es}) of the analyte between the organic solvent and the liquid sample [36]. Its biggest drawback is the use of a large volume of organic solvent. SPE isolates analytes based on a simple chromatographic process [35]. Compared to LLE, SPE consumes less organic solvent. However, the enrichment factor of LLE and SPE is limited by partial injection of elutes.

In the past 30 years, numerous miniaturized sample preparation techniques have been invented to displace the LLE and SPE by taking advantages of miniaturized sample preparation devices, namely high speed, simultaneous sample concentration, automation and possibility for direct injection of all analytes into the analytical instrument with reduced amount or even without organic solvent [9, 10, 22, 37]. The other purposes include saving time and labor in the laboratory and during on-site working. Among these techniques, SPME in the coated fiber format (fiber SPME) is the first and most successful miniaturized sample preparation technique, which was invented by Pawliszyn in the early 1990s [38]. Afterward, the International Unit of Pure and Applied Chemistry (IUPAC) defined the microextraction techniques as those using a substantially smaller extraction phase than the sample volume [39]. Typically, the amount of extraction phase is <100 µL or <10 mg and the sample volume >1 mL [39]. Some other formats of SPME were introduced in the past two decades, for example, SPME Arrow [26, 40-44]. Beside the non-exhaustive SPME, exhaustive needle trap microextraction (NTME) [9, 31] and in-tube extraction (ITEX) have also been invented and well-employed [45-58].

2.2.1. Non-exhaustive microextraction techniques

SPME

In the original fiber SPME, the fused silica or metal fiber is coated with less than 1 µL of polymer and/or solid sorbent [11]. SPME fiber partially extracts analytes by direct exposure to the sample matrix (direct immersion (DI mode)) or via sample headspace (HS mode). These extraction processes are based on the partition equilibrium between the SPME coating and the sample matrix or headspace (Figure 3). DI mode is specifically used for extraction of less or non-volatile chemicals from a liquid or solid sample. While HS mode is especially suitable to eliminate the effect of high-molecular-weight interferences by extracting semi-volatile and volatile compounds from the sample headspace. In an SPME extraction process, only a small portion of the analytes are adsorbed/absorbed to the extraction phase and subsequently, they can be completely desorbed into the GC or LC for analysis. The characteristics of comprehensive injection of analytes by SPME device enable its comparable sensitivity to SPE. SPME technique dramatically reduces the time and labor compared to other multi-step sample preparation techniques by integrating sampling, extraction, pre-concentration, and sample injection into a two-step process. Furthermore, the SPME technique only needs few milliliters or no organic solvent by using solvent desorption or thermal desorption, respectively. Thus, SPME has been complimented as a great achievement in analytical science and widely accepted by international organizations and laboratories.

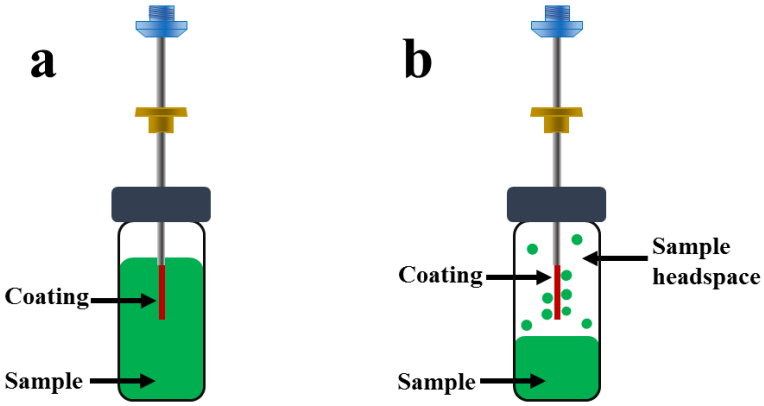

Figure 3. SPME extraction modes: (a) direct immersion (DI) and (b) headspace (HS).

Powerful SPME technique is applicable for environmental, food, fragrance, drug, in *vivo,* and in *vitro* analysis [11]. To develop a proper SPME method for a specific application, it is essential to understand the SPME theory to minimize the number of experiments that need to be conducted [11].

SPME theory

In a DI SPME process, SPME fiber is directly exposed to the sample for a predetermined amount of time. The equilibrium is reached between two phases, the fiber coating, and the sample matrix. The equilibrium conditions can be described by equation (3):

$$C_0 V_s = C_S^{\infty} V_s + C_f^{\infty} V_f \tag{3}$$

where C_0 is the original concentration of analytes in the sample, C_S^{∞} and C_f^{∞} are the equilibrium concentrations of analytes in the sample and the fiber coating, respectively. The V_s and V_f are the volumes of sample and the fiber coating, respectively.

Distribution of the analytes between the fiber coating and the sample matrix at equilibrium is a constant and can be expressed as K_{fs}:

$$K_{fs} = \frac{C_f^{\infty}}{C_S^{\infty}} \tag{4}$$

Therefore, equations (3) and (4) can be rearranged into equation (5):

$$C_f^{\infty} = C_0 \frac{K_{fs} V_s}{K_{fs} V_f + V_s} \tag{5}$$

The mass of analytes (n) that is extracted by the fiber coating can be calculated from equation (6):

$$n = C_f^{\infty} V_f = C_0 \frac{K_{fs} V_s V_f}{K_{fs} V_f + V_s} \tag{6}$$

When the sample volume $V_s \gg K_{fs} V_f$, equation (6) can be simplified to equation (7),

$$n = C_f^{\infty} V_f = C_0 K_{fs} V_f \quad (7)$$

Equation (7) exactly shows the linear relation between the analyte amount extracted by the fiber coating and analyte concentration in the sample matrix, which indicates the quantitative property of the SPME technique. On the other hand, the affinity of the coating material to the analytes, and the coating volume determines the sensitivity of the SPME. Therefore, researchers take a great effort to design and construct new materials with higher affinity to analytes and/or develop new SPME devices with a larger volume of coating [10, 22, 59].

In headspace SPME, there are three phases: sample, fiber coating, and sample headspace. The overall equilibrium of the analytes is achieved in this three-phase system. Equation (8) describes the equilibrium situation:

$$C_0 V_s = C_S^{\infty} V_s + C_h^{\infty} V_h + C_f^{\infty} V_f \quad (8)$$

where C_h^{∞} and V_h are the equilibrium concentration of analytes in the headspace and the headspace volume, respectively.

The sample-to-headspace and headspace-to-fiber distributions are subsequently defined as $K_{hs} = C_h^{\infty}/C_S^{\infty}$ and $K_{fh} = C_f^{\infty}/C_h^{\infty}$, respectively. Equation (8), therefore, can be rearranged to be equation (9):

$$n = C_f^{\infty} V_f = C_0 \frac{K_{fh} K_{hs} V_s V_f}{K_{fh} K_{hs} V_f + K_{hs} V_h + V_s} \quad (9)$$

If we assume that the $K_{fs} = K_{fh} K_{hs}$, equation (9) can be simplified to equation (10),

$$n = C_0 \frac{K_{fs} V_s V_f}{K_{fs} V_f + K_{hs} V_h + V_s} \quad (10)$$

Notably, equations (6), (7) and (10) only apply for liquid polymer coated SPME fiber, which extract analytes via absorption [11]. For solid sorbent-coated SPME fiber, the surface binding active sites should be taken into consideration in the adsorption process [60]. The equilibrium amount of analyte on the solid sorbent-coated SPME fiber can be estimated by equation (11):

$$n = C_0 \frac{K V_s V_f \left(C_{f\,max} - C_f^{\infty}\right)}{V_s + K V_f \left(C_{f\,max} - C_{fA}^{\infty}\right)} \quad (11)$$

where K is the adsorption equilibrium constant (affinity constant) of the analyte and $C_{f\,max}$ is the maximum concentration of active sites on the coating. In practice, normally more than one analyte with an affinity for the extraction phase exist in a sample. Thus, the existence of another compound (B) will affect the amount of analyte (A) extracted by the fiber due to the competitive nature of the adsorption process. The analyte A extracted on the fiber in the presence of a competing compound B is given by equation (12):

$$n = C_0 \frac{K_A V_s V_f \left(C_{f\,max} - C_{fA}^{\infty}\right)}{\left(1 + K_B C_{fB}^{\infty}\right) V_s + K_A V_f \left(C_{f\,max} - C_{fA}^{\infty}\right)} \quad (12)$$

where K_A and $K_B$are the adsorption equilibrium constants for analyte A and competing compound B, respectively. C_{fA}^{∞} and C_{fB}^{∞} are the equilibrium concentration of analyte A and competing compound B in the coating, respectively.

From above equations, the quantitation of analytes in the sample by SPME is very strict to the distribution of analytes between the fiber coating and the sample/sample headspace, which is affected by temperature, agitation, ionic strength, pH and matrix polarity of the sample. Therefore, careful calibration and optimization are needed to develop a robust quantitative SPME method.

Further, to address other issues during SPME implementation, other concepts have also been developed such as SPME Arrow, thin film SPME, in-tube SPME and 96-blade configured SPME [22].

SPME Arrow

SPME Arrow (introduced in 2015 by CTC Analytics AG, Switzerland) is an excellent alternative to SPME fiber that is based on a completely redesigned SPME device. This aims to combine the advantages of the conventional SPME fiber and the stir bar sorptive extraction, while still eliminating the disadvantages in these two techniques (Figure 4) [26, 40-44, 58, 61]. In the SPME Arrow device, a stainless-steel rod is used to replace the traditional fused silica or metal fiber. Further, the Arrow tip design at the end of the rod enables the complete closure of the SPME Arrow device when withdrawn the sorbent-coated rod into the outer stainless-steel sheath and allow the SPME Arrow gently penetrates through the injector and sample vial septa. This closed SPME system can avoid the physical damage and contamination of the coating during the transfer process [10]. The design of Arrow tip and stainless-steel rod is very different to the conventional SPME fiber, which only allows for the retraction of the extraction phase and thereby having a larger potential risk by the contaminants from ambient air to enter inside the outer capillary and the fiber. On the other hand, the coating volume of SPME Arrow, 3.8-11.8 µL [10], is much larger than 0.028-0.612 µL of SPME fiber [11], which improves the SPME capacity and extraction efficiency when using the same coating material (Equation (7)). Further improvement in SPME Arrow extraction efficiency (and sensitivity of the whole analysis) can be obtained with higher affinity coating materials.

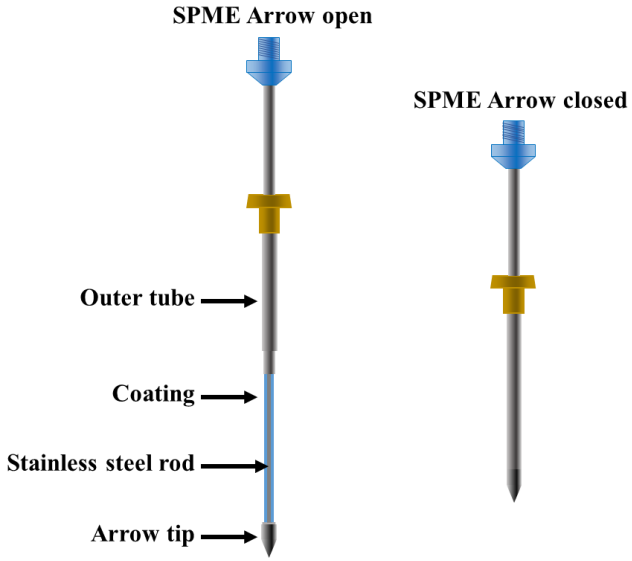

Figure 4. SPME Arrow.

Nowadays, PAL RTC and RSI autosamplers are compatible with SPME Arrow devices by using CTC Composer software for static extraction. In our group, commercial PDMS, PDMS/DVB, Carbon WR/PDMS, PDMS/Carboxen 1000 SPME Arrows has been used for amines, monoterpenes, and aldehydes analysis in the laboratory and boreal forest [26, 42].

2.2.2. Exhaustive microextraction techniques

Needle trap microextraction

Needle trap microextraction (NTME) (since 2001) was derived from other needle-based extraction methods, e.g. solid phase dynamic extraction, by using a sorbent bed packed needle device (19-22 gauge) instead of coating on the inner wall of the needle, to achieve exhaustive extraction (Figure 5) [62, 63]. The sample flow (gas or liquid) continuously passing through the sorbent bed by an extra pump or gas-tight syringe. The trapped analytes have subsequently been desorbed in the injection port of an analytical instrument. The whole process is simple and fast. In addition, it also has great potential for automation even though it has not been commercialized. Because of the exhaustive nature of the NTME device, additional care must be taken from the user to ensure that no breakthrough occurs during extraction. NTME quantitation is simply performed by determining the exhaustively extracted analytes in reference to the pre-determined instrument detector response calibration [9, 31].

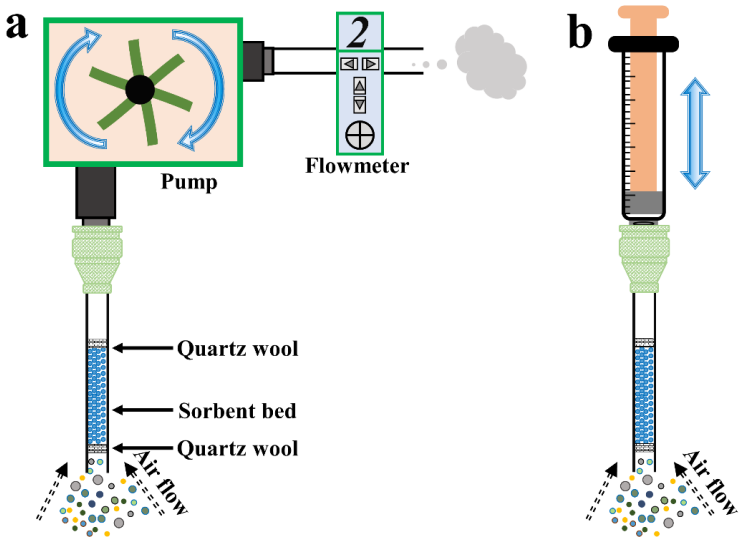

Figure 5. Needle trap device processed with (a) a pump and (b) a syringe.

The NTME process can be interpreted as frontal chromatography since the continually applied sample flow to the sorbent bed. The breakthrough occurs when the sorbent bed is saturated by the analytes [9, 64-66]. Lovkvist et al. made a model to appropriately interpret the theory of NTME process based on the frontal chromatography assumption [64]. The volumetric flow rate for the sample can be calculated by equation (13)

$$Q = \left(\frac{k_p A}{\mu}\right)\left(\frac{\Delta p}{L}\right) \quad (13)$$

where Q is the flow rate of the sample in the needle, k_p is the permeability of the sorbent bed, A is the cross-sectional area of the needle, μ is the viscosity of the sample, Δp is the pressure drop of the sample through the needle and L is the length of the packed sorbent bed.

On the other hand, the breakthrough time (t_b) can be calculated by equation (14) by defining the breakthrough level as 5% of analyte mass exiting the end of the sorbent bed.

$$t_b = \frac{L(1+k)}{v}\left[0.903 + \frac{5.360}{N} + \frac{4.603}{N^2}\right]^{-1/2} \quad (14)$$

where v is the linear flow rate of the gas sample through the sorbent bed, N is the theoretical plate number of the sorbent bed, k is the retention factor. Thus, breakthrough volume (V_b) can be obtained by equation (15).

$$V_b = A\emptyset L(1+k)\left[0.903 + \frac{5.360}{N} + \frac{4.603}{N^2}\right]^{-1/2} \quad (15)$$

where V_b is the breakthrough volume, $\emptyset$ is the porosity of the sorbent bed. k was defined as:

$$k = K_{es}\frac{V_S}{V_v} \quad (16)$$

where K_{es} is the distribution constant between the sorbent phase and sample, V_S is the volume of the sorbent phase and V_v is the void volume of the sorbent bed.

The above three equations give clear guidance to construct the NTME device for exhaustive extraction. To obtain a high-volume flow rate, large breakthrough volume and consequent sensitive NTME method, the needle geometry, the physical and chemical properties of the sorbent material and sample type should be kept in consideration. A larger diameter of a needle with a longer sorbent bed can be used to increase the capacity.

NTME has been utilized for on-site measurement of airborne VOCs in the air [31, 63, 67-69], but it is still tricky for the quantitation of trace level environmental VOCs at pg L^{-1} level due to the small amount of sorbent packed in the needle which essentially restricts the flow rate and total sampling volume. In the literature reported, only 1.9 mL min^{-1} flow rate can be used to avoid the breakthrough [31]. The thermal desorption (TD) is high relying on the inlet temperature of an analytical instrument, thus, an independent TD unit can efficiently improve its applicability.

In-tube extraction (ITEX)

ITEX is another exhaustive sample preparation technique that was commercialized by CTC Analytics AG in 2006 [54]. In the first generation of ITEX, the ITEX device could only be mounted on a special head of the modified autosampler. To standardize the ITEX technique, an upgraded ITEX system, which named as ITEX 2, was therefore introduced in 2009 and match with any PAL-type autosampler without modification [49].

Compared to the conventional NTME device, ITEX is fully automated and employed a stainless-steel needle that is divided into two sections (Figure 6). The lower part is an ordinary needle cannula with a hole on the side for septum penetration in both the GC inlet or sample vial and the upper part is a

tube with a larger diameter to pack the sorbent material. The ITEX tube is connected to a glass syringe that has a 1.3 mL volume size. For headspace dynamic extraction, the syringe plunger is moved up and down (defined as one stroke) to let the sample pass through the packing material. Higher extraction yield can be achieved with higher stroke number and adjustable extraction flow rate. In addition, the upper part of the ITEX needle is surrounded by a heater to avoid sample condensation in the syringe and to facilitate thermal desorption to the inlet system of the analytical instrument (only GC is available now), respectively. Before desorption, a fixed volume of helium is aspirated into the syringe as desorption volume from the GC inlet. Then the heater is heated up rapidly to the desorption temperature and the desorbed analytes are injected with a fixed desorption flow rate into the injection port of the GC system. The external thermal desorption outside the GC injector enables the independent desorption temperature to the injector temperature. After desorption, the syringe plunger is lifted over the side hole of the syringe, and nitrogen flow is introduced to flush the packing material at elevated temperature, which is also controlled by the extra heater.

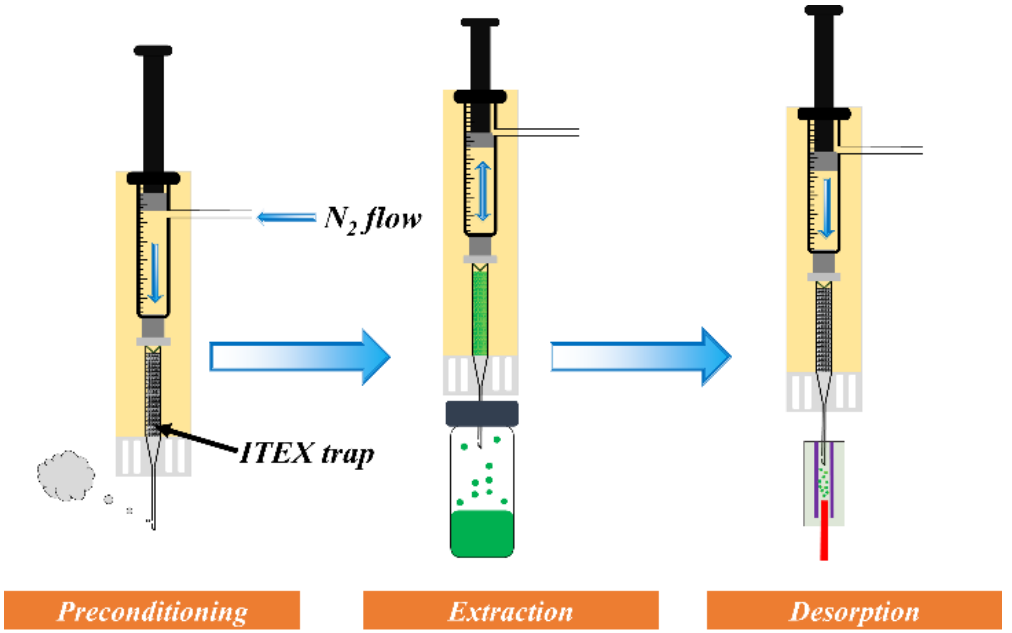

Figure 6. ITEX stages in headspace dynamic extraction mode.

ITEX has been utilized for analyzing VOCs but only limited to dynamic headspace extraction mode [45-57]. It has the potential for dynamic extraction like other needle trap-based extraction methods due to its larger sorbent volume and automation. The theory in NTME section is also fitting for the ITEX technique, therefore the sorbent material affinity to the target analytes and permeability of the packing are essential in ITEX.

2.2.3. Comparison of solid phase microextraction and needle trap-based techniques

The nonexhaustive SPME is applicable to a wider range of sample types than NT-based techniques [10]. While exhaustive techniques are much better in sensitivity, at least one magnitude better than non-exhaustive ones. Further, NT-based techniques are more time-efficient. SPME and ITEX are applicable either manually or automatically. Automation is the trend in analytical chemistry, but

manual extraction is still needed especially for the remote or poor region. Because of the exhaustive nature, NT-based techniques are less selective than nonexhaustive SPME.

In summary, the above-mentioned techniques are all available to combine sampling and sample preparation into a single step to skip the tedious sample preparation procedure. By using a miniaturized sampling device, collected analytes can be introduced into an analytical instrument directly. In this aspect, such microextraction techniques break the boundary of the sampling and sample preparation concepts. In addition, little or no organic solvents are needed in their applications that make them meet the requirement of the concept of 'Green Analytical Chemistry'.

2.3. Trends in the development of analytical process

Analytical chemistry has gained great achievements in the past three decades, but its development will never stop, and it is continued to achieve faster operation, higher method sensitivity, better selectivity, automation, intelligentization, and so on.

2.3.1. New materials

The advances taken in material science have been utilized in analytical chemistry especially as new sampling [70] and sample preparation [59, 71, 72] materials. As shown in equations (7) and (15), selecting an appropriate material for sampling and sample preparation devices can ensure favorable distribution constants between the material and analytes. Consequently, a satisfactory method sensitivity can be achieved. However, depending on the application purposes, from selective extraction of target compounds from a complex matrix to universal screening of organic pollutants in atmospheric air and wastewater, specific and non-specific materials should be employed, respectively. Owing to the limited material options in the commercial market, researchers attempt to design and construct alternative materials with special advantages beyond only selectivity, e.g. sorption capacity, physical and chemical stability.

2.3.1.1. Non-specific materials

Nanofibers

Nanofibers are widely used in many areas of analytical chemistry because of their features of 1) nanometer scale size which results in large surface area to volume ratio and consequently leads to high adsorption capacity, 2) good chemical and mechanical stability, 3) alterable surface group by functionalization, 4) superior suitability for online extraction/separation systems over nanoparticle materials which can cause leakage and blockage in the tubes or valves, 5) easy to pack into tubes in the format of mats and cotton-like bundles, and 6) appropriate permeability which results in low backpressure [73-76].

The most often used technique to produce nanofibers is electrospinning, in which a high voltage draw a viscous polymeric solution into long continuous nanofibers and then these are solidified in the air before reaching the collector (Figure 7) [77]. A wide selection of different polymers has been directly electrospun into nanofibers while inorganic nanofibers have been prepared by calcination of electrospun nanofibers with additional precursors embedded into the polymer matrix [76, 77]. In recent years, solution blow spinning and electroblowing have emerged as higher production rate alternatives to electrospinning [78-83]. Both methods rely on a high-velocity gas flow to draw the solution into nanofibers that enables significantly enhanced production rates compared to conventional needle-based electrospinning.

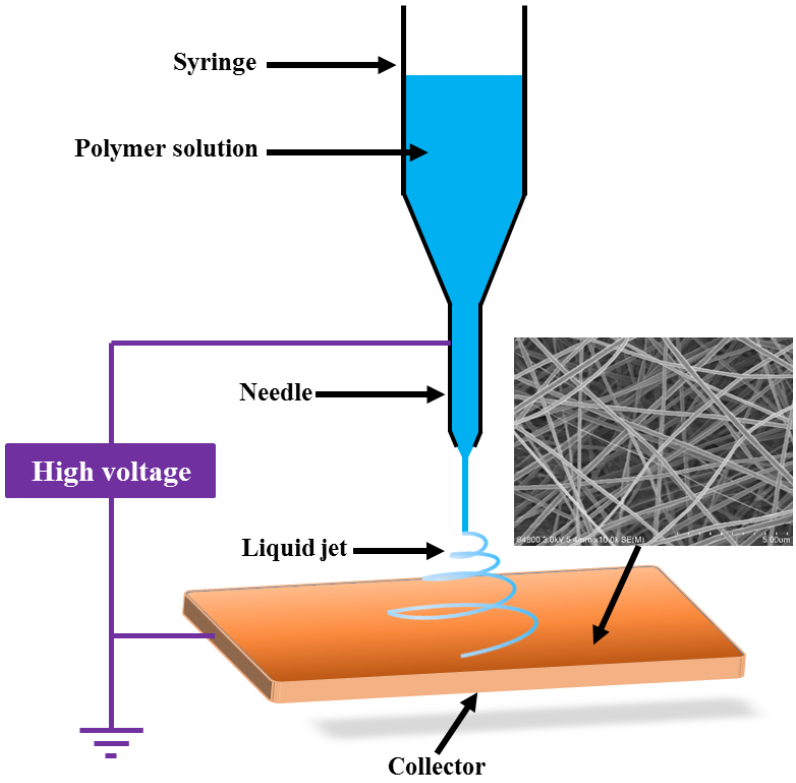

Figure 7. Schematic illustration of the electrospinning process.

On the other hand, bio-, synthetic, functionalized, co- and blended polymers together with composite materials have also been applied for preparation of nanofibers by electrospinning technique using direct or indirect fabrication approaches on a substrate [76].

2.3.1.2. Specific materials

The specific materials can extract a certain analyte or a group of analytes with exceptional selectivity over other interfering compounds in the sample. The exceptional selectivity contributes to improving the number of analytes extracted, the signal-to-noise ratio of the analysis and identification process with decreased size of the error. Size exclusion and chemical group bonding are the two main driving forces to provide the selectivity. The former is achieved by the porous structure and the latter is by the surface functional groups.

Metal organic framework

Metal organic framework (MOF) is a type of multidimensional material, which is formed by linking a metal cluster or metal ion with organic ligands [84]. MOFs features include versatile pore sizes and huge specific surface areas due to their tunable compositions [85]. Since it was introduced in 1995 by Yaghi [86], tremendous research progress has been made to synthesize new MOFs to provide tolerable porosity, hydrophobicity, hydrophilicity, water stability, and/or thermal stability to meet the diverse requirements of real applications [86-95].

The conventional way to synthesize MOFs is by the hydrothermal synthesis approach, in which a mixture containing the metal cluster/ion precursor and organic linker was sealed in a Teflon-lined autoclave and heated using a temperature gradient or constant temperature for a period. The obtained MOFs are generally particles with crystalline structure [96, 97].

The applicability of MOFs is widened using other synthesis methods, e.g. atomic layer deposition (ALD) and molecular layer deposition (MLD), which can automatically assemble a MOFs film layer-by-layer (Figure 8) [98-102]. ALD is a thin film deposition technique based on alternate pulses of gaseous precursors separated by inert purge gas [103]. The precursors react only on the surface, which leads to a self-limiting growth mechanism. ALD enables accurate control over film thickness, superior conformality even on complicated 3D structures, and large area uniformity.

MLD is a closely related method to ALD. In MLD, layers of whole molecules are deposited during one self-limiting reaction step. MOF thin film is either directly deposited by ALD and MLD or indirectly by using post-deposition treatments [98-102]. In 2013, Leo et al. reported to deposit metal-organic ligand film by ALD and then converted it into a MOF film with an additional solvent conversion step [100]. ZIF-8, ZIF-61, ZIF-67, and ZIF-72 films have been produced by ALD deposition of different metal oxide (ZnO) films and their conversion with a relevant organic linker vapor [102]. Lausund et al. reported that MLD deposited Zr-BDC composite can be converted into UIO-66 in acetic acid vapor [99].

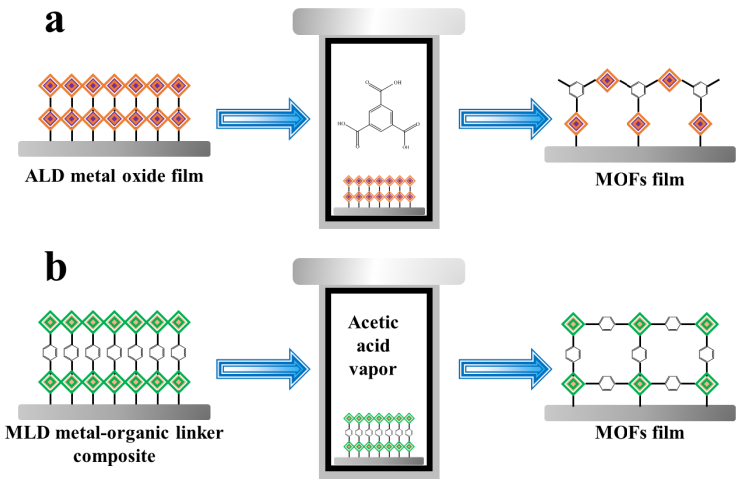

Figure 8. MOFs films synthesized by (a) ALD-conversion and (b) MLD-conversion methods.

Ordered mesoporous silica

Ordered mesoporous silica (OMS) materials are good alternatives to classical sorbents, such as porous carbon-based materials, due to their well-defined pore-size distribution, pore structure, and modifiable surface characteristics (Figure 9) [104-108]. Regardless of the traditional and most well-known utilization of OMSs in liquid chromatographic (LC) columns [109], the implementation of OMSs in extraction science is gaining increasing research interests. For the isolation of analytes from different matrices, functionalization is needed to adjust the surface properties of OMSs to weaken or enhance their natural hydrophilicity and acidity due to the silanol groups [110-112]. Currently, great efforts have been made on the development and investigation of OMS materials with certain pore size and

surface group to provide their specific selectivity to the target compounds [111]. Despite the excellent pore and surface properties, their physical and mechanical stabilities are also comparable or superior to other well-known materials, e.g. MOFs and porous carbon-based materials.

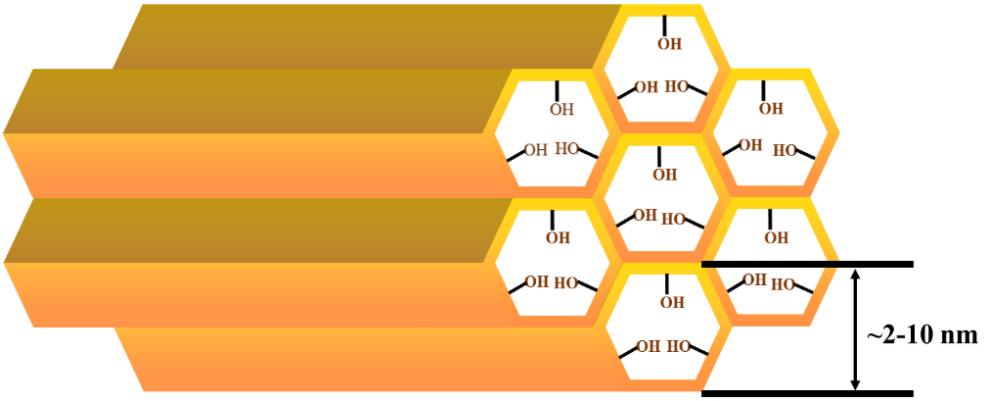

Figure 9. Ordered mesoporous silica with two-dimensional hexagonal pore structure.

2.3.2. Automation

Automation is needed in analytical chemistry to save the labor for repetitious operations, obtain exceptional repeatability, and improve the sample throughput in analytical procedures [113, 114]. The ideal automated analytical system can complete all analytical procedures (sampling, sample preparation, analysis, and data handling) without human intervention [11]. However, this is difficult to achieve in practice due to the large differences in sample type, sampling conditions and properties of analytes, for example.

The major breakthroughs in the development of such kind of a system have generally been started from an individual procedure, such as only sampling, sample preparation, analysis or by combining several steps into one [9, 113-116]. Air is the simplest matrix, compared to liquid and solid, and easiest to achieve automation for its sampling [117, 118]. In the sample preparation procedure, automation for SPME-based techniques is a mature approach, which is achieved by commercial autosamplers that enable to handle the preconditioning, extraction, enrichment, desorption and injection steps with all sample types [11, 119, 120]. In addition, ITEX technique has also been fully automated [10, 45-57].

2.3.3. New platform

Aerial drone, which is also named as unmanned aerial vehicles, remotely piloted aircraft system or simply drone, have grown very popular over the last decade [121]. Their use has expanded from the military use to scientific applications [122]. To date, the aerial drone has been used as the carrier for air sampling devices, sensors, and MS to replace or complement the traditional ways to sampling air or continuous monitoring of VOCs at high altitudes or difficult access places [121-131]. In addition, the use of electrically powered engines in aerial drone limits the potential contamination sources [125]. These merits enable the potential applicability of an aerial drone as a carrier for miniaturized air sampling systems such as SPME Arrow and ITEX (Figure 10).

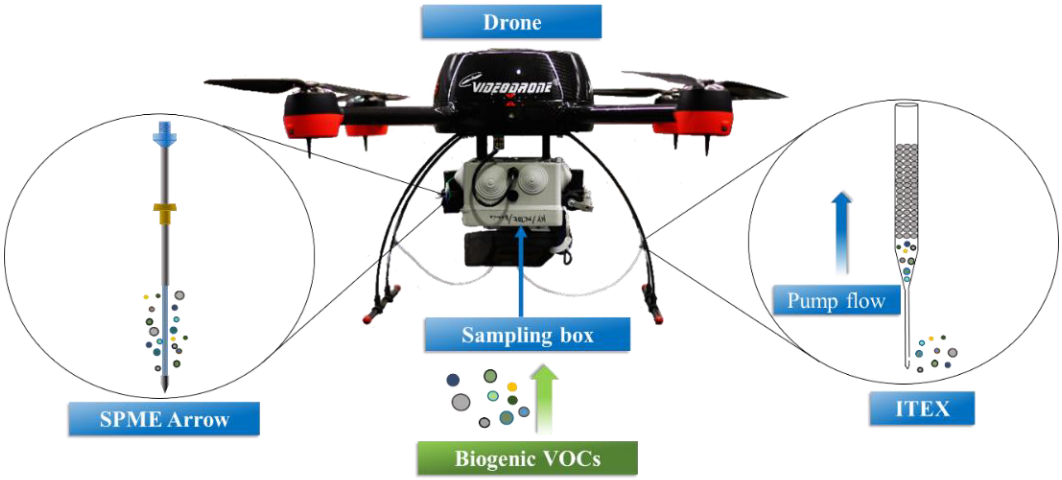

Figure 10. GeoDrone X4L drone furnished with a box for SPME Arrow and ITEX sampling.

2.3.4. Applications

The applications of the analytical process include environmental, food and biogenic analysis. In environmental analysis, the focus is usually on the determination of organic pollutants [120, 132, 133], and monitoring of VOCs in air, especially those of small and polar compounds [23, 24, 26, 42, 69, 120, 134-138]. In food analysis, determination of food quality related VOCs is the main aspect [139, 140]. In the biogenic analysis, the accurate measurement of biomarkers aids the early-stage disease diagnosis [141-144].

3 Experimental

This section describes the chemicals (Table 1), instruments and equipment (Table 2), and methods and experimental conditions used in this thesis. Detailed information is available in ***Papers I-V***.

Table 1. List of chemicals used in the study.

Compound	Supplier	Purity	Paper
1,2,3-Trimethylbenzene	Sigma-Aldrich (St. Louis, USA)	90%	***IV***
1,2,4-Trichlorobenzene	Fluka (The Netherlands)	≥99.0%	***I***
1-Naphthylamine	Fluka (The Netherlands)	≥99.0%	***I***
2-Ethyl-1-hexanol	Sigma-Aldrich (St. Louis, USA)	≥99.6%	***IV***
2-Methylimidazole	Sigma-Aldrich (St. Louis, USA)	99.9%	***IV***
2-Pentylfuran	Alfa Aesar (Karlsruhe, Germany)	98%	***III-IV***
4-Methyl-1-hexene	Tokyo Chemical Industry Ltd (Tokyo, Japan)	>99%	***IV***
Acetaldehyde	Sigma-Aldrich (St. Louis, USA)	≥99.5%	***IV***
Acetic acid	Merck (Darmstadt, Germany)	100%	***I***
Acetone	Honeywell (Honeywell GmbH, Seelze, Germany)	≥99.8%	***III-IV***
Acetonitrile	Sigma-Aldrich (St. Louis, USA)	HPLC grade	***IV***
Acetophenone	The British Drug Houses Ltd (Poole, England)		***III-IV***
Allyl methyl sulfide	Alfa Aesar (Karlsruhe, Germany)	98%	***IV***
Alpha-pinene	Sigma-Aldrich (St. Louis, USA)	98%	***I, IV***
Aniline	Aldrich-Chemie (Steinheim, West-Germany)		***I, III***
Atrazine	Sigma-Aldrich (St. Louis, USA)		***I***
Benzaldehyde	Fluka (The Netherlands)	≥99%	***IV***
Benzyl acetate	Fluka (The Netherlands)	≥99.9%	***III***
Benzyl alcohol	Fluka (The Netherlands)	99.5%	***III***
Carbon disulfide	Sigma-Aldrich (St. Louis, USA)	≥99%	***IV***
Decafluorobiphenyl	Fisher Scientific (Loughborough, Leics, UK)	99.99%	***IV-V***
Decanal	Sigma-Aldrich (St. Louis, USA)	≥98%	***IV***
Delta-3-carene	Sigma-Aldrich (St. Louis, USA)	90%	***IV***
Diethylamine	Fluka (The Netherlands)	≥99.7%	***III***
Dimethyl sulfide	Sigma-Aldrich (St. Louis, USA)	≥99%	***IV***
Dimethylformamide	Sigma-Aldrich (St. Louis, USA)	99.9%	***III-IV***
Ethanol	VWR Chemicals (Pennsylvania, USA)	100%	***III-IV***
Ethylamine	Fluka (The Netherlands)	70% in water	***III***
Ethylbenzene	Sigma-Aldrich (St. Louis, USA)	99%	***IV***
Helium	AGA (Espoo, Finland)	99.996%	***I-V***
Heptanal	Fluka (The Netherlands)	>95%	***IV***

Table 1. List of chemicals used in the study. (Continued)

Hexachlorobenzene	Sigma-Aldrich (St. Louis, USA)	99%	***I***
Hexachlorobutadiene	Merck (Darmstadt, Germany)	96%	***I***
Hexanal	Sigma-Aldrich (St. Louis, USA)	98%	***IV***
Hexylcyclohexane	Tokyo Chemical Industry Ltd (Tokyo, Japan)	>98%	***IV***
Hydrochloric acid	Oy FF-Chemicals Ab (Haukipudas, Finland)	0.1 and 1 M	***II***
Isoprene	Sigma-Aldrich (St. Louis, USA)	99%	***IV***
Longifolene	Fluka (The Netherlands)	≥99%	***IV***
Methanol	Fisher Scientific (Loughborough, Leics, UK)	HPLC grade	***I-II, IV-V***
Methyl isobutyl ketone	Sigma-Aldrich (St. Louis, USA)	98.5%	***IV***
Methyl propyl sulfide	Alfa Aesar (Karlsruhe, Germany)	99%	***IV***
Nonanal	Sigma-Aldrich (St. Louis, USA)	≥95%	***IV***
Octanal	Sigma-Aldrich (St. Louis, USA)	99%	***IV***
p-Cymene	Sigma-Aldrich (St. Louis, USA)	99%	***IV***

Table 1. List of chemicals used in the study. (Continued)

Phenolic mixture in dichloromethane (20 mg mL^{-1})	AccuStandard, Inc. (New Haven, CT)		***I***
Poly(vinyl chloride)	Sigma-Aldrich (St. Louis, USA)		***II***
Polyacrylonitrile (Mw=150 000)	Sigma-Aldrich (St. Louis, USA)		***III-V***
Potassium hydroxide	VWR Chemicals (Pennsylvania, USA)		***I-II***
p-Xylene	Sigma-Aldrich (St. Louis, USA)	99%	***IV***
Sodium chloride	Fisher Scientific (Loughborough, Leics, UK)		***I-II***
Terephthalic acid	Fluka (The Netherlands)	≥99.0%	***I***
Tetrahydrofuran	Sigma-Aldrich (St. Louis, USA)	≥99.9%	***II-IV***
Toluene	VWR Chemicals (Pennsylvania, USA)	HPLC grade	***III-IV***
Triethylamine	Sigma-Aldrich (St. Louis, USA)	99%	***III***
Triethylamine hydrochloride	Sigma-Aldrich (St. Louis, USA)	≥99.0%	***II***
Trimesic acid	Sigma-Aldrich (St. Louis, USA)	95%	***I***
Trimethylamine hydrochloride	Sigma-Aldrich (St. Louis, USA)	98%	***I-II***
Ultrapure water	Millipore DirectQ-UV, Billerica, MA, USA		***I-IV, V***
Zeolitic imidazolate framework-8	Sigma-Aldrich (St. Louis, USA)		***II***

Table 2. List of instruments and equipment.

Instrument/Equipment	Model and manufacture	Paper
Autosampler	PAL RTC, CTC Analytics AG, Zwingen, Switzerland	***I-IV***
Acrodisc syringe filter	1 mm pore size, Gelman Laboratory, MI	***I***
Aerial Drone	Geodrone X4L, VideoDrone Finland Oy, Muurame, Finland	***V***
ALD reactor	F-120, ASM Microchemistry Ltd., Helsinki, Finland	***I***
Bare ITEX	BGB Analytik AG, Zürich, Switzerland	***IV***
Bare SPME Arrow	BGB Analytik AG, Zürich, Switzerland	***I-III, V***
Blender	Bosch, Gerlingen, Germany	***II-III***
Denuder sampler	URG, Chapel Hill, USA	***III***
Electronic shaker	IKA VIBRAX-VXR, Breslau, Germany	***II***
Gas chromatograph	6890 N, Agilent Technologies, Palo Alto, USA	***I-V***
GC capillary column	HP-5 (30m length, 0.25mm id, with 0.25 mm film), Agilent Technologies, Palo, USA	***I***
GC capillary column	InertCap™ (30 m length × 0.25 mm i.d.) GL Sciences, Tokyo, Japan	***II-V***
Headspace vial	20mL, Phenomenex, Torrance, California, USA	***I-V***
Homogenizer	IKA Ultra-Turrax	***II***
ITEX	Tenax TA/Carbosieve S-III, CTC Analytics AG, Zwingen, Switzerland	***IV***
ITEX	Tenax GR, CTC Analytics AG, Zwingen, Switzerland	***IV-V***
ITEX	Tenax TA, CTC Analytics AG, Zwingen, Switzerland	***IV-V***
ITEX	Carbosieve S-III, CTC Analytics AG, Zwingen, Switzerland	***IV***
ITEX	Carboxen-1000, CTC Analytics AG, Zwingen, Switzerland	***IV***
Mass spectrometer	5973C, Agilent Technologies, Palo Alto, USA	***I-II, V***
Mass spectrometer	5975C, Agilent Technologies, Palo Alto, USA	***I-IV***
Membrane filter	0.45 mm pore size, Millipore, Ireland	***I***
Microwave digestion system	CEM Mars 5, CEM Corporation, Matthews, NC, USA	***III***
Microwave plasma-atomic emission spectrometer	MP-AES 4200, Agilent Technologies, Palo Alto, USA	***III***
Minitab 18 statistical software	Minitab, State College, USA	***I***
Nylon filter	0.45 µm, Nalgene, Rochester, NY, USA	***V***
PTFE/silicone septum screw-cap	Phenomenex, Torrance, California, USA	***I-V***
Scanning electron microscope	S-4800, Hitachi, Japan	***I-IV***
SPME Arrow	Carbon WR (sorbent film thickness 120 µm, sorbent length 20 mm), CTC Analytics AG, Zwingen, Switzerland	***I, III, V***

Table 2. List of instruments and equipment. (Continued)

SPME Arrow	PDMS/Carboxen-1000 (sorbent film thickness 120 µm, sorbent length 20 mm), CTC Analytics AG, Zwingen, Switzerland	***II-III***
SPME Arrow	PDMS (sorbent film thickness 120 µm, sorbent length 20 mm), CTC Analytics AG, Zwingen, Switzerland	***III***
SPME Arrow	PDMS/DVB (sorbent film thickness 120 µm, sorbent length 20 mm), CTC Analytics AG, Zwingen, Switzerland	***III, V***
SPME fiber	PDMS, Supelco, Bellefonte, PA, USA	***I***
SPME fiber	PDMS/DVB, Supelco, Bellefonte, PA, USA	***I***
SPME fiber	PA, Supelco, Bellefonte, PA, USA	***I***
Surface Area and Porosity Analyzer	ASAP 2010, Micromeritics Co., Norcross, GA, USA	***II***
Surface Area and Porosity Analyzer	Auto Sorb-1, Quantachrome Instruments, Boynton Beach, Florida, USA	***III***
Teflon vessel	500 mL	***I***
Thermogravimetric analyzer	STARe system, Mettler Toledo, Switzerland	***I-IV***
Water purification system	Millipore DirectQ-UV, Billerica, MA, USA	***I-V***
X-ray diffractometer	X'Pert Pro-MPD, PANalytical, The Netherlands	***I***
X-ray diffractometer	X'Pert PW3710 MPD, PANalytical, The Netherlands	***III***
X-ray photoelectron spectroscope	PHI Quantum 2000, Physical Electronics, Inc., Chanhassen, MN, USA	***II***

3.1. Materials synthesis and fabrication for microextraction devices

3.1.1. Metal organic frameworks for solid phase microextraction Arrows

Atomic layer deposition (ALD)- and molecular layer deposition (MLD)-conversion methods were employed to directly synthesize and immobilize metal organic frameworks (MOFs) onto the high-aspect-ratio solid phase microextraction (SPME) Arrow (Figure 11). The former approach (ALD) was first used to deposit an Al_2O_3 or Fe_2O_3 film, which was further converted into the MOF coating in an H_2BDC or H_3BTC vapor. The latter approach (MLD) was utilized to deposit an amorphous film that contained the Zr-BDC. The amorphous-to-crystalline conversion was completed by the acetic acid vapor ***(Paper I)*** [99].

ZIF-8 was purchased from Sigma Aldrich and its particle size, surface area, and density were ~4.9 µm, 1300-1800 $m^2\ g^{-1}$ (Langmuir surface area), and 0.35 g cm^{-3}, respectively (Data provided by the manufacturer) ***(Paper II)***.

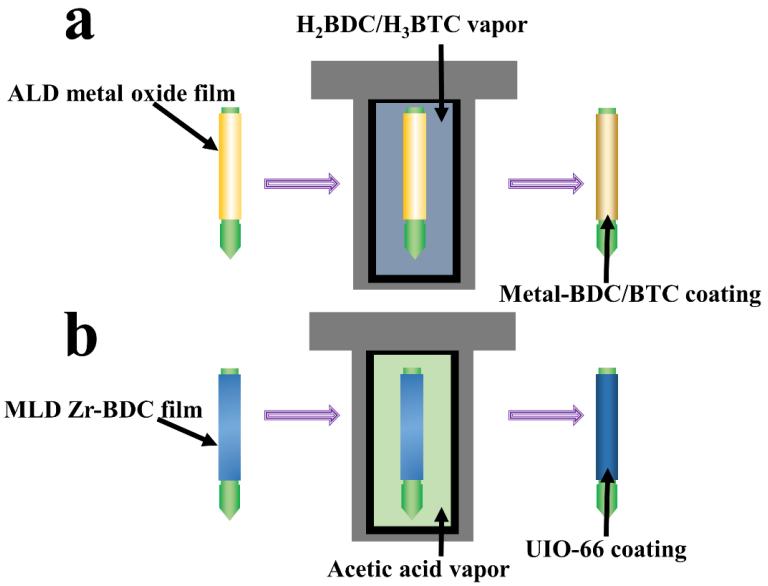

Figure 11. Scheme of the procedure to coat MOFs films onto SPME Arrow by (a) ALD- and (b) MLD-conversion methods.

3.1.2. Ordered mesoporous silicas for solid phase microextraction Arrows

Ordered mesoporous silica (OMS) materials, MCM-41, SBA-15, and KIT-6, were synthesized via hydrolytic sol-gel process [145-147]. A structure-directing agent was dissolved in a pH-adjusted aqueous solution and which then directed the polymerization and condensation of silica source. Once the synthesis process was completed, the structure-directing agent was removed from the silica particles by calcination.

The surface group and pore size were modified by a surface grafting approach (Figure 12) [148]. Titanium alkylphosphate was grafted on MCM-41, SBA-15 and KIT-6 in argon protected atmosphere by using titanium (IV) isopropoxide ($Ti(OPri)_4$) and phosphorus oxychloride ($POCl_3$) as the grafting

agents. The unreacted $Ti(OPri)_4$ and $POCl_3$ were eliminated by toluene. The alkoxy groups were hydrolyzed by water (***Papers III and V***).

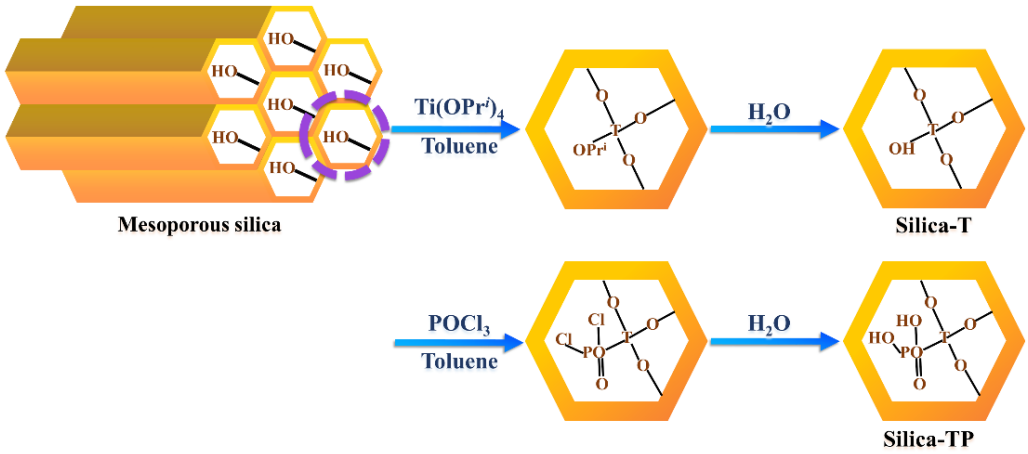

Figure 12. Scheme of the synthesis of functionalized OMS materials.

ZIF-8 and OMS particles were immobilized on bare SPME Arrows by using poly(vinyl) chloride (PVC) and PAN as the adhesive (Figure 13). The adhesive was first dissolved in the organic solvent (THF or DMF) and then mixed with the materials under shaking. This viscous material/adhesive suspension was therefore used to fabricate coatings by dipping the bare SPME Arrow in this suspension and then dried in an oven or under nitrogen flow (***Papers II and III***). The ZIF-8 particles have restricted pore size, which was further adjusted by hydrochloride acid vapor.

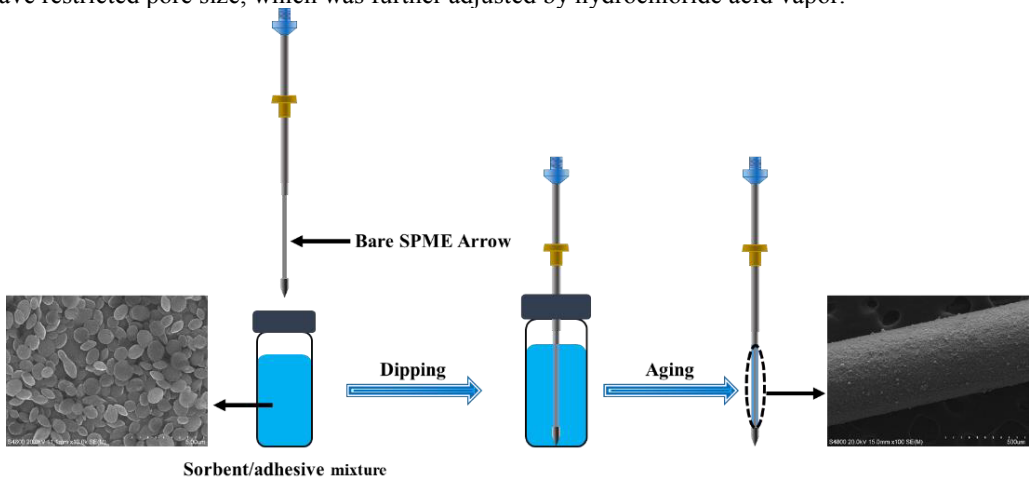

Figure 13. Immobilization of ZIF-8 and OMS particles on SPME Arrow.

3.1.3. Nanofibers packed in-tube extraction

Polyacrylonitrile (PAN) nanofibers were straightforwardly electrospun from a PAN/DMF solution and collected on a grounded silicon wafer.

ZnO, ZIF-8/ZnO and porous ZnO nanofibers were synthesized sequentially. First, ZnO nanofibers were obtained by calcining the electroblowed $Zn(NO_3)_2 \cdot 4H_2O$ composite nanofibers in air. Then ZnO nanofibers were converted to ZIF-8/ZnO nanofibers in the 2-methylimidazole (HmIM) vapor [79]. To this end, ZIF-8/ZnO nanofibers were annealed in the air to form porous ZnO nanofibers (***Papers IV and V***).

The nanofibers packed ITEXs were fabricated by sequentially packing deactivated silicon wool, nanofibers, deactivated silicon wool, and spring into an empty ITEX tube.

3.2. Material characterization

A Hitachi S-4800 field emission-scanning electron microscopy was used for observing the surface morphology of the synthesized materials. A few nanometer Au-Pb layer was sputtered onto the materials in advance. The image J software determined the average diameters of the nanofibers from the SEM images by measuring 100 individual nanofibers in each sample.

A Mettler Toledo STAR^e system equipped with a TGA 850 118 thermobalance was used for testing the thermal stability of the synthesized materials with a heating rate of 10 ºC min^{-1} under the nitrogen flow.

The crystalline structures of the MOF coatings were characterized on a PANalytical X'Pert Pro MPD diffractometer. A PANalytical X'Pert3 diffractometer equipped with a monochromatic Cu Kα radiation source powered at 40 kV and 40 mA (λ=1.54056 Å) was used to perform the analyses of OMS materials.

A PHI Quantum 2000 instrument was used for examining the X-ray photoelectron spectroscopy spectra of the ZIF-8 coatings.

The contents of T and P in OMS materials were determined by an Agilent MP-AES 4200 microwave plasma-atomic emission spectrometer after a total dissolution in 65% HNO_3 and 1% HF using a CEM MARS 5 microwave digestion system.

The specific surface area, pore size and pore volumes of the synthesized materials were determined by nitrogen physisorption measurements at 77 K with an Autosorb-1 instrument. The samples were degassed at 200 °C for 5 h prior to analysis. The BET surface area was determined in the pressure range of 0.05-0.20 P/Po, while the pore size distribution was assessed using the NLDFT model for cylindrical pores.

3.3. Construction of the permeation systems

The permeation systems for standard volatile organic compounds (VOCs) and internal standard (ISTD) were developed for online dynamic ITEX method development.

3.3.1. Permeation system for standard volatile organic compounds

In the permeation system for the standard VOCs (Figure 14a), standard chemicals were first capped into commercial sample vials individually and then placed in a metal cylinder and kept at 30 °C in an oven. A slow nitrogen flow (2 mL min^{-1}) flushed the metal cylinder and mixed with the constantly vaporized analytes. To dilute the analyte concentration, the analyte flow was diluted by an extra nitrogen flow (6 L min^{-1}). The combined flow was guided to the modified extraction port of the auto-

sampler. Copper tubing, which was shorter than one meter, was used for the sampling and connection lines to eliminate the memory effect for the analytes. It could be completely cleaned by flushing with nitrogen for a few hours. This same system was used for air sampling by connecting the air sample flow to the extraction port instead of the total diluted standard flow from the permeation system.

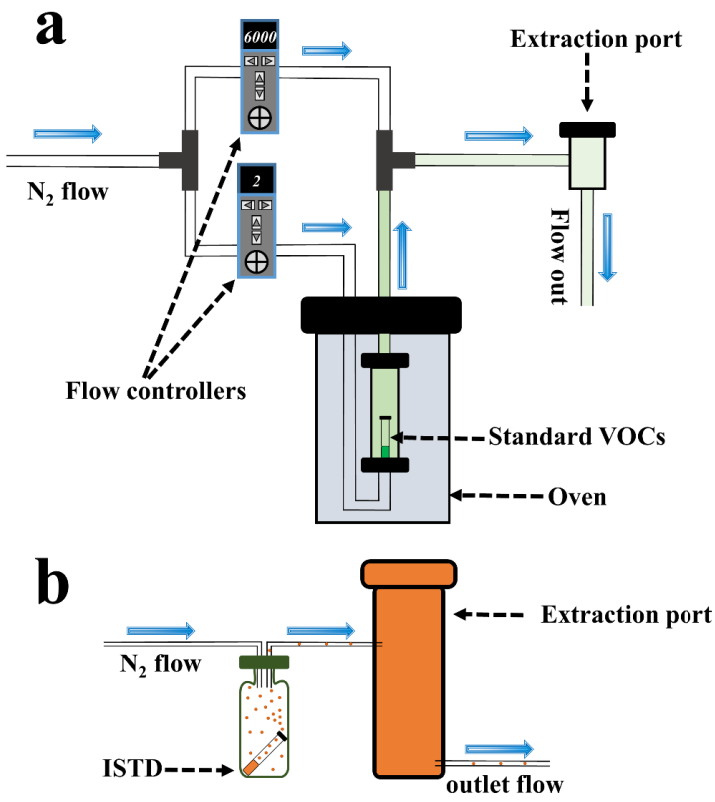

Figure 14. Permeation systems for (a) standard VOCs and (b) ISTD.

3.3.2. Permeation system for internal standard

The permeation system for internal standard (ISTD) was similar to that for standard VOCs (Figure 14b). In a GC vial with insert tube, the ISTD standard, decafluorobiphenyl, was capped and placed in a 20 mL headspace vial. A nitrogen flow (216 mL min^{-1}) was introduced to flush the permeated ISTD (at 40 °C) to the ISTD extraction port without further dilution.

3.4. Construction of the air sampling unit for the drone

Remote controlled drone (Geodrone X4L) was furnished with a sampling box that contained air pump, ITEX and SPME Arrow systems (Figure 15). More specifically, the sampling system consisted of two SPME Arrow holders with opening/closing system, two on/off valves for gas flow control and tubes for ITEX connection with sampling pump. Sampling box included also a remote-controlled operating system. The smartphone app Juice SSH mobile was used to remotely access to the operating system

Raspbian to control the hardware Raspberry Pi (Raspberry Pi Foundation) in the drone box. The operating system was connected by the 3G modem (Huawei) to control the ITEX pump, valves, SPME holders, and to their opening/closing systems.

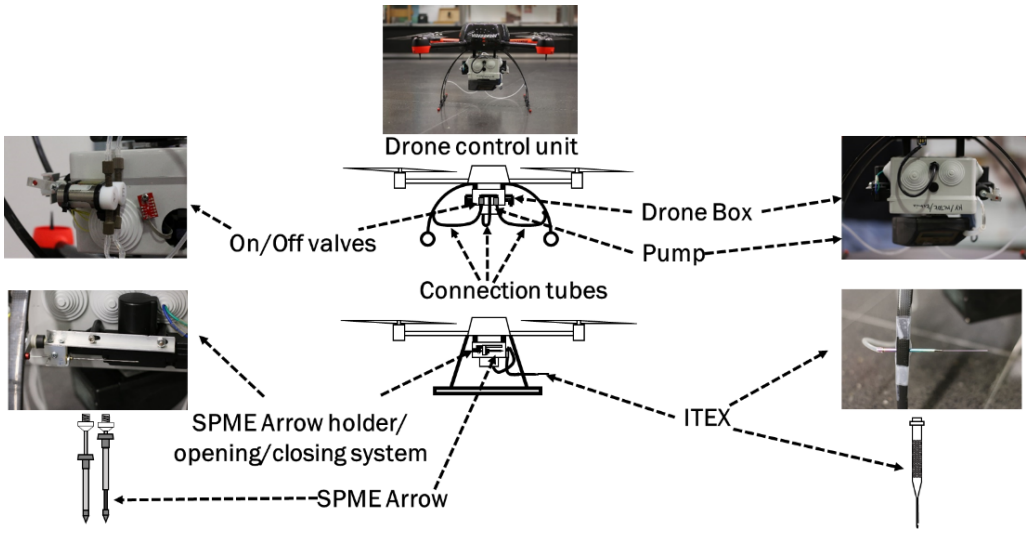

Figure 15. Aerial drone as a carrier for new miniaturized air sampling systems.

3.5. Thermal desorption units

3.5.1. Thermal desorption unit for blade solid phase microextraction

In order to fast and convenient test ALD- and MLD-converted MOFs, a thermal desorption unit (TDU) was constructed for thermal desorption (TD) of MOFs coated silicon wafer (blade SPME). The TDU comprises of a TD oven, a temperature controller, a N_2 flow line, and a cryotrap device (Figure 16). A used GC injector was utilized as the oven for thermal desorption and an electronic temperature controller for the adjustment of the TD oven temperature. A 21-gauge needle was connected to the oven to introduce analytes into the GC-MS system. To obtain narrow GC peaks, a liquid nitrogen based cryotrap (controlled by a magnetic valve) was utilized to refocus the desorbed analytes before the GC-MS analysis.

3.5.2. Thermal desorption unit for in-tube extraction

The TDU device for manual ITEX desorption was similar to that used for blade SPME. The differences were that the ITEX penetrated through the TD oven and then the GC inlet septum and there was a three-port valve to control the nitrogen flow either for ITEX preconditioning or for desorption gas filling (Figure 17). The TDU device consisted of a TD oven, a temperature controller, a Teflon hollow cylinder, a gas pressure valve, a gas flowmeter, and a three-port valve.

In step #1, the three-port valve switched the nitrogen flow to the metal tube, which was connected to ITEX located in the GC oven for preconditioning. After sampling or extraction, the valve switched the nitrogen flow to the Teflon cylinder, where the ITEX was placed and backflushed by the nitrogen flow to remove the residual air in the ITEX to avoid any oxidation during desorption (step #2). Then, the ITEX was connected to a plastic syringe with a homemade connector, and the syringe was filled with a certain volume of nitrogen (step #2). Finally (step #3), the ITEX was moved to the hot TD oven (kept

at 250 ºC) and at the same time, the needle went into the hot GC inlet. At this point, the TD oven rapidly heated the ITEX while the user injected the desorption gas to establish efficient thermal desorption.

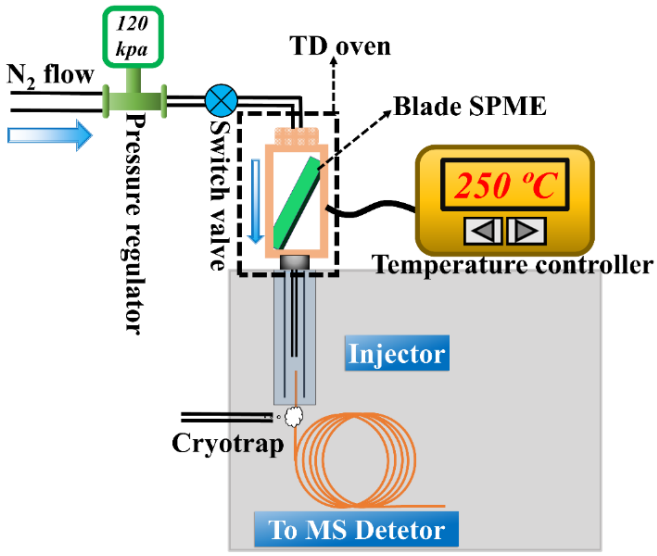

Figure 16. Scheme of the thermal desorption unit used for manual blade SPME and GC-MS analysis.

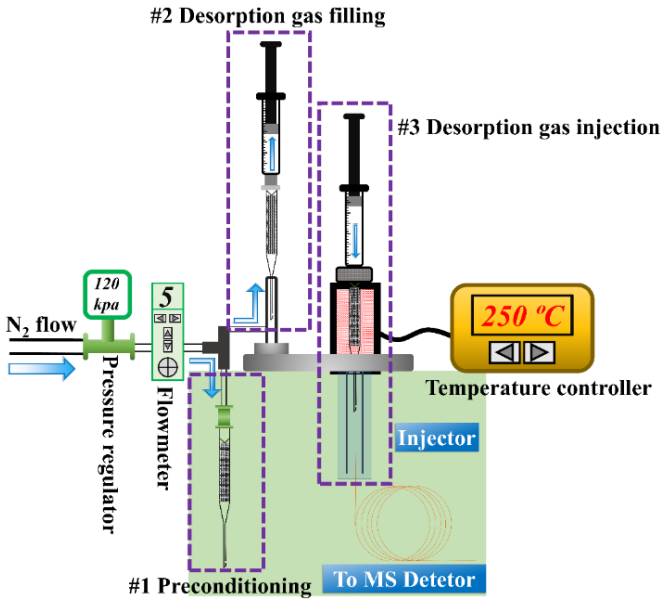

Figure 17. Scheme of thermal desorption unit used for ITEX preconditioning and desorption by manual operation.

3.6. Gas chromatography-mass spectrometry conditions

Conventional gas chromatography-mass spectrometry (GC-MS) was utilized for the analysis of analytes. The types of GC-MS, GC capillary columns, GC oven temperature program, MS conditions, and referred papers were listed in Table 3.

Table 3. Analytical conditions used with different GC-MS systems.

Instrument	GC conditions	MS conditions	Column type	Paper
Agilent 6890 N GC, Agilent 5973C MS, Agilent 5975C MS	Injector, 250 °C; transfer line, 280 °C; oven T.P.[a], 50 °C (2 or 7 min)-10 °C min^{-1}-160 °C-20 °C min^{-1}-280 °C (5 min); helium, 1.2 mL min^{-1}	Ion source, 230 °C; quadrupole, 150 °C; EI mode (70 eV); *m/z*[b], 40-300	HP-5 (30 m×0.25 mm×0.25 μm)	***I***
Agilent 6890 N GC, Agilent 5973C MS, Agilent 5975C MS	Injector, 280 °C; transfer line, 280 °C; oven T.P., 70 °C-25 °C min^{-1}-150 °C-3 °C min^{-1}-180 °C-20 °C min^{-1}-280 °C (2 min); helium, 120 kPa	Ion source, 230 °C; quadrupole, 150 °C; EI mode (70 eV); *m/z*, 40-300	HP-5 (30 m×0.25 mm×0.25 μm)	***I***
Agilent 6890 N GC, Agilent 5973C MS, Agilent 5975C MS	Injector, 270 °C; transfer line, 250 °C; oven T.P., 40 °C (5 min)-30 °C min^{-1}-250 °C (4 min); helium, 1.2 mL min^{-1}	Ion source, 230 °C; quadrupole, 150 °C; EI mode (70 eV); *m/z*, 30-300	InertCap™ for Amines (30 m ×0.25 mm)	***II***
Agilent 6890 N GC, Agilent 5975C MS	Injector, 260 °C; transfer line, 250 °C; oven T.P., 40 °C (2 min)-20 °C min^{-1}-250 °C (5 min); helium, 1.2 mL min^{-1}	Ion source, 230 °C; quadrupole, 150 °C; EI mode (70 eV); *m/z*, 20-350	InertCap™ for Amines (30 m ×0.25 mm)	***III***
Agilent 6890 N GC, Agilent 5975C MS	Injector, 250 °C; transfer line, 250 °C; oven T.P., 40 °C (2 min)-20 °C min^{-1}-250 °C (10 min); helium, 1.2 mL min^{-1}injector	Ion source, 230 °C; quadrupole, 150 °C; EI mode (70 eV); *m/z*, 15-350	InertCap™ for Amines (30 m ×0.25 mm)	***IV***
Agilent 6890 N GC, Agilent 5973C MS	Injector, 250 °C; transfer line, 250 °C; oven T.P., 40 °C (2 min)-20 °C min^{-1}-250 °C (5 min); helium, 1.2 mL min^{-1}	Ion source, 210 °C; quadrupole, 150 °C; EI mode (70 eV); *m/z*, 15-300	InertCap™ for Amines (30 m ×0.25 mm)	***V***

[a]T.P.: temperature program
[b]*m/z*: mass-to-charge ratio

3.7. Solid phase microextraction and in-tube extraction procedures

3.7.1. Static solid phase microextraction procedures

Blade SPME, SPME fiber, or SPME Arrow were carried out either manually or automatically. In the manual operation, few milliliters of the aqueous sample with a stir bar and solid NaCl were capped into a headspace vial equipped with a PTFE/silicone septum screw cap. KOH and sulfuric acid were utilized to adjust the pH value of the solution. During extraction, the stirring bar was agitated at the maximum speed. The automated SPME operation was about the same as in the manual one except no stir bar was used because the agitation was achieved differently by the agitation device in the PAL RTC autosampler.

3.7.2. Dynamic solid phase microextraction Arrow procedures

In the dynamic SPME Arrow procedure, extraction phase of SPME Arrow was exposed in the modified extraction port, which was connected to the standard flow of VOCs instead of the headspace vial. The

standard flow of VOCs was adjusted to have humidity of less than 1% or about 50%. All other steps, preconditioning and desorption, were the same as in the static extraction mode.

3.7.3. Headspace dynamic in-tube extraction

The PAL Cycle Composer (CTC analytics AG) and PAL RTC autosampler controlled and performed the headspace dynamic ITEX process. The detailed description can be found in ***Paper III***.

3.7.4. Online dynamic in-tube extraction

To allow online dynamic extraction by ITEX, the PAL Cycle Composer was modified to allow its operation with two different extraction steps, firstly with the ISTD and then with air sample. In addition, the PAL RTC autosampler need to be modified to allow dynamic extraction (Figure 18).

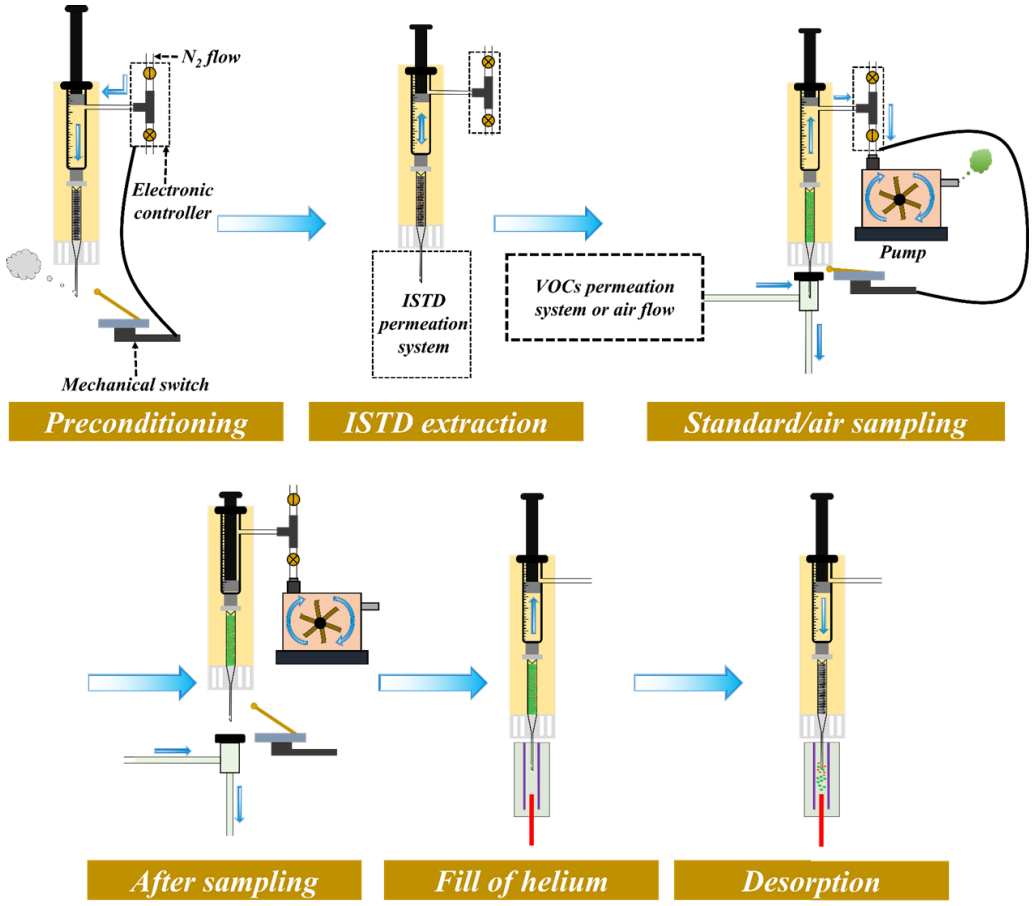

Figure 18. Online dynamic ITEX procedures.

A laboratory-made mechanical switch (with electronic controller) was used to automatically switch between the sample (air or standards) and nitrogen flow inside the ITEX. Always at the beginning, the ITEX device sampled a constant small amount of ISTD from the ISTD permeation system. Then, ITEX was moved to sample at the air/standard sampling port. Now the syringe plunger was raised up and the

sampling pump took the sample continuously into the ITEX. The more detailed description can be found in ***Paper III***. For air sampling, the total diluted standard flow from the permeation system was replaced by an airflow.

3.7.5. Aerial drone as the platform of microextraction sampling systems

The aerial drone was the platform to carry the SPME Arrow and ITEX devices for air sampling in the difficult access areas. During the flight, the drone box was remotely controlled to open/close the SPME Arrow and turn on/off the sampling pump of the ITEX before and after sampling. After sampling and landing of the drone, the SPME Arrow and ITEX were desorbed in the GC inlet and TDU, respectively, for on-site measurement with a conventional GC-MS. To evaluate the extraction phase selectivity and the effect of drone horizontal and vertical displacements on the sampling, the drone carried the microextraction sampling systems to collect air samples at different horizontal distances, heights and with different times.

3.8. Sampling and sample pretreatment

3.8.1. Air samples

The atmospheric air sampling by the online dynamic ITEX was conducted from the 12th to 30th of July and from 12th to 19th of November 2018 in Kumpula Campus, University of Helsinki, Helsinki, Finland.

The atmospheric air samples for SPME Arrow analysis were collected at SMEAR (Station for Measuring Ecosystem-Atmosphere Relations) II station in a Scots pine forest at Hyytiälä in southern Finland [137, 149]. The sampling site was located about 15 m from a 127-m high mast for atmospheric and flux measurements (61°50′50.55″N, 157 24°17′39.77″E, 181 m above the sea level). The sampling was done from 23rd to 26th of October 2018. The denuder sampler for air located at 2 m above the ground vegetation and 3 m from the closest tree. A three-channel annular denuder coated with 0.1 M phosphoric acid was connected to a peristaltic pump with a flow rate of 1 m^3 h^{-1}. The sampling time ranged from 4 to 13.5 h. After sampling, the denuder was rinsed three times with 5 mL of Milli-Q water and the eluent was stored at 4 ℃ for further analysis. Totally 12 samples were collected.

SPME Arrow and ITEX sampling with the aerial drone was performed from 22nd to 26th of October 2018 at a soccer field area (61.844400° N - 24.287033° E) in SMEAR II station. In addition, 8 samples were collected in the forest next to the SMEAR II tower (61.846350° N - 24.295333° E - 23 October 2018) and Siikaneva wetland (fen) area (26 October 2018). The later was in Ruovesi (61.833266° N, 24.192550°E) 8 km far from SMEAR II station, a well-known site for carbon and energy studies and soil processes [150].

The online dynamic ITEX system sampled the indoor air on 31st of July 2018 from a chemistry laboratory, Department of Chemistry, University of Helsinki, Helsinki, Finland.

Exhaled air samples were collected from a smoker and a non-smoker with the online dynamic ITEX system.

3.8.2. Liquid samples

Influent and effluent wastewater samples were from Viikinmäki municipal wastewater treatment plant (WWTP), which is in Helsinki, Finland. The samples were collected into pre-cleaned plastic bottles

and stored in the refrigerator at 4 ºC prior to analysis. Samples were filtered through cotton wool to remove large particles followed by additional filtration.

The urine sample was collected from a young male volunteer (28 years old) without additional pretreatment and analyzed immediately.

3.8.3. Solid samples

Ten types of fruiting bodies of mushroom were collected from a forest near Kumpula Campus of the University of Helsinki (Helsinki, Finland) on the 1st of September 2016 and 8th of October 2018. The first batch of samples was stored overnight at +4 ºC and the second batch was pretreated without storage. The samples were cut and mixed 10% (w/v) trichloroacetic acid or formic acid solution and then homogenized, centrifuged, and the supernatant was collected.

The salmon sample was purchased from a local supermarket in Helsinki and it was stored at room temperature for 0, 1, 2, 3, and 4 days to track the food spoilage.

3.9. Software

Minitab 18 statistical software (Minitab, State College, USA) was used for the experimental design and data analysis. ADAP-GC (Automated Data Analysis Pipeline) was used for pre-processing untargeted mass spectrometry-based omics data, an algorithm included in Mzmine2 software, was used for the detection, deconvolution, and alignment of the chromatographic peaks [151, 152]. The identification of the aligned peaks was done by comparison of their mass spectra and retention indices to NIST2014 mass spectral database. R 3.5.1 was used for the development of ANOVA, linear regression, principal component analysis (PCA) and cluster analysis (CA) [153].

4 Results and discussion

The main objective of this work was to evaluate the performance and applicability of different sorbent materials in miniaturized microextraction techniques, e.g. SPME Arrow and ITEX (***Papers I, II, III and IV***). Development of corresponding analytical methods is another objective (***Papers I, II, III and IV***). Developed SPME Arrow and ITEX devices in ***Paper III*** and ***IV*** were further coupled with an aerial drone for air sampling in the boreal forest to test the applicability of the whole system (***Paper V***). The developed materials were also compared with commercial materials in terms of extraction capacity, extraction selectivity and extraction kinetics (***Papers I-V***).

4.1. Development of new materials for microextraction techniques

Extraction phase is the crucial part in microextraction techniques that affect e.g. sensitivity, selectivity, robustness, reusability, repeatability, and reproducibility of an analytical method. In this thesis, MOFs, OMSs, and electrospun nanofibers were utilized due to their advantageous porous structure and surface chemical properties, which provide excellent adsorption and high affinity to VOCs.

4.1.1. Solid phase microextraction Arrow coatings

MOFs coatings

MOF materials in this study were synthesized via ALD- and MLD-conversion methods and purchased from the chemical supplier.

The first criteria to select a proper MOF is its hydrophobicity. Literature reported MIL-53 (Fe), MIL-100 (Fe), MIL-53 (Al), and MIL-100 (Al), which used H_2BDC or H_3BTC as the organic linker, are hydrophobic and water stable [88]. This inspired us to synthesize these MOFs for high humidity samples. Al-BDC/BTC and Fe-BDC/BTC films were obtained after conversion of ALD deposited metal oxide (Al_2O_3 or Fe_2O_3, ~200 nm thickness) film in organic linker (H_2BDC or H_3BTC) vapor (***Paper I***). In this approach, conversion temperature and time are the key points. The high boiling points of H_2BDC and H_3BTC resulted in high conversion temperature. However, to avoid the decomposition of organic linker bed and to reuse it, the conversion temperature should be lower than the boiling points of organic linkers. In literature, 100 ºC was utilized for 2-methylimidazole (boiling point 275 ºC) vaporization [102]. Based on these considerations, heating at 330 and 350 ºC were utilized for Al/Fe-BTC and Al/Fe-BDC conversion, respectively. The coating thickness of MOFs was further increased with longer conversion time (40 h vs 2 h) that enable higher extraction capacity. The resulted films had a ~2 μm thicknesses and crystalline structures (Figures 19a-b and 20a-d). Another approach is to convert the MLD deposited organic-inorganic composite film (Zr-BDC) into crystalline and porous UIO-66 film in acetic acid vapor (***Paper I***). In this way, pre-heating (10-20 min) is the essential step to eliminate the condensation of acetic acid droplets and consequent Zr-BDC decomposition. Besides that, a proper acetic acid volume (4 mL), conversion time (≥23 h) and temperature (≥200 ºC) were needed to complete the Zr-BDC-to-UIO-66 conversion process thoroughly. This resulted in a UIO-66 film with ca. 7.5 μm thickness (Figures 19c-d and 20e).

ZIF-8 is another hydrophobic MOF material. It can enrich target analytes by absorption, e.g. aromatic compounds, but it has a weak capability to adsorb C_3 or larger compounds due to its nominal aperture size of 3.4 Å [154, 155]. Therefore, its pore size was enlarged in this study by acidification with HCl to improve its applicability to retain aliphatic amine compounds (***Paper II***). After exposing ZIF-8 to the headspace of 1 M HCl solution, its pore size converted to be 2-50 nm. The higher mass-to-mass ratio of PVC/ZIF-8 in tetrahydrofuran (THF) can improve the stability of the coating while decreasing

its extraction capacity and uniformity. As a result, the coating made by 6:1 of PVC/ZIF-8 in 1 mL THF provided the highest extraction efficiency and excellent uniformity. Five cycles of dipping resulted in an optimal coating thickness (~70 µm) (Figures 19e-f).

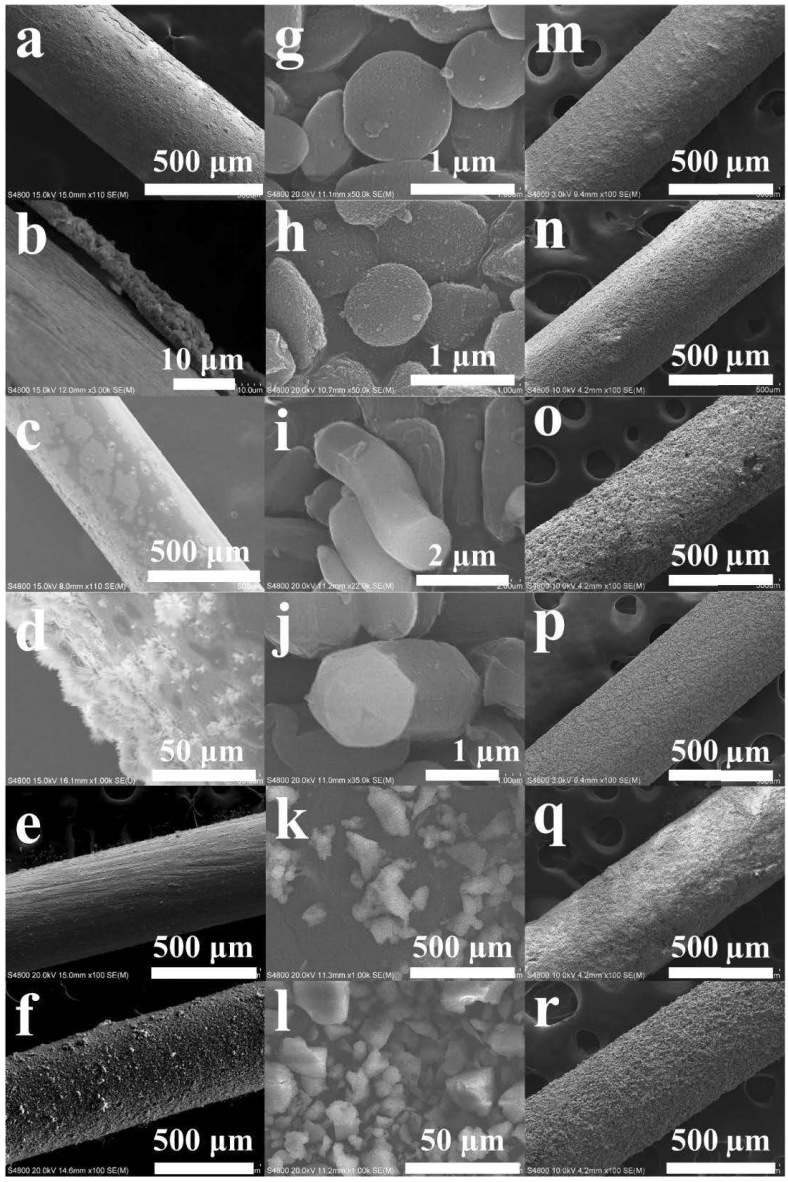

Figure 19. SEM images of (a and b) Fe-BDC, (c and d) UIO-66, (e) A-ZIF-8/PVC (one dipping cycle), (f) A-ZIF-8/PVC (five dipping cycles) coated SPME Arrows, and (g) MCM-41, (h) MCM-TP, (i) SBA-15, (j) SBA-TP, (k) KIT-6 and (l) KIT-TP OMSs, and (m) MCM-41-, (n) MCM-TP-, (o) SBA-15-, (p) SBA-TP-, (q) KIT-6- and (r) KIT-TP-coated SPME Arrows.

Ordered mesoporous silica coatings

MCM-41, SBA-15, and KIT-6 were the representative OMS materials. MCM-41 and SBA-15 have two-dimensional (2D) hexagonal pore structure but different pore sizes, 4 nm and 8 nm, respectively [156, 157]. On the other hand, KIT-6 has a similar pore size (10 nm) with SBA-15 but a 3D cubic mesoporous structure [158]. They are all thermally stable (up to 600 ºC) and weakly acidic, which suggested their strong affinity to basic compounds. Their acidity was further enhanced by modifying with titanium-phosphate (-TP) groups [159-161]. The surface modification process had no obvious effect to the pore structures (Figures 20f-h) and morphologies (Figures 19g-l) of OMSs but led to their smaller pore sizes (Figures 20i-k) and weaker thermal stability. However, they are still suitable for thermal desorption (usually under 300 ºC). In ***Paper III,*** PAN replaced PVC as the adhesive due to its higher thermal stability. However, 12 dipping cycles were needed to prepare a satisfactory thickness of OMS coatings (~20 µm). Aging time needed to be extended to 18 h in the GC inlet at 250 °C under helium flow.

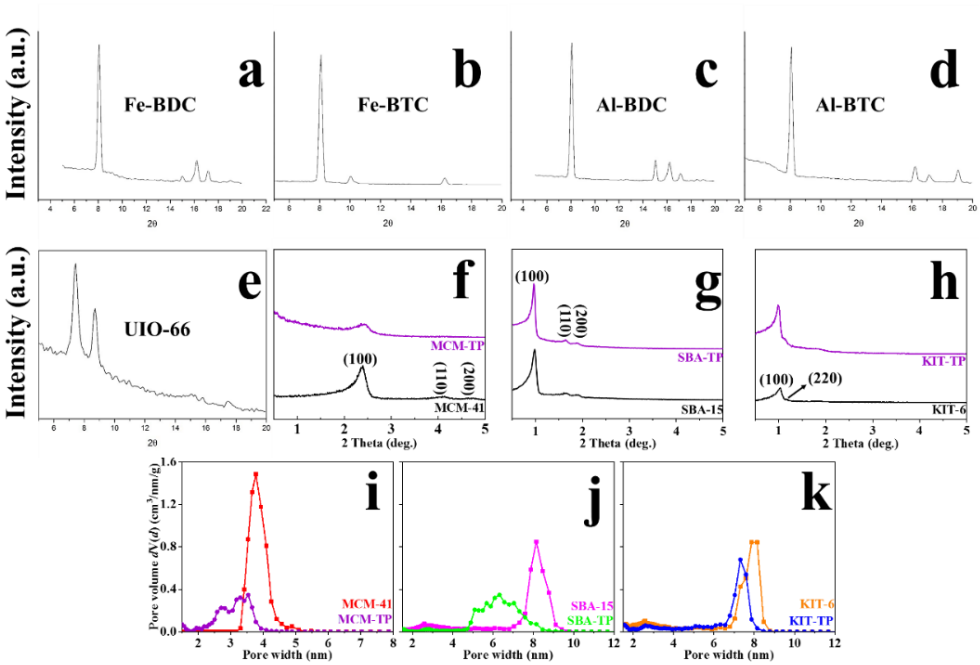

Figure 20. XRD patterns of (a) Fe-BDC, (b) Fe-BTC, (c) Al-BDC, (d) Al-BTC, (e) UIO-66, (f) MCM-41 and MCM-TP, (g) SBA-15 and SBA-TP, (h) KIT-6 and KIT-TP, and pore size distributions of (i) MCM-41 and MCM-TP, (j) SBA-15 and SBA-TP, and (k) KIT-6 and KIT-TP.

4.1.2. In-tube extraction packing material

Nanofibers are particularly suitable as the packing material for the ITEX because of their good permeation for gas flow. For example, 50 mg of PAN nanofibers packed into ITEX showed similar permeability with that of ca. 50 mg of 60/80 mesh particulate sorbent packed ITEX. Furthermore, the thermal stability of the nanofibers synthesized in this study was over 285 ºC. This meets well the requirement for thermal desorption applications. All the nanofibers prepared had a diameter less than 1 µm with excellent nanostructure (Figure 21).

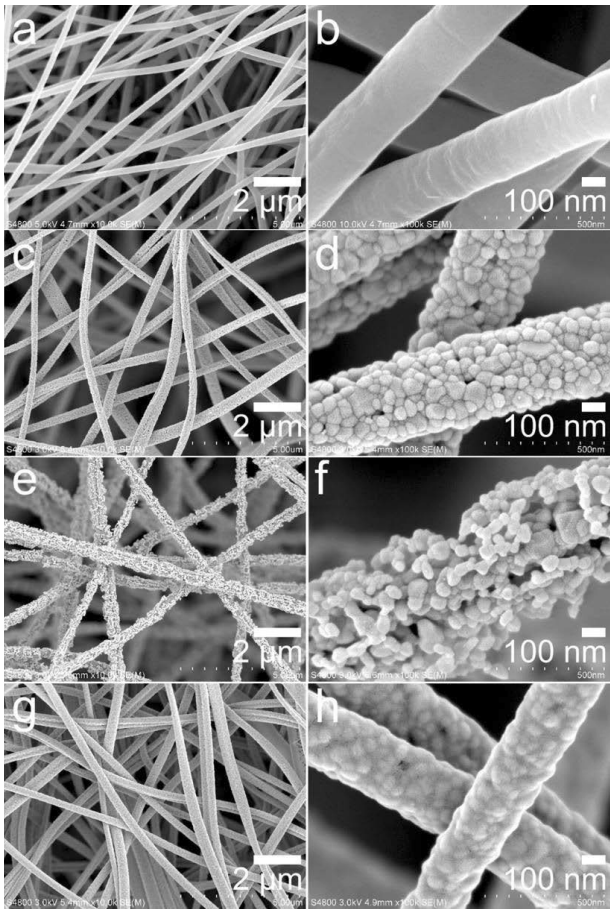

Figure 21. Scanning electron microscopy images of (a-b) 10 % PAN, (c-d) ZnO, (e-f) porous ZnO and (g-h) ZnO/ZIF-8 core/shell nanofibers.

4.2. Comparison of laboratory-made and commercial solid phase microextraction devices

Laboratory-made and commercial coatings of SPME Arrow were compared in terms of extraction affinity, extraction selectivity and extraction kinetics (Table 4).

ALD- and MLD-converted MOF coatings had higher extraction affinity to aromatic compounds due to the π-π interactions between the aromatic rings and organic linker (***Paper I***). Among them, Fe-BDC and Fe-BTC coatings owned exceptional hydrophobicity and opened Fe^{3+} sites, which prevented interferences due to water and facilitated their high affinity to chlorinated phenols, respectively (Figure 22) [162-166]. Besides phenols, some other aromatic compounds, e.g. naphthalene, 1,2,4-trichlorobenzene, and hexachlorobenzene, also interacted well with laboratory-made materials. On the contrary, PA coating exhibited low extraction affinity to phenols in high humidity condition as the consequence of its hydrophilicity. Another laboratory-made MOF coating, UIO-66, preferentially extracted small polar, aliphatic polar and aromatic compounds and its adsorption performance decreased with the increase of the molecular mass of the analytes, e.g. pyridine, aniline, and 1-naphthylamine. Commercial coatings showed advantages in extracting nonpolar compounds

Table 4. Comparison of laboratory-made and commercial SPME Arrow coatings

	Laboratory-made coatings	Commercial coatings	Comparison items
Paper I	Fe-BDC (~2 μm)[a]	PDMS (100 μm), PDMS/DVB (65 μm), PA (85 μm) and Carbon WR/PDMS (120 μm)	Extraction affinity and extraction selectivity
Paper I	Fe-BTC (~2 μm)	PDMS (100 μm), PDMS/DVB (65 μm), PA (85 μm) and Carbon WR/PDMS (120 μm)	Extraction affinity and extraction selectivity
Paper I	Al-BDC (~2 μm)	PDMS (100 μm), PDMS/DVB (65 μm), PA (85 μm) and Carbon WR/PDMS (120 μm)	Extraction affinity and extraction selectivity
Paper I	Al-BTC (~2 μm)	PDMS (100 μm), PDMS/DVB (65 μm), PA (85 μm) and Carbon WR/PDMS (120 μm)	Extraction affinity and extraction selectivity
Paper I	UIO-66 (~7.5 μm)	PDMS (100 μm), PDMS/DVB (65 μm), PA (85 μm) and Carbon WR/PDMS (120 μm)	Extraction affinity and extraction selectivity
Paper II	Acidified ZIF-8 (~70 μm)	PDMS/Carboxen-1000 (120 μm)	Extraction affinity, extraction selectivity and extraction kinetics
Paper III	MCM-41 (~20 μm)	PDMS (120 μm), Carbon WR/PDMS (120 μm), PDMS/Carboxen-1000 (120 μm) and PDMS/DVB (120 μm)	Extraction affinity, extraction selectivity and extraction kinetics
Paper III	MCM-TP (~20 μm)	PDMS (120 μm), Carbon WR/PDMS (120 μm), PDMS/Carboxen-1000 (120 μm) and PDMS/DVB (120 μm)	Extraction affinity, extraction selectivity and extraction kinetics
Paper III	SBA-15 (~20 μm)	PDMS (120 μm), Carbon WR/PDMS (120 μm), PDMS/Carboxen-1000 (120 μm) and PDMS/DVB (120 μm)	Extraction affinity, extraction selectivity and extraction kinetics
Paper III	SBA-TP (~20 μm)	PDMS (120 μm), Carbon WR/PDMS (120 μm), PDMS/Carboxen-1000 (120 μm) and PDMS/DVB (120 μm)	Extraction affinity, extraction selectivity and extraction kinetics
Paper III	KIT-6 (~20 μm)	PDMS (120 μm), Carbon WR/PDMS (120 μm), PDMS/Carboxen-1000 (120 μm) and PDMS/DVB (120 μm)	Extraction affinity, extraction selectivity and extraction kinetics
Paper III	KIT-TP (~20 μm)	PDMS (120 μm), Carbon WR/PDMS (120 μm), PDMS/Carboxen-1000 (120 μm) and PDMS/DVB (120 μm)	Extraction affinity, extraction selectivity and extraction kinetics
Paper V	MCM-41-Ti (~20 μm)	Carbon WR/PDMS (120 μm) and PDMS/DVB (120 μm)	Extraction affinity and extraction selectivity

[a] coating thickness

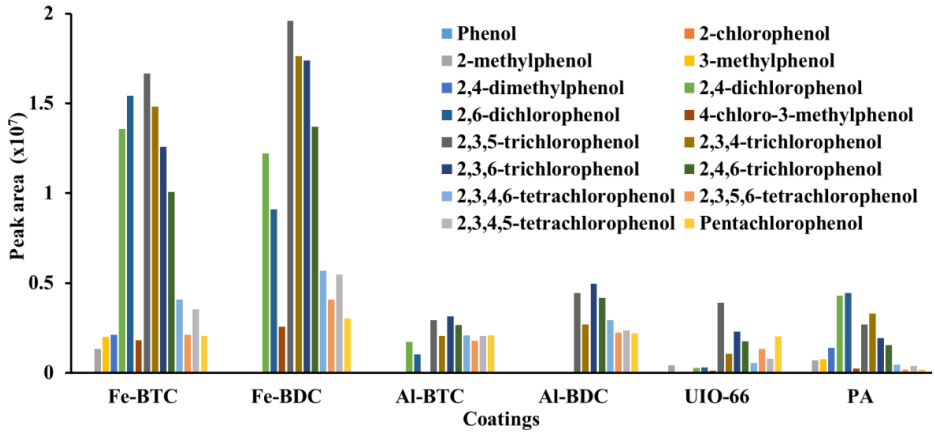

Figure 22. Comparison (in terms of GC-MS peak areas) of laboratory-made Fe-BDC, Fe-BTC, Al-BDC, Al-BTC, and UIO-66 coatings with commercial PA coating for extraction of chlorinated phenols.

Acidified ZIF-8 coating showed an exceptional affinity and selectivity to low-molecular-weight aliphatic amines (LMWAAs) (***Paper II***). HCl treated ZIF-8 has 2-50 nm of pore size, which led to 12.9 times increase in extraction efficiency of template trimethylamine (TMA), compared to the untreated ZIF-8 (Figure 23a). With the help of adhesive PVC, the acidified ZIF-8 coating thickness was increased from 5 µm to 70 µm (Figures 19e-f) and a 10-times increase in the extraction capacity was obtained. To this end, the A-ZIF-8/PVC coating even showed 3.3 times higher extraction capacity to TMA than that of PDMS/Carboxen-1000 coating, which was the best commercial option for LMWAA extraction (Figure 23). PVC coated SPME Arrow showed weak affinity towards TMA and therefore indicated the extraction of TMA in an A-ZIF-8/PVC coated SPME Arrow was caused by the acidified-ZIF-8.

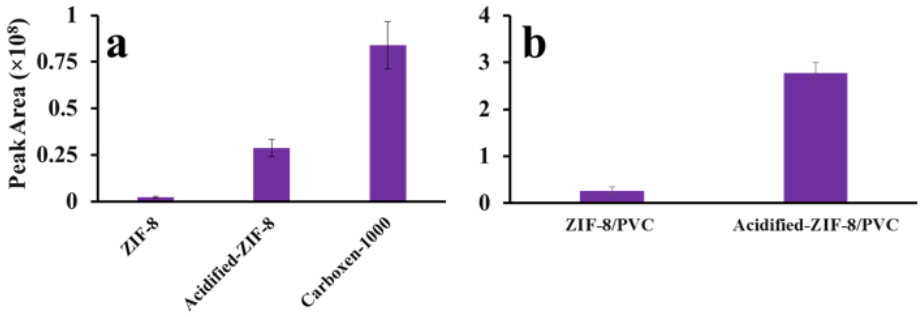

Figure 23. Extraction performance for trimethylamine with (a) ZIF-8-, acidified ZIF-8- and PDMS/Carboxen-1000-SPME Arrows, and (b) ZIF-8/PVC- and acidified-ZIF-8/PVC-SPME Arrows.

The enlarged pore size of ZIF-8 also facilitated its fast extraction kinetics for capturing LMWAAs. A-ZIF-8/PVC coating can reach the extraction equilibrium at 5 min for TMA and triethylamine (TEA), while with the PDMS/Carboxen-1000 coating it takes 15 min (Figure 24).

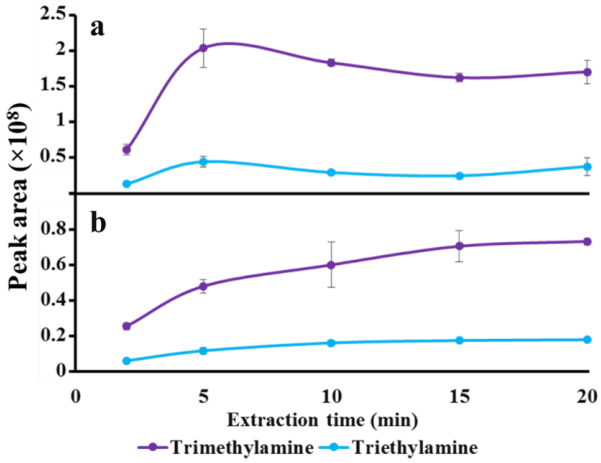

Figure 24. Extraction time profiles with (a) acidified-ZIF-8/PVC- and (b) PDMS/Carboxen-1000-SPME Arrows.

To evaluate the selectivity of A-ZIF-8/PVC coating to LMWAAs, it was used to analyze samples with complex matrices (wastewater, salmon, and mushroom) together with PDMS/Carboxen 1000 coating. All the SPME Arrow results showed excellent selectivity of A-ZIF-8/PVC coating (Figure 25) to TMA and TEA.

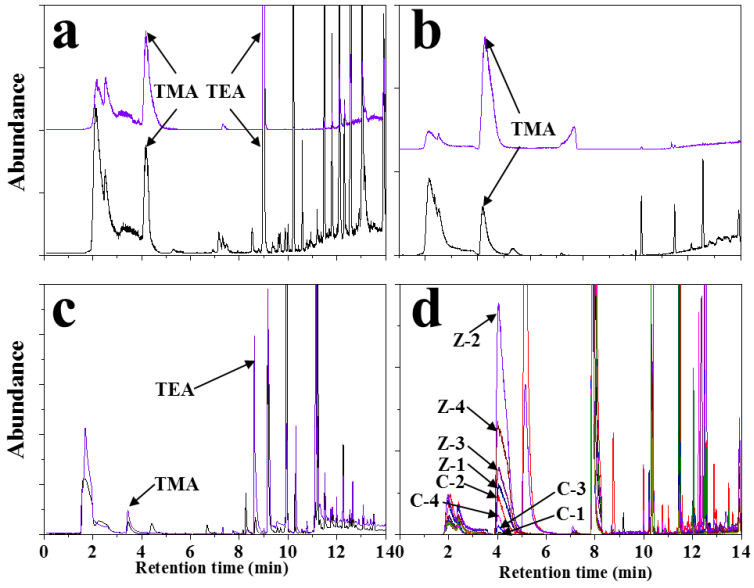

Figure 25. Comparison of A-ZIF-8/PVC and PDMS/Carboxen-1000 coatings for SPME Arrow extraction of LMWAAs from (a) influent wastewater, (b) effluent wastewater, (c) salmon and (d) mushroom samples. In (a-c), A-ZIF-8/PVC and PDMS/Carboxen-1000 chromatograms are in purple and black, respectively. In Figure d, Z represented the mushroom sample extracted by A-ZIF-8/PVC coating, and C by PDMS/Carboxen-1000 coating. The numbers following letters Z and C correspond to the mushroom sample number.

OMS coatings were prepared as the alternatives of A-ZIF-8/PVC coating for selective extraction of LMWAAs with a more systematic study (***Papers III and V***). The extraction affinity of OMS and commercial coatings to primary ethylamine (EA), secondary diethylamine (DEA), tertiary TEA and aromatic aniline were compared. Under the ideal and dry (<1% humidity) conditions, competing compounds did not interfere with the interaction between analytes and coating materials. OMS coatings extracted 18.6-102.5, 4.8-10.8 and 2.6-4.0 times more EA, DEA and TEA, respectively, than the best commercial coating (PDMS-DVB) (Figure 26a). Pore size and surface acidity of the OMS materials determined the extraction efficiency for LMWAAs when the extraction time (10 min) was far from equilibrium (like in the case of MCM-41, SBA-15, and KIT-6). Grafted -TP groups enhanced the surface Lewis and Brønsted acidity of OMSs but decreased the pore size and consequently reduced the extraction capacity. On the other hand, the hydrophilic nature of OMSs predicted that the extraction performance of OMS coatings would drop dramatically when working in a high humidity atmosphere. As expected, with 50% humidity, water molecules occupied a tremendous amount of extraction sites on the OMS surface but the extraction capacity of OMS coatings to EA, DEA, and TEA was still 11.6-53.3, 3.3-8.4 and 1.8-3.6 times higher than that of PDMS-DVB (Figure 26b). Interestingly, OMS with smaller pore size and 2D channels can restrict the water molecules more effectively when compared to neutral and hydrophobic PDMS/DVB, which pore size is 40 nm. Therefore, pore size is the decisive parameter for LMWAAs extraction and controlling water affinity.

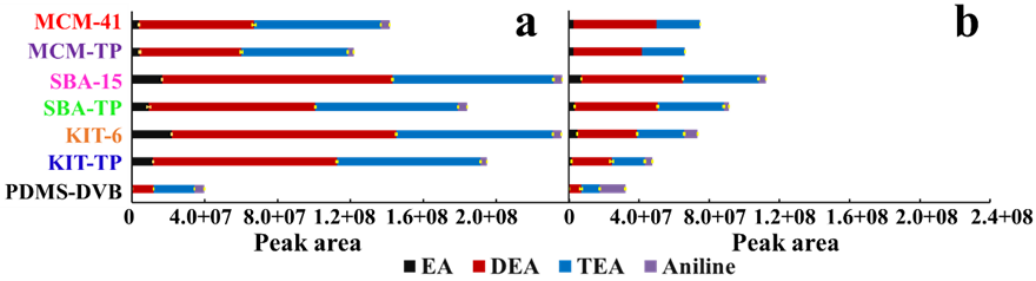

Figure 26. Comparison of ordered mesoporous silicas and PDMS-DVB coated SPME Arrows for extraction of ethylamine, diethylamine, triethylamine and aniline at (a) <1% and (b) 50% humidity.

Further, the prevention of interferences by OMS, which had narrower pore size, was not only limited to water molecules but also other low affinity competing compounds (Figure 27). To this end, MCM-41 and MCM-TP, which had 2-4 nm pore size, 2D pore structure, acidic surface, and nonaromatic structure, thereby provided the highest selectivity to LMWAAs.

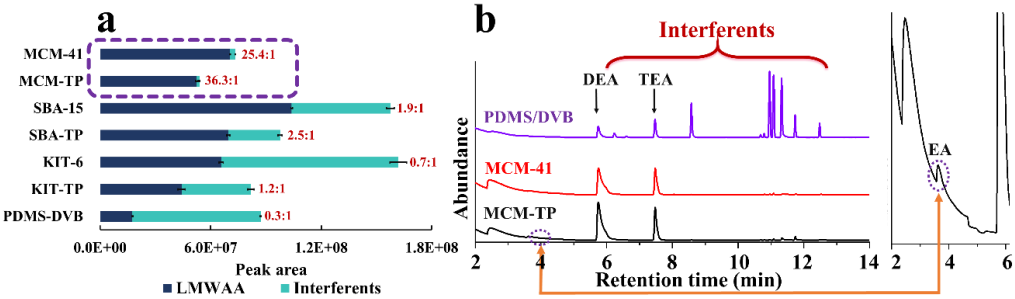

Figure 27. (a) Selectivity comparison towards LMWAA and b) representing GC-MS chromatograms of LMWAAs with MCM-41, MCM-TP, and PDMS-DVB-SPME Arrows.

The selectivity of MCM-41-based and commercial coatings to LMWAA was further tested in natural samples, atmospheric air, and urine. Ammonia, dimethylamine, EA, DEA, and TEA were identified in the urine sample by all coatings but MCM-41 and MCM-TP coatings provided much clearer baseline and more intense amine peaks compared to that of PDMS/DVB coating (Figure 28). In the air sampling, the MCM-41-Ti coating successfully adsorbed alkylamines, which were not found by commercial coatings. Further, the number of adsorbed compounds by MCM-41-Ti coating was 2-3 times smaller than that by commercial coatings, thus showing the good selectivity of the MCM-41-Ti.

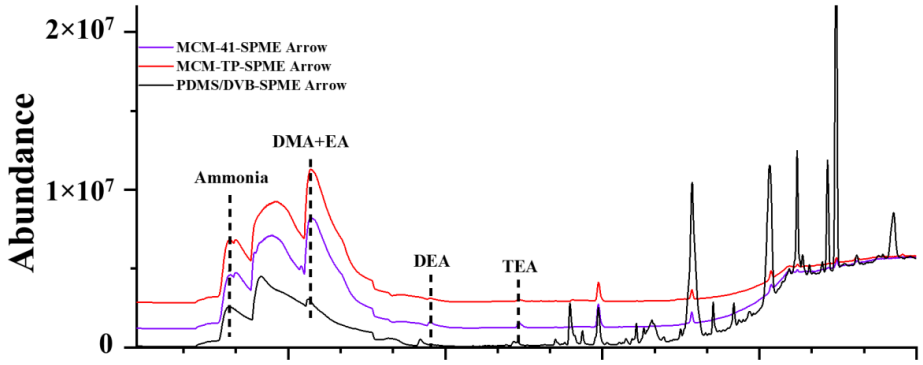

Figure 28. GC-MS chromatograms of the urine samples after extraction by MCM-41, MCM-TP, and PDMS-DVB coated SPME Arrows.

The acidity of MCM-41 and MCM-TP coatings allowed them to reach extraction equilibrium for EA, DEA, and TEA within 20 and 30 min, respectively. However, PDMS-DVB needed 60 min for equilibrium (Figure 29).

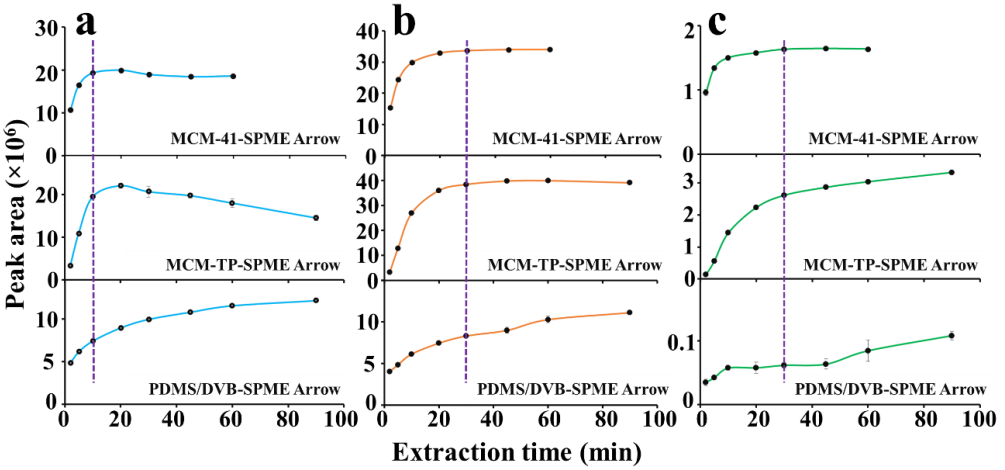

Figure 29. Extraction kinetics with MCM-41, MCM-TP and PDMS-DVB SPME Arrows for extraction of a) TEA, b) DEA and c) EA.

4.3. Comparison of laboratory-made and commercial in-tube extraction

The nanofibers packed ITEXs were compared with commercial ITEXs for extraction of a wide range of VOCs with different polarity, volatility, and molecular mass. The VOCs selected are widely distributed in the atmosphere and present at trace level concentrations.

Among these ITEXs, PAN-ITEX exhibited the highest extraction affinity to alcohols, aldehydes, and ketones due to the rich amine and imide group on the surface of PAN nanofibers (Figure 30). Inorganic ZnO, ZIF-8/ZnO and porous ZnO nanofibers packed ITEXs were only selective to few compounds with small extraction capacity which can be interpreted by their physical and chemical structures, e.g. inaccessible pore size and weak surface functional groups. Tenax TA/Carbosieve S-III multilayer packed ITEXs extracted more analytes because of the synergistic effect by combing the microporous Carbosieve S-III and mesoporous Tenax TA. As expected, single layer microporous Carbosieve S-III or Carboxen 1000 packed ITEXs showed the worst extraction capacity.

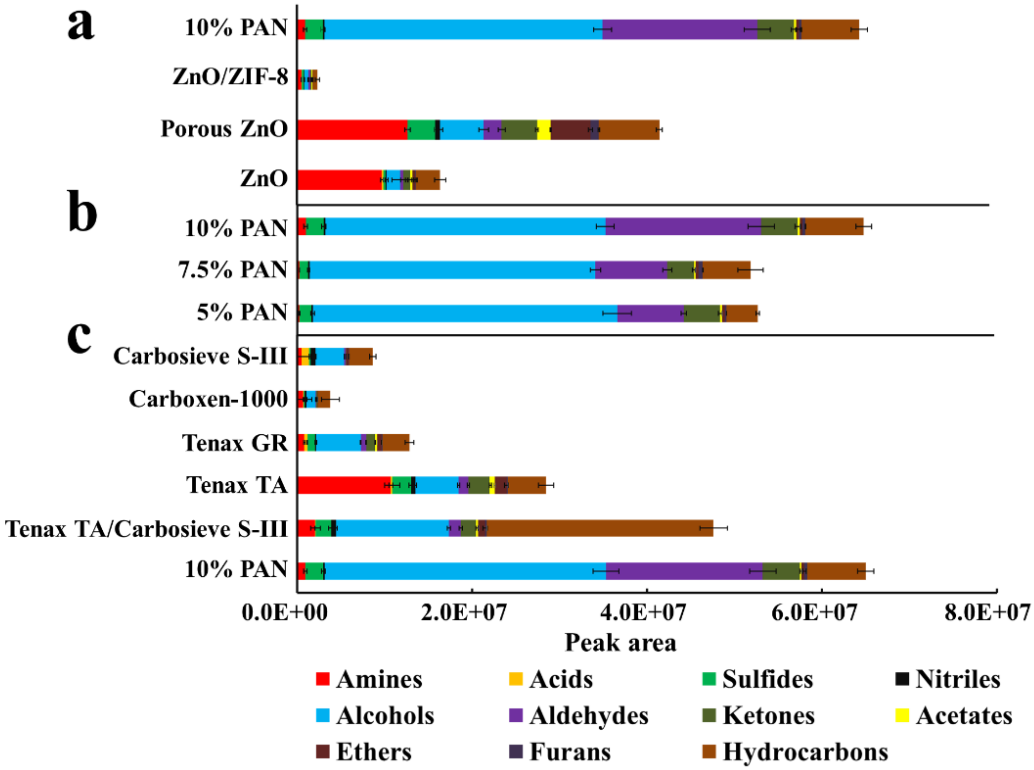

Figure 30. Comparison of laboratory-packed and commercial ITEXs for the extraction of different VOCs.

In three types of PAN-ITEXs, in which the PAN nanofibers were electrospun by 5, 7.5 and 10 wt.% PAN/DMF solutions, 10% PAN-ITEX had the best extraction affinity to most analytes due the larger volume of sorbent phase (180±40 and 290±40 nm for 7.5 and 10% PAN nanofibers, respectively). It is worth to mention that in electrospinning technique, the viscosity of the polymer solution is crucial to prepare uniform and nanometer diameter fibers. The improper concentration of the polymer solution can cause the particulate structure of nanofibers or make it impossible for electrospinning.

In the following study (***Paper V***), the selectivity of 10% PAN-ITEX was also tested by analyzing the air sample. The extraction efficiency of analytes by 10% PAN-ITEX was aldehydes>alcohols>hydrocarbons>ketones>acids and that by Tenax TA- and Tenax GR-ITEXs was alcohols>ketones>hydrocarbons>aldehydes. These results were in good agreement with those achieved in ***Paper III***.

4.4. Reusability and reproducibility of laboratory-made microextraction devices

The reusability test was performed for Fe-BDC, UIO-66, A-ZIF-8/PVC, MCM-41, and MCM-TP coated SPME Arrows. Under optimal operation condition, Fe-BDC coating had the shortest lifetime, 80 extraction and desorption cycles, among all laboratory-made coatings due to its 2 µm coating thickness (***Paper I***). All other coatings could be used over 100 cycles. Particularly, the A-ZIF-8/PVC coating did not show a significant decrease in the extraction efficiencies of template TMA and TEA after 130 extraction and desorption cycles (Figure 31) (***Paper II***). With A-ZIF-8/PVC, the RSD% of the two analytes was less than 13%, which also indicate its good repeatability. Since the adhesive PAN is more robust than PVC, the OMS/PAN coating can reach the lifetime of at least 150 extraction and desorption cycles (***Paper III***).

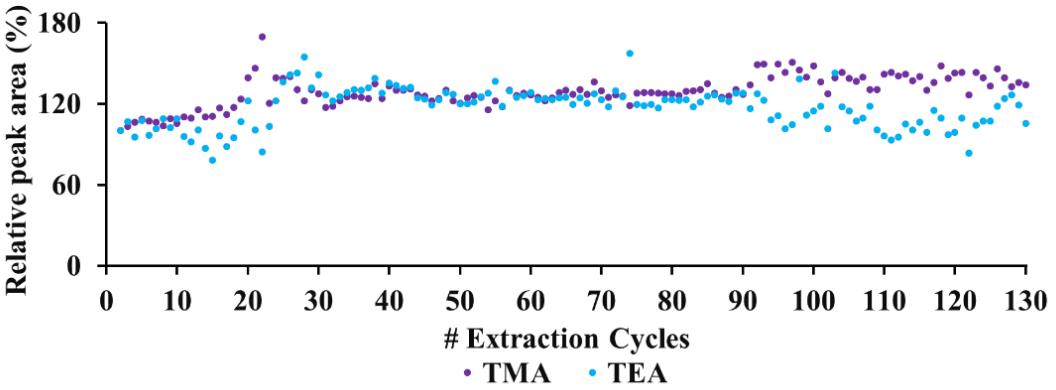

Figure 31. Reusability of acidified-ZIF-8/PVC SPME Arrow. The peak area of the second extraction was set as 100%.

One of the aims was to construct the 10% PAN-ITEX for long-term nonstop measurements of VOCs in air. Thanks to the design of inner packed sorbent and automated operation, 1500 extraction and desorption cycles was achieved by 10% PAN-ITEX and therefore it can be an ideal sampling device for long-term air monitoring (***Paper IV***).

The reproducibility of dipped A-ZIF-8/PVC coating was evaluated by preparing five A-ZIF-8/PVC coatings in a batch. The RSD% (n=5) was lower than 16% which reveals the good applicability of dipping method for SPME Arrow coating preparation (***Paper I***).

The reproducibility test for 10% PAN-ITEX was more demanding because of its long-term and nonstop application, which requires a spare one in case the used ITEX is accidentally broken and need to be replaced by a new one. Consequently, average RSD of 15 template compounds, including alcohols, aldehydes, sulfides, and nitriles, was only 9.7%, which is acceptable for ITEX replacement during the campaign without further calibration (***Paper IV***).

In terms of the number of compounds and total peak area of these compounds, excellent reproducibility was obtained by testing MCM-41-Ti-SPME Arrow and 10% PAN-ITEX sampling systems in one drone flight (***Paper V***).

4.5. Performance of laboratory-constructed permeation systems

The permeation systems that were constructed in the laboratory, for either VOCs or internal standard (ISTD), needed to be validated before using them for online dynamic ITEX method development. Widely distributed alcohols, ketones, aldehydes, and hydrocarbons in the atmosphere in Helsinki were selected as the template compounds for validation of the VOCs permeation system. On the other hand, the ISTD selected should not exist in atmosphere, give no inference to the analysis result, be non-reactive to all the other compounds and be easily trapped by 10% PAN.

Triplicate measurements of template compounds with 0.5, 1, 2, 5, 10, 15, 20, 30, 45, and 60 min sampling times were performed by 10% PAN-ITEX in dynamic mode. The analysis results showed RSDs ranging from 0.26 to 3.2%, which indicated the constant emission and flow of VOCs from the permeation system and the excellent repeatability and suitability of 10% PAN-ITEX for dynamic sampling. Further, the reliability of ISTD permeation system was proved by a consecutive 22 extractions, which showed RSD to be only 2.1%. This result confirmed the accuracy of ISTD addition into the ITEX before each air sampling.

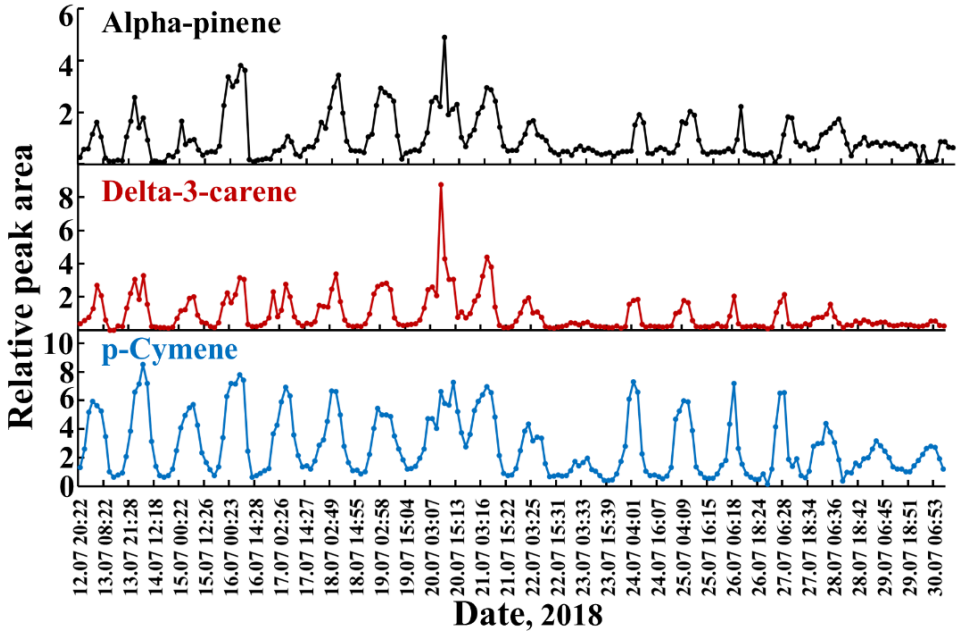

Figure 32. Variation of alpha-pinene, delta-3-carene, and p-cymene concentrations in atmospheric air at Kumpula Campus in July 2018, using 10% PAN ITEX-GC-MS method. Y-axis is the relative peak area of analyte (relative to ISTD).

The online dynamic ITEX system for air sampling is complicated and comprises of 10% PAN-ITEX, ISTD permeation system, airflow tubes, controlling software, GC-MS, PAL autosampler, and electronics for switching valves. Therefore, its reliability was examined for a consecutive 19-days

campaign. The successfully analyzed results proved preliminary that the system was robust and reliable. It proved to be suitable for a long-term campaign by running a sequence without any manual operation or even for on-site measurements by remote control. Figure 32 shows the relative peak area (analyte/ISTD) variation of alpha-pinene, delta-3-carene, and p-cymene, which are important precursors for aerosol formation, during these 19 days. In addition, this system is also feasible to analysis indoor and exhaled air. The components in the indoor air were similar to that in outdoor air except some chemicals used in chemistry laboratories such as ethyl acetate, chloroform, and pyridine. This is due to the ventilation system of the building, which is feeding the outdoor air into the laboratory. The successful analysis of exhaled air indicated the applicability of the system for the sampling of high humidity air.

4.6. Optimization of solid phase microextraction Arrow conditions

Sample volume

Based on the equation (7), SPME technique is independent with sample volume when $V_s \gg V_f$. However, in our cases, the size of the sample vial, extraction mode (HS or DI), SPME Arrow exposure and water amount in the headspace were the limitations to the sample volume. For HS extraction of phenols and amines (***Papers I, II and III***), to fully expose the 2 cm long coating in a 20 mL of sample vial and reduce the water condensation on the coating surface, the sample volume was controlled to be 5 or 7.5 mL. For DI extraction of hexachlorobutadiene and hexachlorobenzene (***Paper I***), 15 mL of sample was needed to fully immerse the coating.

Sample pH

pH is highly important for HS SPME to release acidic or basic analytes into the sample headspace. While it is not recommended to adjust the sample pH in DI SPME mode to guarantee the coating reusability. In ***Paper I***, low pH (pH=1) increased the extraction efficiency of Fe-BDC coating to chlorinated phenols due to analytes' acidity. However, for amines analysis by A-ZIF-8/PVC and OMS coated SPME Arrows (***Papers II and III***), a strong base (KOH) addition is the key point to neutralize and transfer amine compounds from the solution into the headspace.

Ionic strength

In all cases (***Papers I, II and III***), the addition of NaCl decrease the analytes' solubility in the sample and consequently improve the SPME Arrow method sensitivity (Figure 33). However, the method sensitivity for analyzing polar amines gained less benefit from NaCl than that for analyzing of medium polar phenols.

Agitation

The maximum agitation speed available in an autosampler (750 rpm) or magnetic stirrer (1400 rpm) was used to promote the transfer of the analytes or narrower the extraction boundary layer (***Papers I, II and III***).

Sample temperature

For amines extraction, the higher extraction temperature raises the amount of water in the sample headspace and its condensation on the coatings, which is thereby risky for the GC-MS analysis. Thus, room temperature and 40 ºC (lowest available temperature in the autosampler) were employed in manual and automated operations, respectively (***Papers II and III***). For extraction of chlorinated phenols, extraction temperature had both positive and negative effects (Figure 33), but to ensure the coating applicability, the extraction temperature could not be over 40 ºC (***Paper I***).

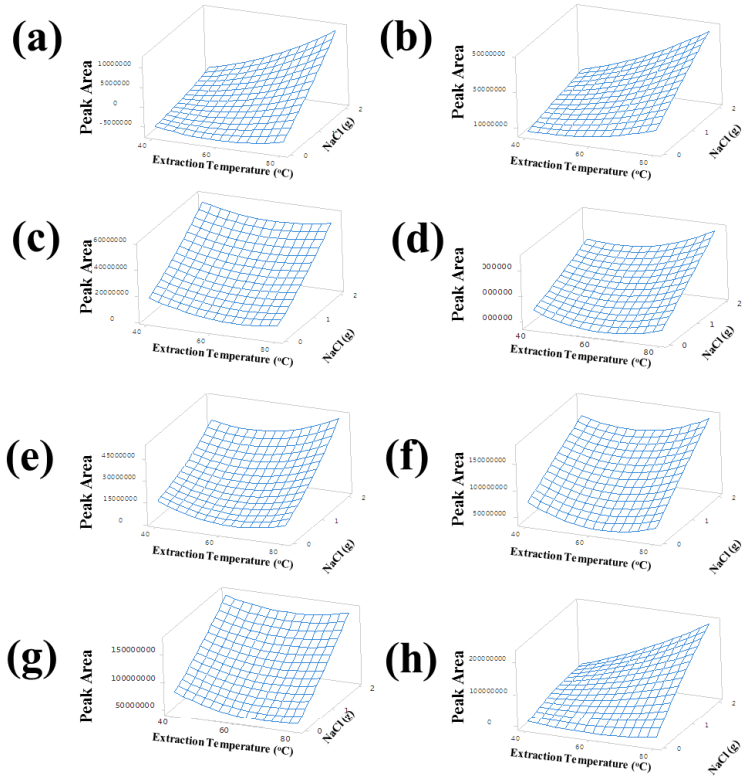

Figure 33. Response surface models of chlorinated phenols using Fe-BDC coated SPME Arrow to show the effect of extraction temperature and NaCl addition. (a) 2,6-dichlorophenol, (b) 2,3,5-trichlorophenol, (c) 2,3,4-trichlorophenol, (d) 2,3,6-trichlorophenol, (e) 2,4,6-trichlorophenol, (f) 2,3,4,6-tetrachlorophenol, (g) 2,3,4,5-tetrachlorophenol, and (h) pentachlorophenol.

Extraction time

Extraction time is one of the most crucial steps of SPME Arrow method development, which determine the feasibility of high sample throughput analysis. The equilibrium time of laboratory-made coatings was 40 min or less. In HS extraction mode, Fe-BDC, A-ZIF-8, and OMSs coatings achieved extraction equilibrium in 5-30 min. but UIO-66 coating needed 40 min, which is due to the slower diffusion kinetic in DI extraction mode (***Papers I, II and III***).

Desorption temperature

The selection of optimal desorption temperature was based on the thermal stability of the coatings, the boiling point of analytes and temperature range of GC. The thermal stability of Fe-BDC, A-ZIF-8/PVC and OMSs/PAN coating was not exceeded 270 ºC, which was, therefore, the highest desorption temperature for these coatings (***Papers I, II, III and V***). On the other hand, the UIO-66 coating was thermally stable up to 480 ºC but 280 ºC was used for the thermal desorption of UIO-66 coating to compromise the GC system (***Paper I***).

Desorption time

Desorption time was a compromise between desorption speed, desorption completion and method sensitivity. For polar amines, 0.5-1 min was enough to obtain 95% desorption of extracted analytes in

the coatings (***Papers II and III***). For low volatile hexachlorobutadiene and hexachlorobenzene, 3 min was enough to complete the desorption step (***Paper I***).

Sample incubation and SPME Arrow preconditioning

In the automated SPME Arrow process, the sample incubation was accompanied by SPME Arrow preconditioning. Therefore, the latter determined the time length of the former. The preconditioning time for all coating was 10 min to eliminate the memory effect on the coatings and consequently, the incubation time was 10 min (***Papers I, II and III***).

4.7. Optimization of in-tube extraction conditions

4.7.1. Online dynamic in-tube extraction

Online dynamic ITEX is an exhaustive technique, in which flow rate is the crucial parameter, which affects the quantitativeness, sample throughput and extraction yield of ITEX method. Based on equations (14) and (15), in an ITEX trap, the breakthrough time (t_b) determined by the linear velocity of the air. On the other hand, the flow rate ≥200 mL min^{-1} was risky to keep the tightness of the packed sorbent in the ITEX device and caused the breakthrough at the beginning of the sampling for low to high volatile template compounds, toluene, delta-3-carene and nonanal (Figure 34). Exhaustive extraction by online dynamic ITEX was achieved by lowering the flow rate to 56- or 35-mL min^{-1}. Further, the ISTD was retained in the ITEX tube over 30 min when the flow rate of 56 mL min^{-1} or lower was used. After considering the quantitation, time resolution and method sensitivity of the analytes, sampling at 56 mL min^{-1} for 30 min was the optimal condition for air sampling.

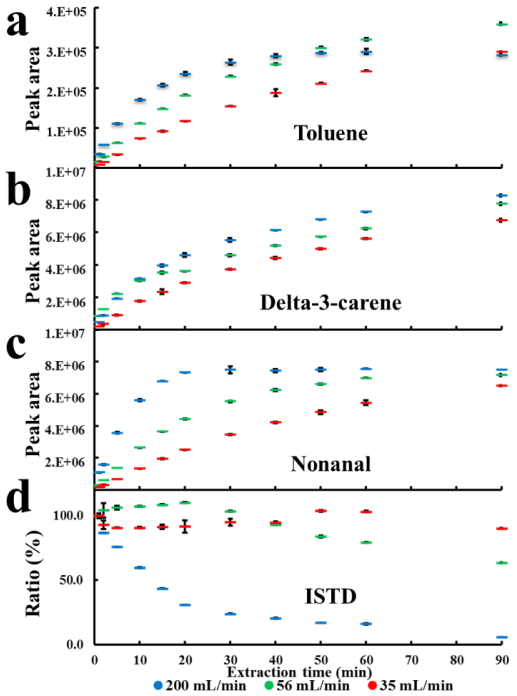

Figure 34. Extraction kinetics of (a) toluene, (b) delta-3-carene, (c) nonanal and (d) ISTD for 10% PAN-ITEX with 200, 56, and 35 mL min^{-1} flow rates.

In addition, ITEX trap and syringe temperature during the extraction showed a negative effect on extraction yield due to the exothermic adsorption process. Desorption temperature and desorption helium volume gave a positive effect on the analysis result. However, the PAN nanofibers were thermally stable up to 285 ºC and the maximum syringe desorption gas volume was 1.3 mL. Therefore, a desorption temperature of 240 °C and desorption volume of 800 µL were utilized, respectively. As an exception, injection speed had no obvious influence on the results.

4.7.2. In-tube extraction sampling accessories

Three types of traps were individually placed in front of the ITEX needle to prevent the aerosol, water or ozone effect on the air sampling with ITEX, which was carried by the drone. They all decreased the total number of compounds detected in the samples and the total peak area of these compounds. However, the positive thing of the trap design was to protect the compounds from oxidation during sampling.

4.8. Performance of the developed solid phase microextraction and in-tube extraction methods

The performance of the developed analytical methods used in this study, which were based on SPME Arrow and ITEX techniques, are summarized in Table 5. SPME Arrow-GC-MS methods gave the limits of quantitation (LOQs) from 0.03 to 10 ng mL^{-1}. Particularly, the LOQs for analyzing of chlorinated phenols, hexachlorobutadiene, and hexachlorobenzene were lower than the maximum allowable concentration in surface water by European Union and in drinking water by US Environmental Protection Agency [167, 168]. Further, MCM-41- and MCM-TP-SPME Arrow-GC-MS methods had a similar method sensitivity. In general, the SPME Arrow methods exhibited wide linear ranges, good linearity, and repeatability.

Table 5. Analytical performance of developed SPME Arrow and ITEX methods

Method	Analytes	LOQs	Linear range	Correlation coefficient (R^2)	RSD (%)	Paper
Fe-BDC-SPME Arrow -GC-MS	Chlorinated phenols	0.17-0.46 ng mL^{-1}	0.5-500 ng mL^{-1}	0.9945-0.9995	0.33-26.4	***I***
UIO-66-SPME Arrow -GC-MS	Hexachlorobutadiene Hexachlorobenzene	0.05-0.07 ng mL^{-1}	0.1-250 ng mL^{-1}	0.9964-0.9994	1.2-24.2	***I***
A-ZIF-8/PVC-SPME Arrow -GC-MS	TMA TEA	1 ng mL^{-1}	1-500 ng mL^{-1}	0.9839-0.9934	2.0-24.1	***II***
MCM-41-SPME Arrow -GC-MS	EA DEA TEA	0.03-5 ng mL^{-1}	0.03-500 ng mL^{-1}	0.9980-0.9984	0.5-20.1	***III***
MCM-TP -SPME Arrow -GC-MS	EA DEA TEA	0.03-10 ng mL^{-1}	0.03-1000 ng mL^{-1}	0.9955-0.9997	0.2-17.4	***III***
Online dynamic ITEX -GC-MS	Toluene p-Xylene Benzaldehyde Acetophenone 1,2,3-Trimethylbenzene	25-120 pg L^{-1}	30-19400 pg L^{-1}	0.9914-0.9989		***IV***

The representative VOCs that existed in atmospheric air in November 2018, Helsinki, Finland were selected as the template compounds for online dynamic ITEX-GC-MS method development. Owing to the exhaustive extraction nature of ITEX technique and large sampling volume (1.68 L of air), the LOQs of online dynamic ITEX-GC-MS method reached to pg L^{-1} level which is much lower than the concentration of some VOCs in atmospheric air and three magnitudes lower than with dynamic headspace ITEX methods [49, 54, 55, 57]. The wide linear range of this method predicted its applicability for long-term tracking of atmospheric air, in which the VOCs concentrations are time-

dependent and variable. Further, only 55 min total analysis time confirmed its suitability for high throughput analysis, which could be still shortened by using fast GC.

4.9. Developed solid phase microextraction Arrow and in-tube extraction methods for natural sample analysis

Wastewater

The concentrations of phenolic in the wastewater samples from Viikinmäki municipal wastewater treatment plant were lower than the LOQs of Fe-BDC-SPME Arrow-GC-MS method due to their restricted consumption in Finland (***Paper I)***. However, LMWAAs, for example, TMA and TEA, were found in high concentrations. A-ZIF-8/PVC SPME Arrow-GC-MS method determined TMA and TEA in influent wastewater to be 71±3 ng mL^{-1} and 271±20 ng mL^{-1}. After wastewater purification, TMA was eliminated (maybe because of high volatility) and TEA was only partially eliminated. These results were in good agreement with those obtained by PDMS/Carboxen-1000 Arrow-GC-MS method (***Paper II)***.

Mushroom

In ***Paper III***, DEA and TEA were detected from all six mushroom samples by MCM-41-and MCM-TP-SPME Arrow-GC-MS methods. Further, the DEA and TEA concentrations, which were determined by these two coatings, were in a good correlation with each other.

Salmon

TMA is the spoilage indicator of salmon. Under room temperature storage, the TMA content in salmon dramatically increased over 150 times in three days, which was obtained by both A-ZIF-8/PVC and PDMS/Carboxen-1000 SPME Arrow-GC-MS methods **(*Paper II*)**.

Atmospheric air

The concentrations of DEA and TEA in SMEAR II station ranged from 6.2 to 103.7 and from 0.1 to 8.6 ng m^{-3}, respectively, during the campaign in October 2018 which indicated the biogenic emission of LMWAAs in the boreal forest even at low temperatures (–1.4-3.3 ºC). On the other hand, snow inhibited these emissions **(*Paper III*)**.

Recovery tests

The recovery tests were performed in wastewater (***Papers I and II***) and mushroom (***Paper III***) samples to further confirm the applicability of the developed SPME Arrow-GC-MS methods and the accuracy of the results. In all SPME Arrow-GC-MS methods, the recoveries (n=3) of analytes were 68.4-105.1% (RSD%=1.3-23.1). As expected, more complicate sample matrix and lower spiking concentration caused lower recovery and higher RSDs values, and vice versa.

Online dynamic ITEX for automated and continuous air sampling

In a consecutive ten days' campaign in November 2018, five VOCs in atmospheric air (Kumpula Campus, University of Helsinki, Helsinki, Finland) were quantitatively monitored (Figure 35). Human activity-produced toluene, p-xylene, and 1,2,3-trimethylbenzene showed a regular day-to-night variation in terms of their concentrations, which were 0.07-1.3, 0.13-2.2, and 0.03-1.1 ng L^{-1}, respectively. However, the rain cleaned the pollutant in the air not only in the rainy days but also a few days after that. Further, benzaldehyde is well resistant to OH radicals and thereby showed relatively constant concentration during the days [169]. Phenol was detected in the campaign and its product acetophenone, formed by HOOH photo formation, concentration varied from 2.7 to 7.5 ng L^{-1} [170].

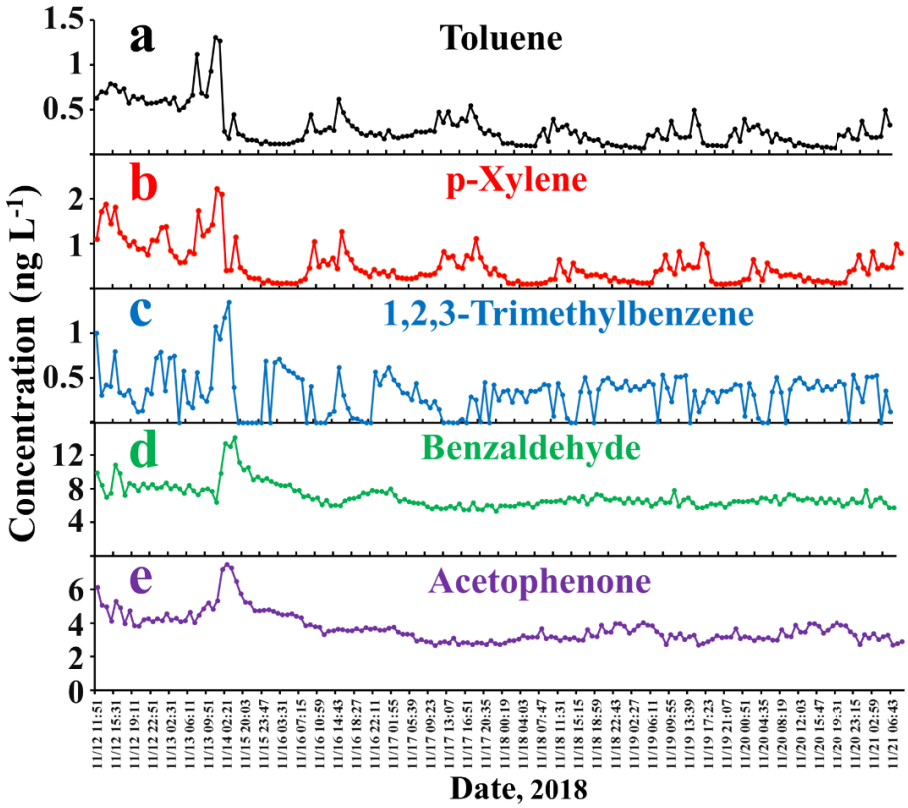

Figure 35. Variation of VOCs concentrations in atmospheric air in Kumpula Campus in November 2018, using 10% PAN ITEX-GC-MS method. (a) toluene, (b) p-xylene, (c) 1,2,3-trimethylbenzene, (d) benzaldehyde, and (e) acetophenone.

4.10. Drone as the platform for the microextraction devices in air sampling

When utilizing a drone as the platform to carry SPME Arrow and ITEX devices for passive and active sampling, the effect of drone horizontal and vertical displacements on the sampling was studied. The drone horizontal displacement had a positive effect, in terms of the number of compounds and total peak area of these compounds, on passive SPME Arrow because of the propellers-produced turbulences and airflow, which enhanced the interaction between the VOCs and SPME Arrow coatings. However, there was no significant influence on active ITEX due to its exhaustive nature.

In the vertical displacement, VOCs vertical profile distribution was the decisive factor to the sampling results. More compounds and larger peak area values of these compounds were measured with a lower sampling altitude (5 m VS 50 m). Eleven out of 28 and 5 out of 18 compounds for the SPME Arrow and ITEX sampling system, respectively, were only detected at a lower altitude. On the other hand, 13 compounds for SPME Arrow and 10 compounds for ITEX were detected in both altitudes.

The SPME Arrow and ITEX sampling in SMEAR II station and Siikaneva wetland were performed to evaluate the system applicability and the difference of air compositions in these two sites (Figure 36). In terms of the total number of compounds and total peak area, wetland air was more complex than forest air, which was found by both SPME Arrow and ITEX sampling systems. Some VOCs

(aldehydes, ketones, and alcohols) existed in both sites (14 and 17 for SPME Arrow and ITEX, respectively). However, 24 out of 38 and 36 out of 53 compounds for SPME Arrow and ITEX only existed in one of these two sampling sites. The contributors to the air differences included the different vegetation distribution at two sampling locations and the sampling time (2 days). Further, the characteristic VOCs in two sampling sites inspired us to process detailed research about the effect of the sampling location on the results. For example, sulphur-containing compounds were specific components (detected by both SPME Arrow and ITEX) in wetland air that indicated the incomplete humification of the organic matter in waterlogged and anoxic conditions [171].

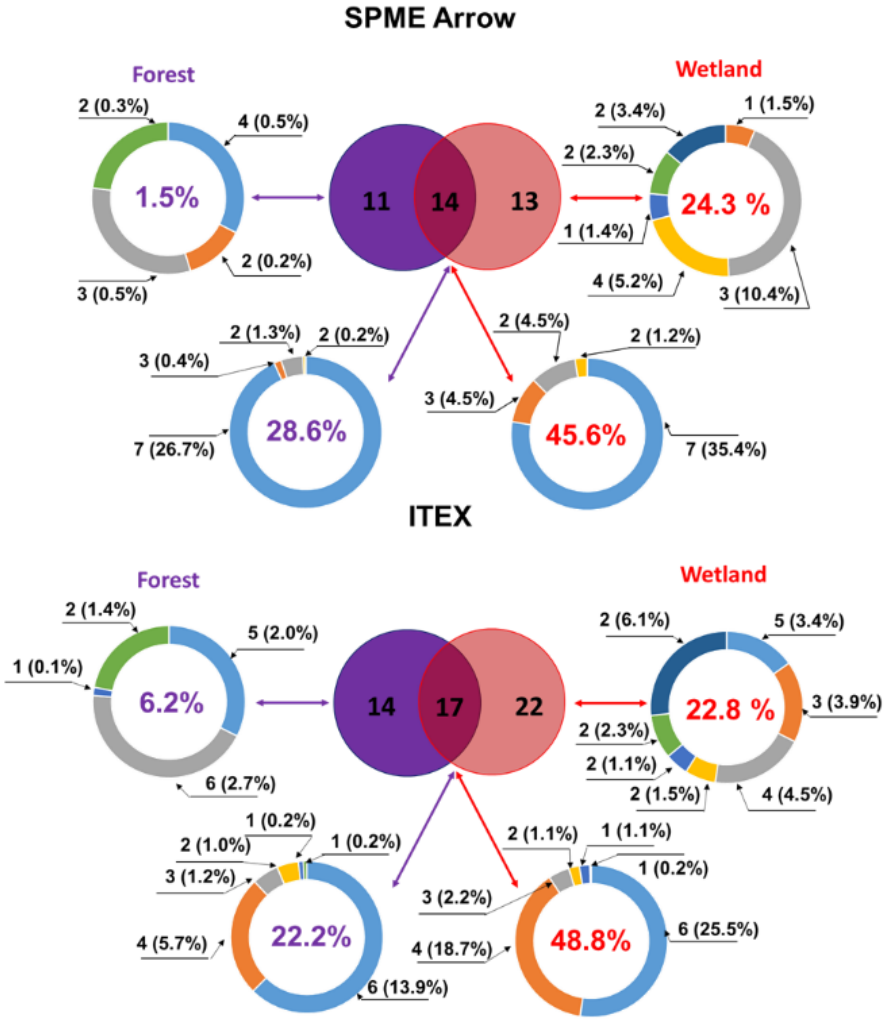

Figure 36. Results obtained for the analysis of air samples collected in difficult access locations by drone using simultaneous SPME Arrow and ITEX sampling systems. Venn diagrams compares samples collected in different places using the same sampling system. Doughnut charts show the results in terms of VOC composition. Number of compounds are noted as black numbers. Relative peak area values are noted as black numbers in brackets. Forest samples **(■)**; Wetland samples **(■)**; Aldehydes **(■)**; Ketones **(■)**; Alcohols **(■)**; Hydrocarbons **(■)**; Acids and derivatives **(■)**; Nitrogen containing compounds **(■)**; Sulphur containing compounds **(■)**.

5. Conclusions

The main goal of this doctoral dissertation was to study the effect of different materials on the performance of microextraction techniques and thereby to develop corresponding analytical methods for environmental, food, and biogenic chemistry studies. An objective was to compare commercially available and newly developed sorbent materials in terms of extraction affinity, extraction selectivity, and extraction kinetics. The potential applicability of an aerial drone as the carrier for new miniaturized passive and active samplers was demonstrated.

ALD- and MLD-conversion methods allowed to fabricate directly iron, aluminum, and Zr-BDC based MOFs for SPME Arrows. In these approaches, coating growth under atomic and molecular level was controlled and followed the gas phase reaction/conversion to form a MOFs coating on the substrate. The post-treatment of ALD and MLD films was crucial to obtain ideal SPME Arrow coatings. Extending the suspension time facilitates the thorough reaction between the metal precursor and organic linker and consequently lead to thicker coating. Appropriate conversion temperature enhanced the organic linker vaporization and prevented its decomposition. The preheated-Zr-BDC film avoided the damaging of Zr-BDC film by condensed acetic acid droplet. Fe-BDC coating was highly hydrophobic because of the unsaturated metal sites and thereby exhibited exceptional selectivity to benzene ring containing compounds. Zr-BDC converted UIO-66 coating was preferentially interacting with small, polar, aromatic, and long chain polar compounds due to its high porosity. Fe-BDC- and UIO-66-GC-MS methods allowed the selective analysis of organic pollutants from influent and effluent wastewater.

Acidified ZIF-8 was applicable as the SPME Arrow coating for selective extraction of LMWAAs from complex sample matrices. The ZIF-8 particles were immobilized on bare SPME Arrow by a physical adhesion approach, with PVC as the adhesive. This approach increased the coating stability and thickness and consequently extraction capacity. The pore size of ZIF-8 can be adjusted by a headspace acidification approach, which increased dramatically the pore accessibility to LMWAAs. The coating fabrication process was reproducible, and the coating was reusable. A-ZIF-8-SPME Arrow-GC-MS method was applicable for the determination of trace level amines in wastewater, salmon and mushroom samples, and the results were comparable with those achieved by commercial PDMS/Carboxen-1000 SPME Arrow system.

MCM-41 and MCM-TP showed an exceptional extraction selectivity and fast kinetics to LMWAAs when compared with commercial and other OMSs coatings. The principles of extraction selectivity and extraction kinetic are size exclusion and acid-base interaction. SPME Arrow with MCM-41 and MCM-TP coatings had two-dimensional channels and a pore width under four nm, which facilitated the extraction of targeted analytes and excluded smaller or larger molecules. The surface acidity of silica materials was enhanced after introducing more acidic Lewis and Brønsted sites by modifying with -TP groups. The MCM-41- and MCM-TP-SPME Arrow-GC-MS methods were successfully used to identify and quantify LMWAAs in mushroom, atmospheric air, and urine samples.

The ITEX tube packed with 10% PAN nanofibers featured excellent permeability and high extraction affinity to biogenic and anthropogenic VOCs compared to other nanofibers and commercially available ITEXs, due to the uniform diameter, rich surface functional groups and good thermal stability of the 10% PAN nanofibers. The system allowed the development of a fully automated online dynamic ITEX-GC-MS method and its application to monitor atmospheric, indoor, and exhaled air samples. Detected VOCs in the air were further identified and/or quantified. This fully automated and robust system is important for long-term campaigns that need reliable sampling and timesaving operation.

The aerial drone was well applicable as the carrier of miniaturized sampling systems for air sampling in difficultly accessible places, such as forest or wetlands. The drone allowed carrying two SPME Arrows (4 in manual mode) and 2 ITEX devices simultaneously during a flight. Sampling by remote control enabled to prevent contaminations and other negative effects on the sampling devices. Accessories, applicable for ITEX devices can be used to eliminate the undesirable chemical reactions during the sampling of VOCs. ITEX sampling was not significantly affected by vertical and horizontal displacements of the drone. Instead, the horizontal displacement had a clear influence on SPME Arrow sampling. The selectivity of MCM-41-Ti-SPME Arrow and PAN-ITEX agreed well with the previous experiments.

The proposed materials and methods demonstrated the great potential for a more accurate and informative analysis of VOCs and hazardous compounds in various sample matrices. They were selective, reusable, and reproducible. Further, they provided better extraction affinity to target analytes compared to commercially available materials. The developed SPME Arrow and ITEX based methods enabled sensitive, timesaving, and laborsaving analysis. Aerial drone proved to be an ideal carrier for the miniaturized sampler for air sampling. However, some improvements are still needed. For example, 1) the ALD and MLD based methods can be improved to deposit thicker SPME Arrow coatings, 2) SPME Arrows can be utilized for the development of online dynamic methods to selectively monitor a certain group of compounds, 3) new materials are needed for selective extraction of other small and polar VOCs through selection of silica substrate and functional groups, 4) the analytical method sensitivity can be further improved by new packing materials in ITEX devices, 5) the online dynamic ITEX system coupled to GC with high-resolution MS detector or GC-MS/MS can provide more informative results, 6) more powerful air pump and battery are required in order to increase the number of air samples during the flight, 7) the conventional GC-MS can be replaced with portable GC-MS to achieve the fast on-site measurements in the difficult access locations.

References

[1] J.W. Robinson, E.M.S. Frame, G.M. Frame II, Undergraduate instrumental analysis, CRC press, 2014.
[2] E.P. Popek, Sampling and analysis of environmental chemical pollutants: a complete guide, Elsevier, 2017.
[3] T.G. Gregoire, H.T. Valentine, Sampling strategies for natural resources and the environment, Chapman and Hall/CRC, 2007.
[4] E. Baltussen, C. Cramers, P. Sandra, Sorptive sample preparation–a review, Analytical Bioanalytical Chemistry, 373 (2002) 3-22.
[5] C.W. Huie, A review of modern sample-preparation techniques for the extraction and analysis of medicinal plants, Analytical Bioanalytical Chemistry, 373 (2002) 23-30.
[6] R.M. Smith, Before the injection-modern methods of sample preparation for separation techniques, Journal of Chromatography A, 1000 (2003) 3-27.
[7] J. Beltrán, F.J. López, F. Hernández, Solid-phase microextraction in pesticide residue analysis, Journal of Chromatography A, 885 (2000) 389-404.
[8] H. Kataoka, Automated sample preparation using in-tube solid-phase microextraction and its application-a review, Analytical Bioanalytical Chemistry, 373 (2002) 31-45.
[9] H.L. Lord, W. Zhan, J. Pawliszyn, Fundamentals and applications of needle trap devices: a critical review, Analytica Chimica Acta, 677 (2010) 3-18.
[10] N. Lorenzo-Parodi, W. Kaziur, N. Stojanović, M.A. Jochmann, T.C. Schmidt, Solventless microextraction techniques for water analysis, TrAC Trends in Analytical Chemistry, 113 (2018) 321-331.
[11] J. Pawliszyn, Handbook of solid phase microextraction, Elsevier, 2011.
[12] C.S. Gordon, J.T. Lowe, Carbon-monoxide detector, US Patents, 1927.
[13] E. Palmes, A.F. Gunnison, Personal monitoring device for gaseous contaminants, American Industrial Hygiene Association Journal, 34 (1973) 78-81.
[14] K.D. Reiszner, P.W. West, Collection and determination of sulfur dioxide incorporating permeation and West-Gaeke procedure, Environmental Science & Technology, 7 (1973) 526-532.
[15] T. Górecki, J. Namieśnik, Passive sampling, TrAC Trends in Analytical Chemistry, 21 (2002) 276-291.
[16] L. Melymuk, P. Bohlin, O.e. Sáňka, K. Pozo, J. Klánová, Current challenges in air sampling of semivolatile organic contaminants: sampling artifacts and their influence on data comparability, Environmental Science & Technology, 48 (2014) 14077-14091.
[17] J. Namiesnik, T. Gorecki, E. Kozlowski, L. Torres, J. Mathieu, Passive dosimeters-an approach to atmospheric pollutants analysis, Science of the Total Environment, 38 (1984) 225-258.
[18] B. Kozdroń-Zabiegata, J. Namieśnik, A. Przyjazny, Use of passive dosimeters for evaluation of the quality of indoor and outdoor air, Indoor Environment, 4 (1995) 189-203.
[19] S. Seethapathy, T. Gorecki, X. Li, Passive sampling in environmental analysis, Journal of Chromatography A, 1184 (2008) 234-253.
[20] B. Vrana, I.J. Allan, R. Greenwood, G.A. Mills, E. Dominiak, K. Svensson, J. Knutsson, G. Morrison, Passive sampling techniques for monitoring pollutants in water, TrAC Trends in Analytical Chemistry, 24 (2005) 845-868.
[21] P.A. Martos, J. Pawliszyn, Time-weighted average sampling with solid-phase microextraction device: implications for enhanced personal exposure monitoring to airborne pollutants, Analytical Chemistry, 71 (1999) 1513-1520.
[22] H. Piri-Moghadam, M.N. Alam, J. Pawliszyn, Review of geometries and coating materials in solid phase microextraction: opportunities, limitations, and future perspectives, Analytica Chimica Acta, 984 (2017) 42-65.
[23] L.M.F. Barreira, G. Duporté, J. Parshintsev, K. Hartonen, M. Jussila, J. Aalto, J. Bäck, M. Kulmala, M.-L. Riekkola, Emissions of biogenic volatile organic compounds from the boreal forest

floor and understory: a study by solid-phase microextraction and portable gas chromatography-mass spectrometry, Boreal Environment Research, 22 (2017) 393-413.
[24] L.M.F. Barreira, J. Parshintsev, N. Kärkkäinen, K. Hartonen, M. Jussila, M. Kajos, M. Kulmala, M.-L. Riekkola, Field measurements of biogenic volatile organic compounds in the atmosphere by dynamic solid-phase microextraction and portable gas chromatography-mass spectrometry, Atmospheric Environment, 115 (2015) 214-222.
[25] B. Eckenrode, Environmental and forensic applications of field-portable GC-MS: an overview, Journal of the American Society for Mass Spectrometry, 12 (2001) 683-693.
[26] L.M.F. Barreira, G. Duporté, T. Rönkkö, J. Parshintsev, K. Hartonen, L. Hyrsky, E. Heikkinen, M. Jussila, M. Kulmala, M.-L. Riekkola, Field measurements of biogenic volatile organic compounds in the atmosphere using solid-phase microextraction Arrow, Atmospheric Measurement Techniques, 11 (2018) 881-893.
[27] G.A. Gómez-Ríos, T. Vasiljevic, E. Gionfriddo, M. Yu, J. Pawliszyn, Towards on-site analysis of complex matrices by solid-phase microextraction-transmission mode coupled to a portable mass spectrometer via direct analysis in real time, Analyst, 142 (2017) 2928-2935.
[28] J.J. Grandy, E. Boyacı, J. Pawliszyn, Development of a carbon mesh supported thin film microextraction membrane as a means to lower the detection limits of benchtop and portable GC/MS instrumentation, Analytical Chemistry, 88 (2016) 1760-1767.
[29] Y.A. Olcer, M. Tascon, A.E. Eroglu, E. Boyaci, Thin film microextraction: towards faster and more sensitive microextraction, TrAC Trends in Analytical Chemistry, 113 (2019) 93-101.
[30] T. Dittmar, B. Koch, N. Hertkorn, G. Kattner, A simple and efficient method for the solid-phase extraction of dissolved organic matter (SPE-DOM) from seawater, Limnology Oceanography: Methods, 6 (2008) 230-235.
[31] I.-Y. Eom, A.-M. Tugulea, J. Pawliszyn, Development and application of needle trap devices, Journal of Chromatography A, 1196 (2008) 3-9.
[32] S.B. Hawthorne, A. Kubatova, Sampling and sample preparation for field and laboratory, Comprehensive Analytical Chemistry, (2002) 587-608.
[33] Y. Su, H. Hung, E. Sverko, P. Fellin, H. Li, Multi-year measurements of polybrominated diphenyl ethers (PBDEs) in the Arctic atmosphere, Atmospheric Environment, 41 (2007) 8725-8735.
[34] S.D. Supowit, I.B. Roll, V.D. Dang, K.J. Kroll, N.D. Denslow, R.U. Halden, Active sampling device for determining pollutants in surface and pore water-the in situ sampler for biphasic water monitoring, Scientific Reports, 6 (2016) 21886.
[35] M.-C. Hennion, Solid-phase extraction: method development, sorbents, and coupling with liquid chromatography, Journal of Chromatography A, 856 (1999) 3-54.
[36] J. Rydberg, Solvent extraction principles and practice, revised and expanded, CRC press, 2004.
[37] R.M. Smith, Before the injection-modern methods of sample preparation for separation techniques, Journal of Chromatography A, 1000 (2003) 3-27.
[38] C.L. Arthur, J. Pawliszyn, Solid phase microextraction with thermal desorption using fused silica optical fibers, Analytical Chemistry, 62 (1990) 2145-2148.
[39] C. Poole, Z. Mester, M. Miró, S. Pedersen-Bjergaard, J. Pawliszyn, Glossary of terms used in extraction (IUPAC Recommendations 2016), Pure and Applied Chemistry, 88 (2016) 517-558.
[40] A. Kremser, M.A. Jochmann, T.C. Schmidt, PAL SPME Arrow-evaluation of a novel solid-phase microextraction device for freely dissolved PAHs in water, Analytical Bioanalytical Chemistry, 408 (2016) 943-952.
[41] A.K. Huba, M.F. Mirabelli, R. Zenobi, High-throughput screening of PAHs and polar trace contaminants in water matrices by direct solid-phase microextraction coupled to a dielectric barrier discharge ionization source, Analytica Chimica Acta, 1030 (2018) 125-132.
[42] A. Helin, T. Rönkkö, J. Parshintsev, K. Hartonen, B. Schilling, T. Läubli, M.-L. Riekkola, Solid phase microextraction Arrow for the sampling of volatile amines in wastewater and atmosphere, Journal of Chromatography A, 1426 (2015) 56-63.

[43] K. Eckert, D. Carter, K. Perrault, Sampling Dynamics for Volatile Organic Compounds Using Headspace Solid-Phase Microextraction Arrow for Microbiological Samples, Separations, 5 (2018) 45.
[44] Ó. Castro, L. Trabalón, B. Schilling, F. Borrull, E. Pocurull, Solid phase microextraction Arrow for the determination of synthetic musk fragrances in fish samples, Journal of Chromatography A, 1591 (2019) 55-61.
[45] L.-C. Salanţă, M. Tofană, S.A. Socaci, C.L. Pop, D. Michiu, A. Fărcaş, Determination of the volatile compounds from hop and hop products using ITEX/GC-MS technique, Journal of Agroalimentary Processes and Technologies, 18 (2012) 110-115.
[46] I. Rasanen, J. Viinamäki, E. Vuori, I. Ojanperä, Headspace in-tube extraction gas chromatography-mass spectrometry for the analysis of hydroxylic methyl-derivatized and volatile organic compounds in blood and urine, Journal of Analytical Toxicology, 34 (2010) 113-121.
[47] D. Michiu, S.A. Socaci, M.A. Jimborean, E. Mudura, A.C. Fărcaş, S.E. Biriş-Dorhoi, M. Tofană, Determination of Volatile Markers from Magnum Hops in Beer by In-Tube Extraction-Gas Chromatography-Mass Spectrometry, Analytical Letters, 51 (2018) 2967-2980.
[48] J. Laaks, M.A. Jochmann, B. Schilling, T.C. Schmidt, Optimization strategies of in-tube extraction (ITEX) methods, Analytical and Bioanalytical Chemistry, 407 (2015) 6827-6838.
[49] J. Laaks, M.A. Jochmann, B. Schilling, T.C. Schmidt, In-tube extraction of volatile organic compounds from aqueous samples: an economical alternative to purge and trap enrichment, Analytical Chemistry, 82 (2010) 7641-7648.
[50] J. Laaks, M.A. Jochmann, B. Schilling, K. Molt, T.C. Schmidt, In-tube extraction-GC-MS as a high-capacity enrichment technique for the analysis of alcoholic beverages, Journal of Agricultural and Food Chemistry, 62 (2014) 3081-3091.
[51] M. Kusano, M. Kobayashi, Y. Iizuka, A. Fukushima, K. Saito, Unbiased profiling of volatile organic compounds in the headspace of Allium plants using an in-tube extraction device, BMC Research Notes, 9 (2016) 133.
[52] M. Kupska, H.H. Jeleń, In-tube extraction for the determination of the main volatile compounds in Physalis peruviana L, Journal of Separation Science, 40 (2017) 532-541.
[53] K. Kędziora-Koch, W. Wasiak, Needle-based extraction techniques with protected sorbent as powerful sample preparation tools to gas chromatographic analysis: Trends in application, Journal of Chromatography A, 1565 (2018) 1-18.
[54] M.A. Jochmann, X. Yuan, B. Schilling, T.C. Schmidt, In-tube extraction for enrichment of volatile organic hydrocarbons from aqueous samples, Journal of Chromatography A, 1179 (2008) 96-105.
[55] T. Hüffer, X.L. Osorio, M.A. Jochmann, B. Schilling, T.C. Schmidt, Multi-walled carbon nanotubes as sorptive material for solventless in-tube microextraction (ITEX2)-a factorial design study, Analytical and Bioanalytical Chemistry, 405 (2013) 8387-8395.
[56] J. Hu, E. Pagliano, X. Hou, C. Zheng, L. Yang, Z. Mester, Sub-ppt determination of butyltins, methylmercury and inorganic mercury in natural waters by dynamic headspace in-tube extraction and GC-ICPMS detection, Journal of Analytical Atomic Spectrometry, 32 (2017) 2447-2454.
[57] A. Akinlua, M. Jochmann, J. Laaks, A. Ewert, T. Schmidt, Microwave-assisted nonionic surfactant extraction of aliphatic hydrocarbons from petroleum source rock, Analytica Chimica Acta, 691 (2011) 48-55.
[58] J. Ruiz-Jimenez, N. Zanca, H. Lan, M. Jussila, K. Hartonen, M.-L. Riekkola, Aerial drone as a carrier for miniaturized air sampling systems, Journal of Chromatography A, 1597 (2019) 202-208.
[59] G.A. Gómez-Ríos, N.R. Garcés, M. Tascon, Smart Materials in Solid Phase Microextraction (SPME), Handbook of Smart Materials in Analytical Chemistry, (2019) 581-620.
[60] H. Lord, B. Bojko, Drug Analysis by SPME, in Handbook of Solid Phase Microextraction, (2012) 335-382.
[61] K.H. Schueler, C. Schillig, Extraction device, US Patents, 2014.

[62] J. Pawliszyn, Needle trap, US Patents, 2002.
[63] J.A. Koziel, M. Odziemkowski, J. Pawliszyn, Sampling and analysis of airborne particulate matter and aerosols using in-needle trap and SPME fiber devices, Analytical Chemistry, 73 (2001) 47-54.
[64] P. Loevkvist, J.A. Joensson, Capacity of sampling and preconcentration columns with a low number of theoretical plates, Analytical Chemistry, 59 (1987) 818-821.
[65] T. Górecki, J. Pawliszyn, Effect of Sample Volume on Quantitative Analysis by Solid-phase MicroextractionPart 1. Theoretical Considerations, Analyst, 122 (1997) 1079-1086.
[66] F.A. Dullien, Porous media: fluid transport and pore structure, Academic press, 2012.
[67] M. Mieth, J.K. Schubert, T. Gröger, B. Sabel, S. Kischkel, P. Fuchs, D. Hein, R. Zimmermann, W. Miekisch, Automated needle trap heart-cut GC/MS and needle trap comprehensive two-dimensional GC/TOF-MS for breath gas analysis in the clinical environment, Analytical Chemistry, 82 (2010) 2541-2551.
[68] M. Mieth, S. Kischkel, J.K. Schubert, D. Hein, W. Miekisch, Multibed needle trap devices for on site sampling and preconcentration of volatile breath biomarkers, Analytical Chemistry, 81 (2009) 5851-5857.
[69] F. Barreira, L. Miguel, Y. Xue, G. Duporte, J. Parshintsev, K. Hartonen, M. Jussila, M. Kulmala, M.-L. Riekkola, Potential of needle trap microextraction-portable gas chromatography-mass spectrometry for measurement of atmospheric volatile compounds, Atmospheric Measurement Techniques, 9 (2016) 3661-3671.
[70] W.G. Cochran, Sampling techniques, John Wiley & Sons, 2007.
[71] B. Buszewski, M. Szultka, Past, present, and future of solid phase extraction: a review, Critical Reviews in Analytical Chemistry, 42 (2012) 198-213.
[72] J. Xu, J. Zheng, J. Tian, F. Zhu, F. Zeng, C. Su, G. Ouyang, New materials in solid-phase microextraction, TrAC Trends in Analytical Chemistry, 47 (2013) 68-83.
[73] Z.-M. Huang, Y.-Z. Zhang, M. Kotaki, S. Ramakrishna, technology, A review on polymer nanofibers by electrospinning and their applications in nanocomposites, Composites Science, 63 (2003) 2223-2253.
[74] F.E. Ahmed, B.S. Lalia, R. Hashaikeh, A review on electrospinning for membrane fabrication: challenges and applications, Desalination, 356 (2015) 15-30.
[75] S. Jiang, Y. Chen, G. Duan, C. Mei, A. Greiner, S. Agarwal, Electrospun nanofiber reinforced composites: a review, Polymer Chemistry, 9 (2018) 2685-2720.
[76] M. Háková, L.C. Havlíková, P. Solich, F. Švec, D. Šatínský, Electrospun nanofiber polymers as extraction phases in analytical chemistry-the advances of the last decade, TrAC Trends in Analytical Chemistry, (2018).
[77] J. Xue, J. Xie, W. Liu, Y. Xia, Electrospun nanofibers: new concepts, materials, and applications, Accounts of Chemical Research, 50 (2017) 1976-1987.
[78] J.L. Daristotle, A.M. Behrens, A.D. Sandler, P. Kofinas, A review of the fundamental principles and applications of solution blow spinning, ACS Applied Materials & Interfaces, 8 (2016) 34951-34963.
[79] J. Holopainen, M.J. Heikkilä, L.D. Salmi, K. Ainassaari, M. Ritala, Zeolitic imidazole Framework-8 (ZIF-8) fibers by gas-phase conversion of electroblown zinc oxide and aluminum doped zinc oxide fibers, Microporous and Mesoporous Materials, 267 (2018) 212-220.
[80] J. Holopainen, M. Ritala, Rapid production of bioactive hydroxyapatite fibers via electroblowing, Journal of the European Ceramic Society, 36 (2016) 3219-3224.
[81] E.S. Medeiros, G.M. Glenn, A.P. Klamczynski, W.J. Orts, L.H.C. Mattoso, Solution blow spinning: A new method to produce micro- and nanofibers from polymer solutions, Journal of Applied Polymer Science, 113 (2009) 2322-2330.
[82] D. Tang, X. Zhuang, C. Zhang, B. Cheng, X. Li, Generation of nanofibers via electrostatic-Induction-assisted solution blow spinning, Journal of Applied Polymer Science, 132 (2015) 42326.

[83] Y. Zhang, L. Gao, N. Deng, M. Ya, H. He, W. Kang, B. Cheng, Fabrication of porous and magnetic Fe/FeNX fibers by electro-blown spinning method for efficient adsorption of Cr (VI) ions, Materials Letters, 212 (2018) 235-238.
[84] J. Lee, O.K. Farha, J. Roberts, K.A. Scheidt, S.T. Nguyen, J.T. Hupp, Metal-organic framework materials as catalysts, Chemical Society Reviews, 38 (2009) 1450-1459.
[85] H.-C. Zhou, J.R. Long, O.M. Yaghi, Introduction to metal-organic frameworks, Chemical Reviews, 112 (2012) 673-674.
[86] O.M. Yaghi, H. Li, Hydrothermal synthesis of a metal-organic framework containing large rectangular channels, Journal of the American Chemical Society, 117 (1995) 10401-10402.
[87] A. Betard, R.A. Fischer, Metal-organic framework thin films: from fundamentals to applications, Chemical Reviews, 112 (2011) 1055-1083.
[88] N.C. Burtch, H. Jasuja, K.S. Walton, Water stability and adsorption in metal-organic frameworks, Chemical Reviews, 114 (2014) 10575-10612.
[89] S.M. Cohen, Postsynthetic methods for the functionalization of metal-organic frameworks, Chemical Reviews, 112 (2011) 970-1000.
[90] Y. Cui, Y. Yue, G. Qian, B. Chen, Luminescent functional metal-organic frameworks, Chemical Reviews, 112 (2011) 1126-1162.
[91] K.J. Gagnon, H.P. Perry, A. Clearfield, Conventional and unconventional metal-organic frameworks based on phosphonate ligands: MOFs and UMOFs, Chemical Reviews, 112 (2011) 1034-1054.
[92] Z.-Y. Gu, C.-X. Yang, N. Chang, X.-P. Yan, Metal-organic frameworks for analytical chemistry: from sample collection to chromatographic separation, Accounts of Chemical Research, 45 (2012) 734-745.
[93] L.E. Kreno, K. Leong, O.K. Farha, M. Allendorf, R.P. Van Duyne, J.T. Hupp, Metal-organic framework materials as chemical sensors, Chemical Reviews, 112 (2011) 1105-1125.
[94] C. Wang, T. Zhang, W. Lin, Rational synthesis of noncentrosymmetric metal-organic frameworks for second-order nonlinear optics, Chemical Reviews, 112 (2011) 1084-1104.
[95] J.-P. Zhang, Y.-B. Zhang, J.-B. Lin, X.-M. Chen, Metal azolate frameworks: from crystal engineering to functional materials, Chemical Reviews, 112 (2011) 1001-1033.
[96] Y.-R. Lee, J. Kim, W.-S. Ahn, Synthesis of metal-organic frameworks: A mini review, Korean Journal of Chemical Engineering, 30 (2013) 1667-1680.
[97] N. Stock, S. Biswas, Synthesis of metal-organic frameworks (MOFs): routes to various MOF topologies, morphologies, and composites, Chemical Reviews, 112 (2011) 933-969.
[98] E. Ahvenniemi, M. Karppinen, Atomic/molecular layer deposition: a direct gas-phase route to crystalline metal-organic framework thin films, Chemical Communications, 52 (2016) 1139-1142.
[99] K.B. Lausund, O. Nilsen, All-gas-phase synthesis of UiO-66 through modulated atomic layer deposition, Nature communications, 7 (2016) 13578.
[100] L.D. Salmi, M.J. Heikkilä, E. Puukilainen, T. Sajavaara, D. Grosso, M. Ritala, Studies on atomic layer deposition of MOF-5 thin films, Microporous and Mesoporous Materials, 182 (2013) 147-154.
[101] L.D. Salmi, M.J. Heikkilä, M. Vehkamäki, E. Puukilainen, M. Ritala, T. Sajavaara, Studies on atomic layer deposition of IRMOF-8 thin films, Journal of Vacuum Science & Technology A: Vacuum, Surfaces, and Films, 33 (2015) 01A121.
[102] I. Stassen, M. Styles, G. Grenci, H. Van Gorp, W. Vanderlinden, S. De Feyter, P. Falcaro, D. De Vos, P. Vereecken, R. Ameloot, Chemical vapour deposition of zeolitic imidazolate framework thin films, Nature Materials, 15 (2016) 304.
[103] R. Mikko, J. Niinistö, Chemical vapour deposition: precursors, processes and applications, Royal Society of Chemistry, 2009.
[104] Z. Alothman, A review: fundamental aspects of silicate mesoporous materials, Materials, 5 (2012) 2874-2902.

[105] M. Sajid, Porous membrane protected micro-solid-phase extraction: a review of features, advancements and applications, Analytica Chimica Acta, 965 (2017) 36-53.
[106] C. Bharti, U. Nagaich, A.K. Pal, N. Gulati, Mesoporous silica nanoparticles in target drug delivery system: A review, International Journal of Pharmaceutical Investigation, 5 (2015) 124.
[107] S. Jun, S.H. Joo, R. Ryoo, M. Kruk, M. Jaroniec, Z. Liu, T. Ohsuna, O. Terasaki, Synthesis of new, nanoporous carbon with hexagonally ordered mesostructure, Journal of the American Chemical Society, 122 (2000) 10712-10713.
[108] S.-H. Wu, C.-Y. Mou, H.-P. Lin, Synthesis of mesoporous silica nanoparticles, Chemical Society Reviews, 42 (2013) 3862-3875.
[109] O. Núñez, K. Nakanishi, N. Tanaka, Preparation of monolithic silica columns for high-performance liquid chromatography, Journal of Chromatography A, 1191 (2008) 231-252.
[110] T. Asefa, Z. Tao, Mesoporous silica and organosilica materials-Review of their synthesis and organic functionalization, Canadian Journal of Chemistry, 90 (2012) 1015-1031.
[111] E. Da'na, Adsorption of heavy metals on functionalized-mesoporous silica: A review, Microporous and Mesoporous Materials, 247 (2017) 145-157.
[112] J.M. Rosenholm, E. Peuhu, J.E. Eriksson, C. Sahlgren, M. Lindén, Targeted intracellular delivery of hydrophobic agents using mesoporous hybrid silica nanoparticles as carrier systems, Nano Letters, 9 (2009) 3308-3311.
[113] S. Armenta, S. Garrigues, M. de la Guardia, Green analytical chemistry, TrAC Trends in Analytical Chemistry, 27 (2008) 497-511.
[114] C.L. Arthur, L.M. Killam, K.D. Buchholz, J. Pawliszyn, J.R. Berg, Automation and optimization of solid-phase microextraction, Analytical Chemistry, 64 (1992) 1960-1966.
[115] S. Risticevic, H. Lord, T. Gorecki, C.L. Arthur, J. Pawliszyn, Protocol for solid-phase microextraction method development, Nature Protocols, 5 (2010) 122.
[116] E.A. Souza-Silva, R. Jiang, A. Rodriguez-Lafuente, E. Gionfriddo, J. Pawliszyn, A critical review of the state of the art of solid-phase microextraction of complex matrices I. Environmental analysis, TrAC Trends in Analytical Chemistry, 71 (2015) 224-235.
[117] F.Y. Lai, C. Rauert, L. Gobelius, L. Ahrens, A critical review on passive sampling in air and water for per-and polyfluoroalkyl substances (PFASs), TrAC Trends in Analytical Chemistry, (2018).
[118] D.S. McLagan, M.E.E. Mazur, C.P.J. Mitchell, F. Wania, Passive air sampling of gaseous elemental mercury: a critical review, Atmospheric Chemistry and Physics, 16 (2016) 3061-3076.
[119] E. Boyacı, A. Rodriguez-Lafuente, K. Gorynski, F. Mirnaghi, E.A. Souza-Silva, D. Hein, J. Pawliszyn, Sample preparation with solid phase microextraction and exhaustive extraction approaches: Comparison for challenging cases, Analytica Chimica Acta, 873 (2015) 14-30.
[120] H. Piri-Moghadam, F. Ahmadi, J. Pawliszyn, A critical review of solid phase microextraction for analysis of water samples, TrAC Trends in Analytical Chemistry, 85 (2016) 133-143.
[121] P. Ventura Diaz, S. Yoon, High-fidelity computational aerodynamics of multi-rotor unmanned aerial vehicles, 2018 AIAA Aerospace Sciences Meeting, (2018), 1266.
[122] K. Peräjärvi, J. Lehtinen, R. Pöllänen, H. Toivonen, Design of an air sampler for a small unmanned aerial vehicle, Radiation Protection Dosimetry, 132 (2008) 328-333.
[123] Y. Avakov, Environmental Monitoring UAV System, US Patents, 2018.
[124] O. Black, J. Chen, A. Scircle, Y. Zhou, J.V. Cizdziel, Adaption and use of a quadcopter for targeted sampling of gaseous mercury in the atmosphere, Environmental Science and Pollution Research, 25 (2018) 13195-13202.
[125] C.-C. Chang, J.-L. Wang, C.-Y. Chang, M.-C. Liang, M.-R. Lin, Development of a multicopter-carried whole air sampling apparatus and its applications in environmental studies, Chemosphere, 144 (2016) 484-492.
[126] J. Chen, A. Scircle, O. Black, J.V. Cizdziel, N. Watson, D. Wevill, Y. Zhou, On the use of multicopters for sampling and analysis of volatile organic compounds in the air by adsorption/thermal desorption GC-MS, Air Quality, Atmosphere & Health, 11 (2018) 835-842.

[127] C.E. Corrigan, G.C. Roberts, M.V. Ramana, D. Kim, V. Ramanathan, Capturing vertical profiles of aerosols and black carbon over the Indian Ocean using autonomous unmanned aerial vehicles, Atmospheric Chemistry and Physics, 8 (2008) 737-747.
[128] Y. Kostyukevich, D. Efremov, V. Ionov, E. Kukaev, E. Nikolaev, Remote detection of explosives using field asymmetric ion mobility spectrometer installed on multicopter, Journal of Mass Spectrometry, 52 (2017) 777-782.
[129] T. Villa, F. Salimi, K. Morton, L. Morawska, F. Gonzalez, Development and validation of a UAV based system for air pollution measurements, Sensors, 16 (2016) 2202.
[130] T.F. Villa, E.R. Jayaratne, L.F. Gonzalez, L. Morawska, Determination of the vertical profile of particle number concentration adjacent to a motorway using an unmanned aerial vehicle, Environmental Pollution, 230 (2017) 134-142.
[131] J. Zhang, Y. Ji, J. Zhao, J. Zhao, Optimal location of a particulate matter sampling head outside an unmanned aerial vehicle, Particuology, 32 (2017) 153-159.
[132] E.M. Dias, C. Petit, Towards the use of metal–organic frameworks for water reuse: a review of the recent advances in the field of organic pollutants removal and degradation and the next steps in the field, Journal of Materials Chemistry A, 3 (2015) 22484-22506.
[133] S. Janhäll, Review on urban vegetation and particle air pollution–Deposition and dispersion, Atmospheric Environment, 105 (2015) 130-137.
[134] A. Fekete, A.K. Malik, A. Kumar, P. Schmitt-Kopplin, Amines in the environment, Critical Reviews in Analytical Chemistry, 40 (2010) 102-121.
[135] X. Ge, A.S. Wexler, S.L. Clegg, Atmospheric amines-Part I. A review, Atmospheric Environment, 45 (2011) 524-546.
[136] X. Ge, A.S. Wexler, S.L. Clegg, Atmospheric amines-Part II. Thermodynamic properties and gas/particle partitioning, Atmospheric Environment, 45 (2011) 561-577.
[137] A.-J. Kieloaho, H. Hellén, H. Hakola, H.E. Manninen, T. Nieminen, M. Kulmala, M. Pihlatie, Gas-phase alkylamines in a boreal Scots pine forest air, Atmospheric Environment, 80 (2013) 369-377.
[138] S.M. Murphy, A. Sorooshian, J.H. Kroll, N.L. Ng, P. Chhabra, C. Tong, J.D. Surratt, E. Knipping, R.C. Flagan, J.H. Seinfeld, Secondary aerosol formation from atmospheric reactions of aliphatic amines, Atmospheric Chemistry and Physics, 7 (2007) 2313-2337.
[139] J.E. Stratton, R.W. Hutkins, S.L. Taylor, Biogenic amines in cheese and other fermented foods: a review, Journal of Food Protection, 54 (1991) 460-470.
[140] M.H.S. Santos, Biogenic amines: their importance in foods, International Journal of Food Microbiology, 29 (1996) 213-231.
[141] M.A. Bain, R. Faull, G. Fornasini, R.W. Milne, A.M. Evans, Accumulation of trimethylamine and trimethylamine-N-oxide in end-stage renal disease patients undergoing haemodialysis, Nephrology Dialysis Transplantation, 21 (2006) 1300-1304.
[142] C.S.J. Probert, T. Khalid, I. Ahmed, E. Johnson, S. Smith, N.M. Ratcliffe, Volatile organic compounds as diagnostic biomarkers in gastrointestinal and liver diseases, Journal of Gastrointestinal and Liver Disease, 18 (2009) 337-343.
[143] K.D.G. Van de Kant, L.J.T.M. van der Sande, Q. Jöbsis, O.C.P. van Schayck, E. Dompeling, Clinical use of exhaled volatile organic compounds in pulmonary diseases: a systematic review, Respiratory Research, 13 (2012) 117.
[144] H. Wolrath, H. Borén, A. Hallén, U. Forsum, Trimethylamine content in vaginal secretion and its relation to bacterial vaginosis, Apmis, 110 (2002) 819-824.
[145] Q. Cai, W.-Y. Lin, F.-S. Xiao, W.-Q. Pang, X.-H. Chen, B.-S. Zou, The preparation of highly ordered MCM-41 with extremely low surfactant concentration, Microporous and Mesoporous Materials, 32 (1999) 1-15.

[146] F. Kleitz, S.H. Choi, R. Ryoo, Cubic Ia 3 d large mesoporous silica: synthesis and replication to platinum nanowires, carbon nanorods and carbon nanotubes, Chemical Communications, 17 (2003) 2136-2137.
[147] D. Zhao, Q. Huo, J. Feng, B.F. Chmelka, G.D. Stucky, Nonionic triblock and star diblock copolymer and oligomeric surfactant syntheses of highly ordered, hydrothermally stable, mesoporous silica structures, Journal of the American Chemical Society, 120 (1998) 6024-6036.
[148] J. Zhang, Z. Ma, J. Jiao, H. Yin, W. Yan, E.W. Hagaman, J. Yu, S. Dai, Layer-by-layer grafting of titanium phosphate onto mesoporous silica SBA-15 surfaces: synthesis, characterization, and applications, Langmuir, 25 (2009) 12541-12549.
[149] P. Hari, M. Kulmala, Station for Measuring Ecosystem-Atmosphere Relations (SMEAR II), Boreal Environmental Research, 10, (2005), 315-322.
[150] H. Hellén, H. Hakola, K.H. Pystynen, J. Rinne, S. Haapanala, C2-C10 hydrocarbon emissions from a boreal wetland and forest floor, Biogeosciences, 3 (2006) 167-174.
[151] T. Pluskal, S. Castillo, A. Villar-Briones, M. Orešič, MZmine 2: modular framework for processing, visualizing, and analyzing mass spectrometry-based molecular profile data, BMC bioinformatics, 11 (2010) 395.
[152] A. Smirnov, W. Jia, D.I. Walker, D.P. Jones, X. Du, ADAP-GC 3.2: Graphical Software Tool for Efficient Spectral Deconvolution of Gas Chromatography-High-Resolution Mass Spectrometry Metabolomics Data, Journal of proteome research, 17 (2017) 470-478.
[153] R Development Core Team, R: A Language and Environment for StatisticalComputing, ISBN 3-900051-07-0, URL, R Foundation for StatisticalComputing, Vienna, Austria, 2008 http://www.R-project.org.
[154] C. Zhang, R.P. Lively, K. Zhang, J.R. Johnson, O. Karvan, W.J. Koros, Unexpected molecular sieving properties of zeolitic imidazolate framework-8, The Journal of Physical Chemistry Letters, 3 (2012) 2130-2134.
[155] K. Zhang, R.P. Lively, C. Zhang, R.R. Chance, W.J. Koros, D.S. Sholl, S. Nair, Exploring the framework hydrophobicity and flexibility of ZIF-8: from biofuel recovery to hydrocarbon separations, The Journal of Physical Chemistry Letters, 4 (2013) 3618-3622.
[156] M. Kruk, M. Jaroniec, A. Sayari, Application of large pore MCM-41 molecular sieves to improve pore size analysis using nitrogen adsorption measurements, Langmuir, 13 (1997) 6267-6273.
[157] D. Zhao, J. Feng, Q. Huo, N. Melosh, G.H. Fredrickson, B.F. Chmelka, G.D. Stucky, Triblock copolymer syntheses of mesoporous silica with periodic 50 to 300 angstrom pores, Science, 279 (1998) 548-552.
[158] F. Kleitz, F. Berube, R. Guillet-Nicolas, C.-M. Yang, M. Thommes, Probing adsorption, pore condensation, and hysteresis behavior of pure fluids in three-dimensional cubic mesoporous KIT-6 silica, The Journal of Physical Chemistry C, 114 (2010) 9344-9355.
[159] A. Corma, V. Fornes, M.T. Navarro, J. Perezpariente, Acidity and stability of MCM-41 crystalline aluminosilicates, Journal of Catalysis, 148 (1994) 569-574.
[160] W. Hua, Y. Yue, Z. Gao, Acidity enhancement of SBA mesoporous molecular sieve by modification with SO42−/ZrO2, Journal of Molecular Catalysis A: Chemical, 170 (2001) 195-202.
[161] A. Ramanathan, R. Maheswari, D.H. Barich, B. Subramaniam, Niobium incorporated mesoporous silicate, Nb-KIT-6: Synthesis and characterization, Microporous and Mesoporous Materials, 190 (2014) 240-247.
[162] E. Bekou, D.D. Dionysiou, R.-Y. Qian, G.D. Botsaris, Extraction of chlorophenols from water using room temperature ionic liquids, ACS Publications, 856 (2003) 544-560.
[163] N. Deng, M. Li, L. Zhao, C. Lu, S.L. de Rooy, I.M. Warner, Highly efficient extraction of phenolic compounds by use of magnetic room temperature ionic liquids for environmental remediation, Journal of Hazardous Materials, 192 (2011) 1350-1357.
[164] S.-H. Huo, X.-P. Yan, Metal-organic framework MIL-100 (Fe) for the adsorption of malachite green from aqueous solution, Journal of Materials Chemistry, 22 (2012) 7449-7455.

[165] R.C. Huxford, J. Della Rocca, W. Lin, Metal-organic frameworks as potential drug carriers, Current Opinion in Chemical Biology, 14 (2010) 262-268.
[166] Y.-K. Seo, J.W. Yoon, J.S. Lee, U.H. Lee, Y.K. Hwang, C.-H. Jun, P. Horcajada, C. Serre, J.-S. Chang, Large scale fluorine-free synthesis of hierarchically porous iron (III) trimesate MIL-100 (Fe) with a zeolite MTN topology, Microporous and Mesoporous Materials, 157 (2012) 137-145.
[167] E.U. Directive, Directive 2013/39/EU of the European Parliament and of the Council of 12 August 2013 amending Directives 2000/60/EC and 2008/105/EC as regards priority substances in the field of water policy, Off J Eur Union L, 226 (2013) 1-17.
[168] S. Yang, J. Liang, S. Luo, C. Liu, Y. Tang, Supersensitive detection of chlorinated phenols by multiple amplification electrochemiluminescence sensing based on carbon quantum dots/graphene, Analytical Chemistry, 85 (2013) 7720-7725.
[169] H. Hellén, H. Hakola, A. Reissell, T.M. Ruuskanen, Carbonyl compounds in boreal coniferous forest air in Hyytiälä, Southern Finland, Atmospheric Chemistry and Physics, 4 (2004) 1771-1780.
[170] C. Anastasio, B.C. Faust, C.J. Rao, Aromatic carbonyl compounds as aqueous-phase photochemical sources of hydrogen peroxide in acidic sulfate aerosols, fogs, and clouds. 1. Non-phenolic methoxybenzaldehydes and methoxyacetophenones with reductants (phenols), Environmental Science & Technology, 31 (1996) 218-232.
[171] A.W. Schroth, B.C. Bostick, M. Graham, J.M. Kaste, M.J. Mitchell, A.J. Friedland, Sulfur species behavior in soil organic matter during decomposition, Journal of Geophysical Research: Biogeosciences, 112 (2007) G04011.